

See discussions, stats, and author profiles for this publication at: <https://www.researchgate.net/publication/308960925>

# Time-Frequency Signal Analysis

Chapter · January 1991

---

CITATIONS

360

READS

1,706

1 author:



Boualem Boashash

Qatar University

526 PUBLICATIONS 17,472 CITATIONS

SEE PROFILE

# Time-Frequency Signal Analysis

By Boualem Boashash

In

## Advances in Spectrum Analysis and Array Processing

### Volume I

Simon Haykin, editor

McMaster University  
Hamilton, Ontario  
Canada



PRENTICE HALL, Englewood Cliffs, New Jersey 07632

# Time-Frequency Signal Analysis

## Table of Contents

	Page Number
<b>9.1 INTRODUCTION .....</b>	<b>418</b>
9.1.1 The Need for Time-Frequency Distributions .....	421
9.1.2 Instantaneous Frequency and Time Delay .....	423
9.1.3 Signals, Bandwidth, and Duration .....	426
9.1.4 Example .....	431
<b>9.2 TIME-FREQUENCY SIGNAL ANALYSIS .....</b>	<b>433</b>
9.2.1 A Natural Approach .....	433
9.2.2 A General Class of TFDs .....	436
9.2.3 Physical Interpretation of TFDs .....	439
9.2.4 Comparison of TFDs .....	440
9.2.5 Discrete-Time TFDs: Implementation, Comparison, and Choice .....	444
<b>9.3 THE WIGNER-VILLE DISTRIBUTION .....</b>	<b>452</b>
9.3.1 Definition and Properties .....	452
9.3.2 Instantaneous Frequency, Average Frequency, and the WVD .....	453
9.3.3 The Analytic Signal: A Necessity .....	454
9.3.4 Implementation of the Discrete WVD .....	455
<b>9.4. DISCRETE INSTANTANEOUS FREQUENCY ESTIMATION .....</b>	<b>461</b>
9.4.1 Discrete Instantaneous Frequency .....	461
9.4.2. Estimation Using the first Moment of the WVD .....	462
9.4.3 Relationship Between Smoothed DIF and TFD IF Estimators .....	464
<b>9.5. THE WIGNER-VILLE DISTRIBUTION OF MODULATED SIGNALS .....</b>	<b>467</b>
9.5.1 WVD of Monocomponent FM Signals .....	467
9.5.2 WVD of Multicomponent Signals .....	469
<b>9.6. WIGNER-VILLEEE ANALYSIS OF RANDOM SIGNALS .....</b>	<b>473</b>
9.6.1 Formulation .....	473
9.6.2 Estimation Procedure .....	475
9.6.3 Coherence Estimation for Nonstationary Signals .....	476
<b>9.7 SIGNAL SYNTHESIS AND TIME-VARYING FILTERING .....</b>	<b>477</b>
9.7.1 Pattern Recognition .....	477
9.7.2 Signal Synthesis Using the WVI .....	478
9.7.3 The Synthesis Algorithm .....	480
9.7.4 Influence of Window length on Synthesis Accuracy .....	482
<b>9.8 SIGNAL DETECTION BY TIME-FREQUENCY ANALYSIS .....</b>	<b>488</b>
9.8.1 Matched-Filter, WVD, and XWVD-Based Detection .....	489
9.8.2 interpretation of the XWVD Detection Scheme .....	492
9.8.3 Examples Using the XWVD Scheme .....	493
<b>9.9 APPLICATIONS .....</b>	<b>495</b>
9.9.1 Detection of Transients .....	495
9.9.2 Machine Noise Identification .....	500
9.9.3 Analysis and Modeling of ECG Signals .....	502
9.9.4 Seismic Exploration, Sonar/Radar Echolocation, Passive Detection, and Oceanography .....	507
<b>9.10 CONCLUSION AND PERSPECTIVES .....</b>	<b>510</b>

# Time-Frequency Signal Analysis

Boualem Boashash

## 9.1 INTRODUCTION

In many applications such as seismic surveying, communications, radar, and sonar, the signal analyst is confronted with the task of processing signals whose spectral characteristics are varying with time. These signals are often referred to as "time-varying" or "nonstationary." An accurate spectrum analysis of such signals cannot be accomplished by the simple use of classical time-domain representations such as correlation methods or frequency-domain representations based on the Fourier transform. Rather, it requires the use of analysis methods that do not assume any condition of stationarity, as does classical spectrum analysis based on the Fourier transform.

For such signals, the concept of *time-frequency distributions (TFDs)* has been introduced. These methods represent an attempt to provide a general solution to the problem of representing nonstationary signals; as such, they may be considered as an

extension to classical Fourier analysis. The approach taken by different authors is briefly reviewed here in the light of recent developments. The concepts will be discussed first for deterministic, then extended to random signals.

A concept intimately related to the selection of TFDs for practical analysis is that of *instantaneous frequency (IF)*. (The IF is a parameter that corresponds to the frequency of a sine wave, that locally fits the signal under analysis.) Physically, it has meaning only for *monocomponent signals*, that is, where there is only one frequency or a narrow range of frequencies varying as a function of time. For *multicomponent signals*, the notion of a single-valued IF becomes meaningless, and a breakdown into its subcomponents is needed.

The first step of any general time-frequency analysis procedure is to determine whether the signal under analysis is monocomponent or multicomponent, and whether the signal is stationary or nonstationary. The analysis tool must therefore possess the following three properties:

- $P_1$ : The tool discriminates between stationary and nonstationary signals.
- $P_2$ : The tool discriminates between monocomponent and multicomponent signals.
- $P_3$ : The tool allows a breakup of the multicomponent signal into its components (in general also time varying).

The second step of the analysis procedure is to break down the multicomponent signal into its subcomponents. The method used is based on a windowing operation in the time-frequency plane. If required, the equivalent time domain signal can be obtained by TFD inversion techniques (Section 9.7).

The third step is to analyze the components to

1. Track as accurately as possible the spectral variation of the component as given by the IF.
2. Indicate at each time the energy concentration of the signal around the IF.

The ideal tool would be a TFD that has the IF as its first moment and the spread about the IF as its second moment and can display these two parameters in a meaningful way. TFDs are linearly related to each other, and many TFDs give the IF by their first moment. The relationship between TFDs and IF estimation is detailed in Section 9.2.

The fourth step is the reconstruction and modeling part of the analysis, where a mathematical model can be given that accurately represents this signal. An appropriate model is

$$s(t) = \sum_{k=1}^N s_k(t) + n(t), \quad (9.1)$$

where  $n(t)$  is a random noise process and the  $s_k(t)$  are monocomponent time-varying signals described by the amplitude envelope,  $a_k(t)$  and the instantaneous frequency  $f_i^k(t)$  such that

$$s_k(t) = a_k(t)e^{j\phi_k(t)}, \quad (9.2)$$

where

$$\phi_k(t) = 2\pi \int_{-\infty}^t f_i^k(\tau) d\tau.$$

Then the analysis problem is to find  $a_k$  and  $f_i^k$  for  $k = 1, N$ . The analysis procedure is shown in Fig. 9.1, and an example of a multicomponent signal is presented in Fig. 9.2. This signal is the sum of a chirp signal, a narrow-band, time-varying signal (hyperbolic FM) and noise. For this example,  $N = 2$ ,  $f_1(t)$  is a linear function of time,  $a_1$  is a constant,  $f_2(t)$  is a nonlinear function of time, and  $a_2(t)$  is some time-varying function.

A method based on one of these TFDs, the *Wigner-Ville distribution (WVD)*, is very effective for tracking the spectral variations of a class of signals of practical

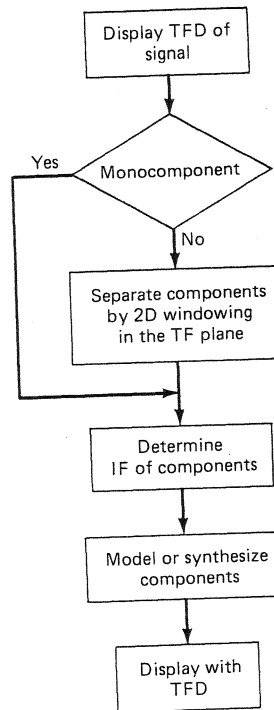


Figure 9.1 Flowchart of a time-frequency analysis system (incorporating component separation and instantaneous frequency estimation).

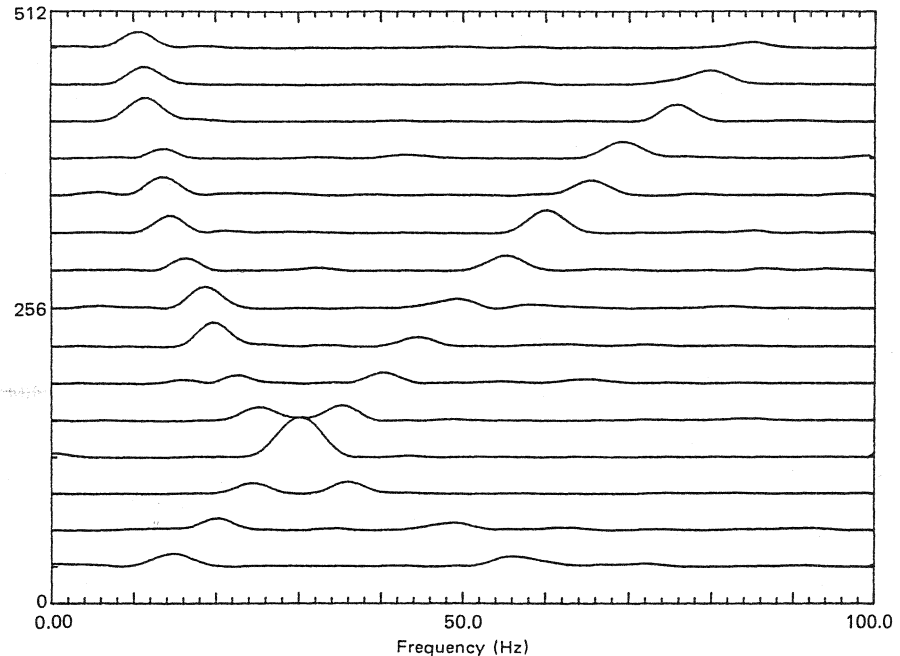


Figure 9.2 A multicomponent signal (a sum of a chirp signal, a hyperbolic FM signal, and noise).

interest, for which the instantaneous frequency plays a central role. It is this form of TFD, therefore, that is dealt with in detail in this chapter.

The properties of the WVD are reviewed, and it is shown how they can be useful for practical analysis with application to diverse areas such as modeling, detection, recognition, and time-varying filtering. The discrete version of the WVD is presented in a simple way that relates to the concept of the *discrete Fourier transform (DFT)*, and the *discrete instantaneous frequency (DIF)* is defined. The application of the method to the analysis of nonstationary random signals and coherence estimation is also introduced and the method of analysis is discussed. The use of the WVD in signal detection is also reviewed. Recent developments and applications are described.

### 9.1.1 The Need for Time-Frequency Distributions

There are two classical representations used in signal theory: the time representation,  $s(t)$ , of a signal, and its frequency representation,  $S(f)$  [1]. In these representations, the variables of time,  $t$ , and frequency,  $f$ , are mutually exclusive. The evaluation of the spectrum,  $S(f)$  at some frequency  $f = f_1$  requires the knowledge of the values of

$s(t)$  in the support of  $s(t)$ , possibly for all  $t$  from  $-\infty$  to  $+\infty$ . This is obtained by calculating the Fourier transform (FT) of  $s(t)$  as follows [2]:

$$S(f_1) = \int_{-\infty}^{+\infty} s(t)e^{-j2\pi f_1 t} dt \quad (9.3)$$

Similarly, the value of the original time function  $s(t)$  at  $t = t_1$  is determined from the values of  $S(f)$ , in the support of  $S(f)$ , possibly  $-\infty < f < \infty$ , by using the inverse Fourier transform

$$s(t_1) = \int_{-\infty}^{+\infty} S(f)e^{j2\pi f t_1} df \quad (9.4)$$

However, often in practice, signals are found for which this property of exclusivity does not hold because these signals are nonstationary, and their spectral content varies with time. These nonstationary signals are of major engineering importance, and it is desirable to analyse them in such a manner that they can be easily interpreted by the analyst.

A good illustration of the limitation of "classical" spectrum analysis is provided by observing that we may find totally different signals  $s_1(t)$  and  $s_2(t)$ , and yet they have the same magnitude (amplitude) spectrum or power spectral density. The reason for this apparent anomaly is that the spectrum of a real signal, defined by its Fourier transform, is in general complex and can be characterized either by real and imaginary parts, or in polar coordinates by magnitude and phase. Therefore, the information that differentiates these two signals,  $s_1$  and  $s_2$ , is contained in the phase spectrum; it contains the information necessary to localize the frequency components in time, or equivalently the time components in frequency. This localization in frequency of a particular time component of the signal is measured by the time (group) delay that is the derivative of the phase spectrum [2]. (See the definition in the next section.)

Similarly, the instantaneous frequency of the signal is a measure of the localization in time of the particular frequency component of the signal [2] and complements the information provided by the time representation,  $s(t)$ , in that it describes the arrangement of the frequency components as they would appear to an observer listening to an audio signal. For, example, in a siren, it would describe whether the sound was proceeding from low frequency to high frequency, or vice versa, or even alternating. These functions, the instantaneous frequency and time delay, describe the "internal organization" of the representation of the signal. Removing this information will lead to an effective scrambling of the signal. A good discussion that illustrates this point—the importance of the phase of the signal—can be found in [3].

To see more clearly this inherent limitation of conventional spectrum analysis, consider the two signals defined by

$$s_1(t) = \Pi_T(t) \cdot \cos(2\pi(f_0 \cdot t + \alpha \cdot t^2/2)) \quad (9.5)$$

$$s_2(t) = \frac{\sin \pi Bt}{\pi t} \cdot \cos 2\pi f_c t \quad (9.6)$$

where  $\Pi(t)$  is a rectangular function of unit amplitude and duration  $T$ ,  $B = \alpha T$ , and  $f_c = f_0$ . Figure 9.3 shows these signals and their spectral densities. The signal  $s_1(t)$  is a chirp signal (i.e., a linear *frequency modulation (FM)* law), and  $s_2(t)$  is a modulated sinc signal. Although  $s_1$  and  $s_2$  are fundamentally different, they have the same magnitude squared spectrum. The information that allows us to discriminate between them is contained in their phase spectrum. This illustrates the need for a more sophisticated and practical general time-varying signal analysis tool, which preserves all the information of the signal and therefore discriminates signals in a better way.

### 9.1.2 Instantaneous Frequency and Time Delay

The notion of instantaneous frequency was defined by Ville [4] as follows,

$$f_i(t) = \frac{1}{2\pi} \frac{d\phi(t)}{dt}, \quad (9.7)$$

where  $z(t) = a(t)e^{j\phi(t)}$  is the analytic signal associated with the real signal,  $s(t)$ , as follows,

$$z(t) = s(t) + j\mathcal{H}[s(t)], \quad (9.8)$$

with  $\mathcal{H}$  representing the Hilbert transform:

$$\mathcal{H}[x(t)] = \frac{1}{\pi} \text{p.v.} \left[ \int_{-\infty}^{+\infty} \frac{x(t - \xi)}{\xi} d\xi \right], \quad (9.9)$$

where *p.v.* denotes the Cauchy principal value.

Similarly, the time (group) delay  $\tau_g(f)$  is defined as

$$\tau_g(f) = -\frac{1}{2\pi} \frac{d\theta(f)}{df} \quad (9.10)$$

where  $\theta(f)$  is the phase of the FT of  $z(t)$ ; that is,

$$Z(f) = A(f)e^{j\theta(f)}. \quad (9.11)$$

As indicated earlier, in many applications it is desirable to estimate the time-frequency laws,  $f_i(t)$  and  $\tau_g(f)$ , of the signal, since they characterize important parameters of the signal. For these applications that arise from practical situations, the signals in general exhibit various restrictions due to their physical origin. These restrictions include such aspects as finite energy, finite message duration, stability, causality, and so forth. It is also observed that these signals always have a finite spectral bandwidth  $B$  containing most of the signal energy. Therefore, even though the model based on the Fourier transform theoretically forbids any double limitation,

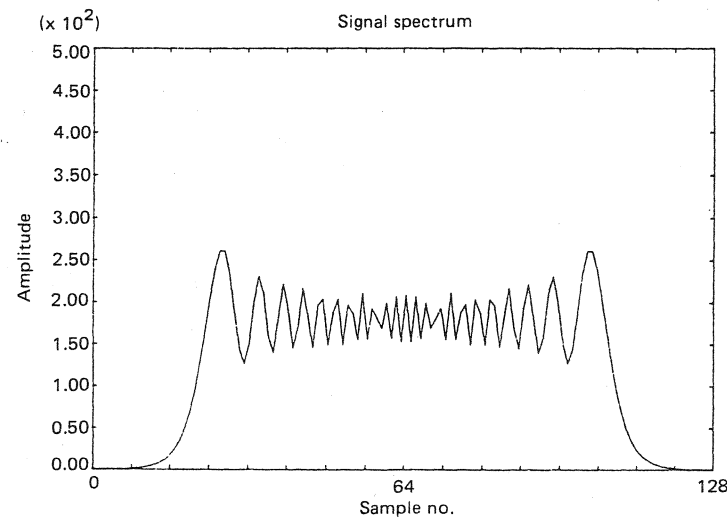
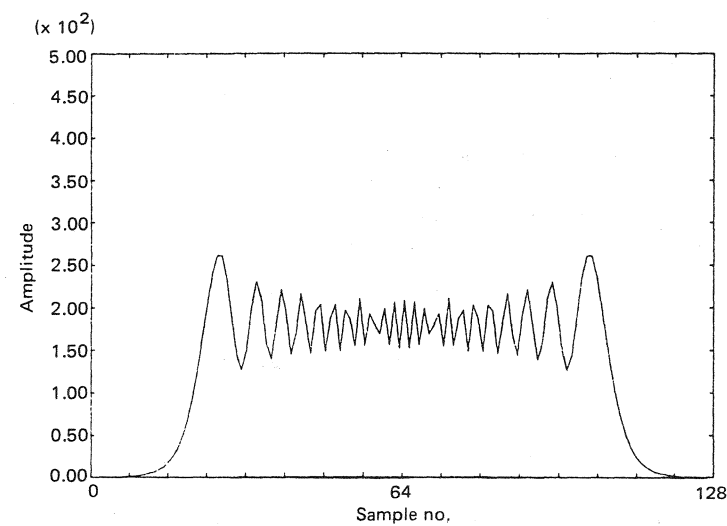
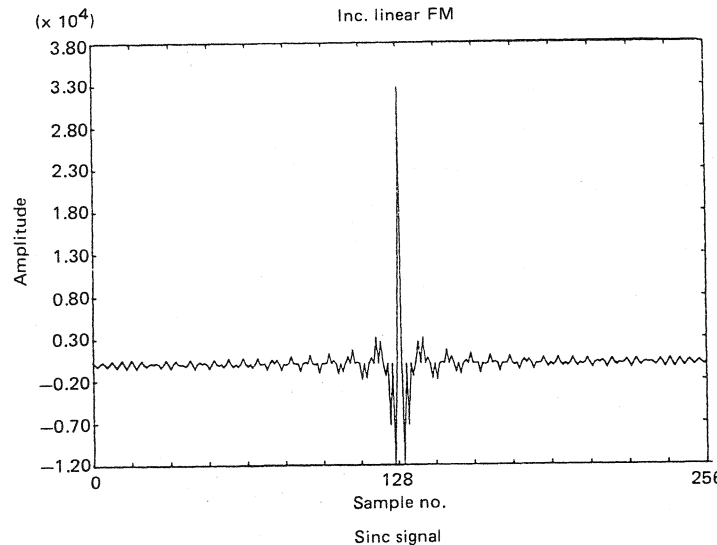
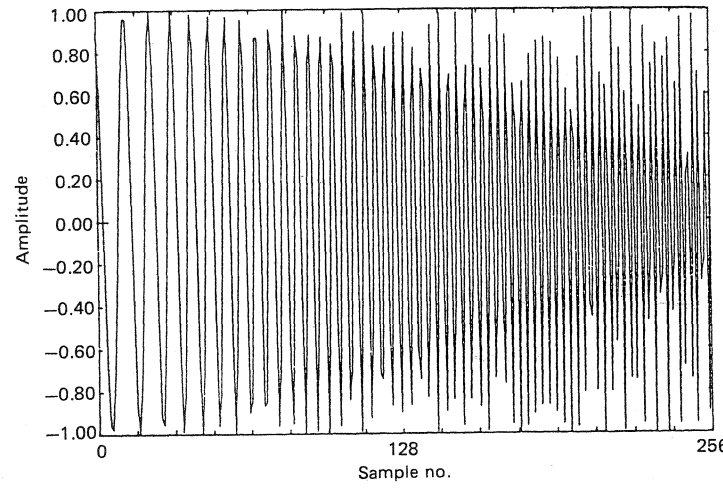


**Figure 9.3** Signals with same spectrum. (a) Chirp signal, (b) spectrum of chirp, (c) modulated sinc signal, (d) spectrum of modulated sinc.

a class of signals with effective finite "duration" and effective finite spectral "bandwidth" will be defined, since this corresponds more closely to the reality of experimentation. A class of signals that describes these properties well is the class of "asymptotic signals" [5] defined next.

### 9.1.3 Signals, Bandwidth, and Duration

Several authors have tried to develop a theoretical basis for the imposition of a double limitation of effective finite bandwidth and effective finite duration.\* The definition commonly used for this purpose was proposed by Gabor [1]. Let  $s(t)$  be a finite-energy signal centered about zero in time and frequency. The *effective duration*,  $T_s$ , and the *effective bandwidth*,  $B_s$ , are, respectively, given by:

$$T_s^2 = \frac{\int_{-\infty}^{\infty} t^2 |s(t)|^2 dt}{\int_{-\infty}^{+\infty} |s(t)|^2 dt} \quad B_s^2 = \frac{\int_{-\infty}^{+\infty} f^2 |S(f)|^2 df}{\int_{-\infty}^{+\infty} |S(f)|^2 df}. \quad (9.13)$$

This definition was found most useful for explicit calculations and comparisons such as those reported in [8].

Based on the foregoing, the signals considered in this chapter are assumed to have the properties of finite energy, bounded maximum amplitude and finite duration; additionally, they are assumed to have a  $BT$  product sufficiently high ( $BT > 10$ ) so that the approximation error involved in assuming band and time limited functions is very small [6]. These restrictions define a class of signals referred to as "asymptotic," the asymptotic behavior being measured by the parameter  $\mu = BT$  (it should be remembered that asymptotic does not only imply large  $BT$ , but also finite

\*To define  $B$  and  $T$ , Landau and Pollack [6] use two parameters  $\varepsilon_T^2$  and  $\eta_B^2$  that measure the fraction of the signal energy lying outside the duration  $T$  and the bandwidth  $B$ . This approach involves defining a percentage of neglected energy by choosing the degree of signal energy concentration  $(1 - \varepsilon_T^2)$  in time (alternatively  $(1 - \eta_B^2)$  in frequency), then solving for  $T$  and  $B$  with the following equations:

$$1 - \varepsilon_T^2 = \frac{1}{E} \int_{-T/2}^{T/2} |s(t)|^2 dt \quad 1 - \eta_B^2 = \frac{1}{E} \int_{-B/2}^{B/2} |S(f)|^2 df, \quad (9.12)$$

where  $S(f)$  is the Fourier transform of  $s(t)$  and  $E$  is the signal energy. These precise measurements are of great interest to the signal analyst because of the immediate physical meaning associated with these parameters. The disadvantage of this approach is that it requires the knowledge of the signal from  $-\infty$  to  $\infty$ , which is outside the range of any measuring device.

Slepian [7] proposed a definition that needs only the actually measured signal: let  $\varepsilon$  be the minimal energy that the measuring apparatus can detect; then two signals whose energy difference is less than  $\varepsilon$  will look similar to the experimenter. Therefore, he or she defines the duration of a given signal  $s(t)$  as the duration of the time-limited signal whose energy difference with the energy of  $s(t)$  is less than  $\varepsilon$ . A similar definition applies for the bandwidth  $B$ . This approach is closer to the reality of experimentation because it links the definitions with the qualities and precisions of the measurement equipment.

energy, finite duration, etc.). The effect of the  $BT$  parameter on the accuracy of calculations involving time-frequency representations is important, since a low- $BT$  product produces results that are difficult to interpret.

*Note 1.* The  $BT$  product provides a measure for the richness of information (the number of degrees of Freedom) contained in the signal. This product could be compared with the number of realisations needed to estimate the *probability density function (PDF)* of a stochastic process. With only a few experiments available, the estimate does not really make sense, and it is hard to define the process by its PDF estimate. Similarly, if there is a short signal, characterizing it by its IF has limited meaning, because there is not enough data to observe any variation. However, if the signal has a long duration, then its IF becomes very meaningful.

### Definitions and Properties of Asymptotic Signals

**Definition 1-1:** An *asymptotic signal*,  $s(t)$ , is referred to as a *monocomponent* (or *invertible*) signal if that signal satisfies two requirements (1) the instantaneous frequency,  $f_i(t)$ , accurately represents the frequency modulation law of the signal and (2) is single-valued and invertible, so that the function  $f_i^{-1}$  exists. (See Fig. 9.4.)

**Definition 1-2:** A finite energy asymptotic signal,  $s(t)$ , is referred to as a *multicomponent signal* if there exists a finite number,  $N$ , of monocomponent signals,  $s_i(t)$ ,  $i = 1, N$  such that the relation  $s(t) = \sum_{i=1}^N s_i(t)$  holds for all values of  $t$  for which  $s(t)$  is defined, that is, if  $s(t)$  can be characterized as the sum of several monocomponent signals, and such that the decomposition is meaningful. This decomposition is not unique; it is application dependent.

*Note 2.* The breaking up of a signal into meaningful components should be seen as a global phenomenon: often, it is the continuous pattern representing the variation as a function of time of the energy concentration in the time-frequency domain that determines whether there is only one or several components. This energy concentration may be measured by the local bandwidth or spread about the instantaneous frequency of the signal (or its subcomponents in the case of a multicomponent signal). This is illustrated in Figs. 9.5(a) and 9.5(b), and the question is studied in detail in [9].

*Property 1-1.* The energy distribution of an asymptotic signal,  $s(t)$ , is concentrated in a finite domain (time bandwidth) of the time-frequency plane, and the degree of concentration is a function of the  $BT$  product [5]. (This is a signal characteristic and is independent of the representation chosen. See Fig. 9.6(a)).

A useful concept is that of "elementary cells" that define the signal concentration, the dimension of the cells depending on the FM law of the signal and the  $BT$  product of the signal. (See Fig. 9.6(b).) One way to define the dimensions of these

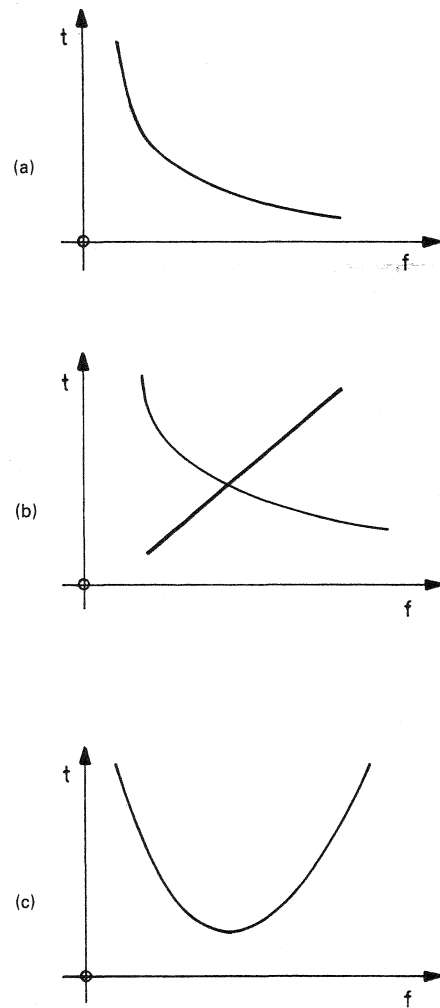


**Figure 9.4** (a) A monocomponent signal. (b) and (c) Nonmonocomponent signals (for a given value of time there are two values of frequency).

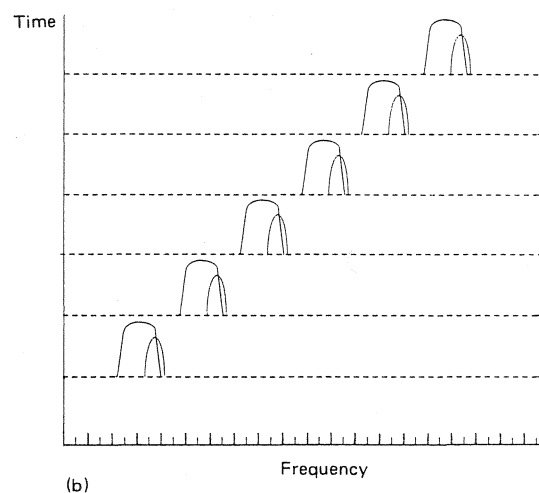
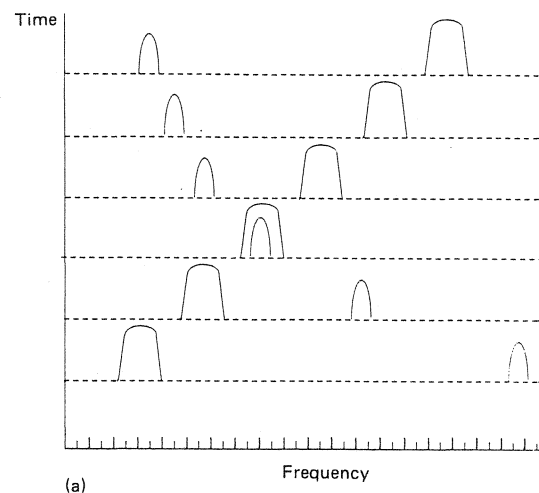


**Figure 9.5** Multicomponent and monocomponent signals. (a) Multicomponent signal: overall, the two components are well separated. (b) Monocomponent signal: overall, the two components are not well separated.

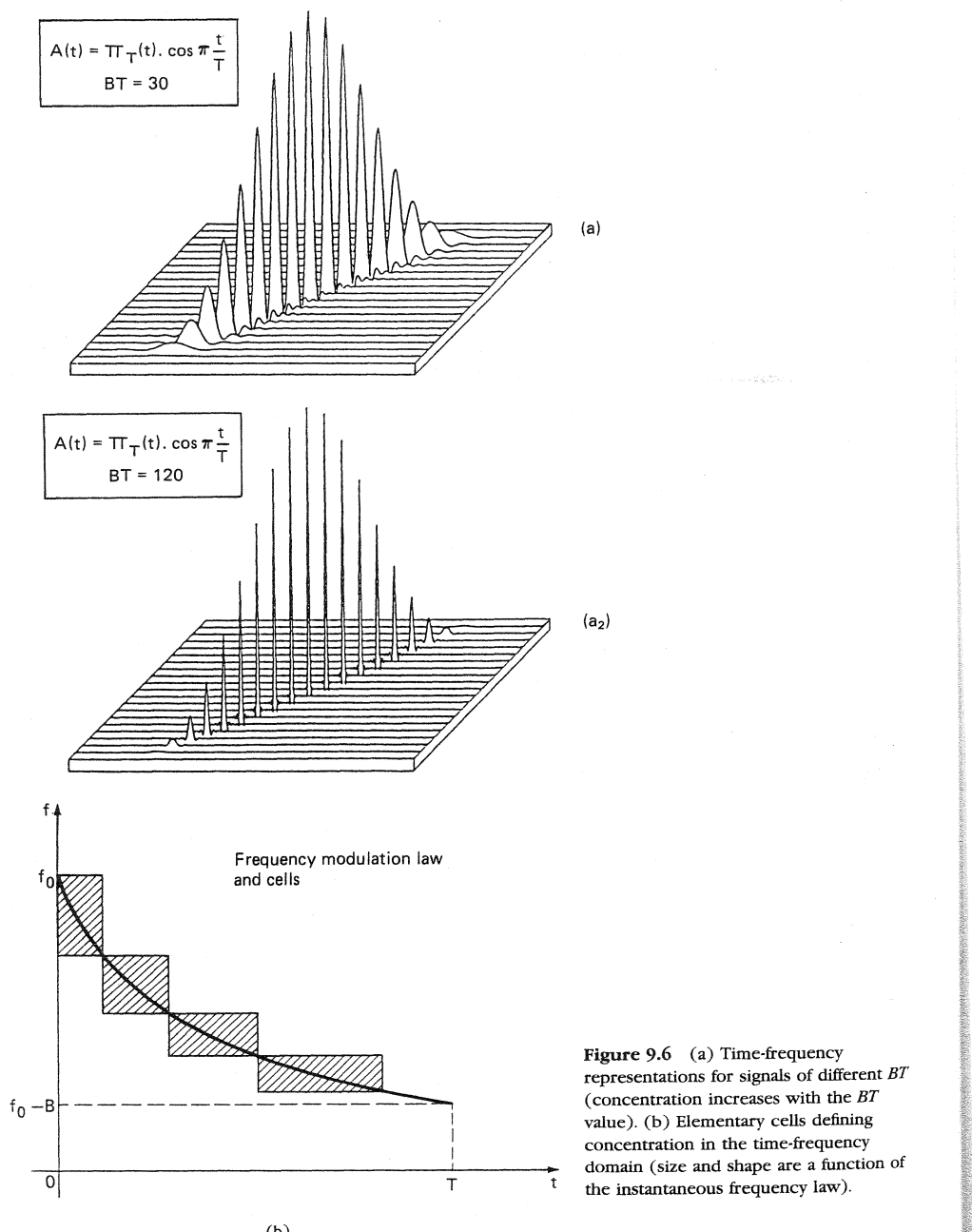


**Figure 9.6** (a) Time-frequency representations for signals of different  $BT$  (concentration increases with the  $BT$  value). (b) Elementary cells defining concentration in the time-frequency domain (size and shape are a function of the instantaneous frequency law).

cells is to introduce the notion of *relaxation time*,  $T_r$ , and *dynamic bandwidth*,  $B_d$ , as follows [10], [5]:

$$T_r(t) = \left| \frac{df_i(t)}{dt} \right|^{-1/2} \quad (9.14)$$

$$B_d(f) = \left| \frac{d\tau_g(f)}{df} \right|^{-1/2} \quad (9.15)$$

#### Property 1-2.

- For a monocomponent asymptotic signal ( $BT$  large), the instantaneous frequency  $f_i(t)$  approaches  $\tau_g^{-1}(f)$ ; that is, these two functions are the inverse of each other [5], [8]. (For this to occur both  $f_i(t)$  and  $\tau_g(f)$  must be monotonic.) In this case, the time-frequency laws have a physical meaning: the instantaneous frequency,  $f_i(t)$ , describes the frequency modulation law of the signal,  $s(t)$ , and  $\tau_g(f)$  represents the time delay of the signal. In other words, it represents the variation of the propagation time as a function of the frequency of an impulse travelling through a linear filter whose impulse response is  $h(t) = s(t)$ .
- For a monocomponent signal, if  $BT$  is small, then  $f_i \neq \tau_g^{-1}$ ; that is, these two functions are not the inverse of each other [5], [8]. In this case, no physical meaning can be associated with these time-frequency laws, although they are mathematically well defined.

**Property 1-3.** Let  $s(t) = a(t) \cdot \cos \phi(t)$  be an FM asymptotic signal; then the analytic signal associated with  $s(t)$  as defined in (9.8) can be approximated by replacing  $\cos \phi(t)$  in the expression of  $s(t)$  by  $e^{j\phi(t)}$ , since

$$\mathcal{H}[s(t)] = \mathcal{H}[a(t) \cos \phi(t)] \cong a(t) \mathcal{H}[\cos \phi(t)] = a(t) \sin \phi(t).$$

This is a consequence of Bedrosian's theorem for large  $BT$  signals [11], [5].

#### 9.1.4 Example

Consider the following asymptotic chirp signal with duration  $T$  and bandwidth  $B$

$$s(t) = \Pi_T(t) \cos \phi(t), \quad (9.16)$$

where  $\phi(t) = 2\pi(f_c t + \alpha t^2/2)$  with  $\alpha = B/T$ . Using Property 1-3, the analytic signal associated with the large  $BT$  signal,  $s(t)$ , is obtained by replacing the cosine function by an exponential function. Thus,

$$z(t) = \Pi_T(t) e^{j\phi(t)} \quad \text{and} \quad f_i(t) = \frac{1}{2\pi} \frac{d\phi}{dt} = f_c + \alpha t. \quad (9.17)$$

Then,  $f_i(t)$  can be considered as an operator mapping the space  $T_t$  of time instants,  $t$ , to the space  $B_f$  of frequencies,  $f$ . The inverse operator,  $g(t) = f_i^{-1}(t)$ ,

represents the inverse mapping and is easily defined by extracting  $t$  as a function of  $f_i(t)$  in (9.17):

$$g(t) = \alpha^{-1}[f_i(t) - f_c(t)]. \quad (9.18)$$

This result is now compared with the time delay,  $\tau_g(f)$ , of the signal. The Fourier transform of the signal,  $z(t)$ , is given by [5]

$$Z(f) \approx \frac{1}{\sqrt{\alpha}} \Pi_B(f - f_c) e^{j\pi[1/4 - \alpha^{-1}(f - f_c)^2]}. \quad (9.19)$$

The time delay,  $\tau_g(f)$ , is easily derived as

$$\tau_g(f) = \frac{1}{2\alpha} 2(f - f_c) = \frac{1}{\alpha}(f - f_c) \quad (9.20)$$

and can be seen to represent the same operator as  $g = f_i^{-1}$ . Exact calculations are given in [12].

For the chirp signal, (9.17) to (9.20) show that  $f_i(t)$  is a unique time-frequency characteristic of the signal. The evaluation of  $f_i(t)$ , then, becomes a problem of fundamental importance in signal processing since in this case ( $BT \gg 1$ ), it represents the unique time-frequency law of the signal. This property is exploited in a variety of applications [13]. When the signal is observed in presence of additive noise, the corresponding instantaneous frequency evaluation for the noisy signal provides a statistical estimation for the instantaneous frequency of the signal. This estimate is useful, but has not been shown to be statistically optimal.

On the other hand, for small  $BT$  signals, two different time-frequency laws can be identified, specifically  $f_i(t)$  and  $\tau_g(f)$ , and therefore, their interpretation becomes less meaningful. (See Fig. 9.7.) However, this does not necessarily preclude the use of the method, but care must be taken in its interpretation [14].

**Estimation of  $f_i$ .** The direct estimation of  $f_i(t)$  as given in (9.7) requires implementation of its discrete-time version, and in the presence of additive noise care must be taken to define carefully the numerical differentiation [15]. (See Section 9.4.) This direct procedure provides the appropriate information regarding the “internal organization of the signal,” but other important information, such as the spread of the signal around its time-frequency law [9], is not available. An alternate method based on TFDs has the advantage that all the information regarding time-frequency law, spread, and so on is presented in one single representation. (See Section 9.4.)

## 9.2 TIME-FREQUENCY SIGNAL ANALYSIS

### 9.2.1 A Natural Approach

Time-frequency signal analysis is a natural extension of time and frequency-domain analysis. It represents signals in a wider space that can display all the signal information in a more accessible way [1]. Such a representation should provide a distribution

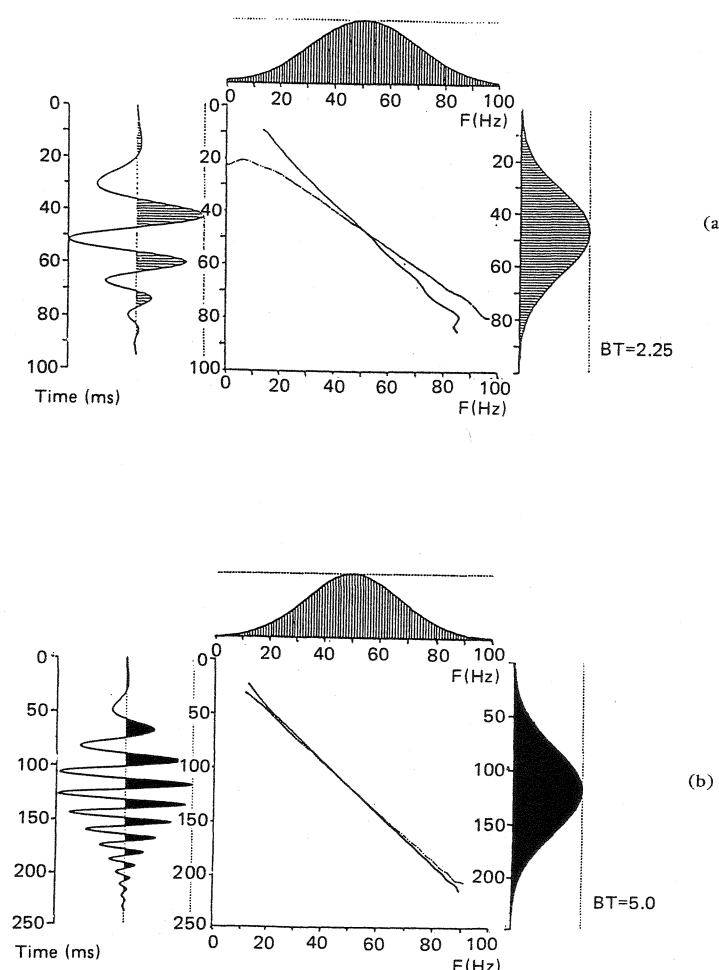


Figure 9.7 Instantaneous frequency and time-delay laws. (a) For low values of  $BT$ , the two laws are represented by different curves. (b) For large values of  $BT$ , the two laws are represented by the same curve.

of signal energy  $E(t, f)$  versus both time and frequency. The time-frequency domain thus defined would (it is hoped) exhibit the time-frequency law of each signal component, thereby making  $f_i(t)$  estimation easier; it could also provide additional information about component amplitude, and the spread of the components around  $f_i(t)$ . Several different attempts have been made at defining such a representation, and a number are shown in Table 9.1.

TABLE 9.1 Popular TFDs and  $g(v, \tau)$ 

$g(v, \tau)$	$p(t, f)$	Representation
1	$\int_{-\infty}^{+\infty} z(t + \tau/2) \cdot z^*(t - \tau/2) \cdot e^{-j2\pi f\tau} d\tau$	[16], [4]
$\cos \pi v\tau$	$\operatorname{Re} \{z(t) \cdot Z^*(f) \cdot e^{-j2\pi f\tau}\}$	[10]
$\frac{\sin \pi v\tau}{\pi v\tau}$	$\int_{-\infty}^{+\infty} \frac{1}{\tau} \int_{t - \tau/2}^{t + \tau/2} z^*(u - \tau/2) \cdot z(u + \tau/2) du e^{-j2\pi f\tau} d\tau$	[17]
$\Pi_{2\Delta}(\tau) \cdot \frac{\sin \pi(\Delta -  \tau ) \cdot v}{\pi v}$	$\left  \int_{t - \Delta/2}^{t + \Delta/2} z^*(u) \cdot e^{-j2\pi f\tau u} du \right ^2$	[18]
$e^{j\pi v \tau }$	$\frac{\delta}{\delta t} \left  \int_{-\infty}^t z(u) \cdot e^{-j2\pi f\tau u} du \right ^2$	[19]
$e^{\frac{4\pi v}{v^2\tau^2/\sigma}}$	$\int \int \frac{\sqrt{\pi}}{\sqrt{\tau^2/\sigma}} e^{-(u - \tau)^2 / 4\tau^2/\sigma} z^*(u - \frac{\tau}{2}) z(u + \frac{\tau}{2}) du d\tau$	[20]

Perhaps the most intuitively appealing time-frequency formulation involves a "discretization" or partitioning of the time domain. We take a slice of the signal by applying a moving window,  $p(t - t_0)$ , to the signal,  $s(t)$ , and then calculate the magnitude squared of the Fourier transform. This method is referred to as the *short time Fourier transform (STFT)* (see Fig. 9.8). The STFT is defined as follows:

$$S_1(t_0, f) = \left| \int_{-\infty}^{+\infty} z(\theta) \cdot p(\theta - t_0) \cdot e^{-j2\pi f\theta} d\theta \right|^2, \quad (9.21)$$

where  $z(t)$  is the analytic signal associated with the real signal  $s(t)$ .

By using a window of width,  $\Delta$ , centered about  $t = t_0$ , and varying  $t_0$ , we may obtain a spectral density that is a function of  $f$  and  $t_0$ . The information that is lost when we use the spectral density of the whole signal is now given by the position,  $t_0$ , of the window, with a resolution determined by the width of this window. The

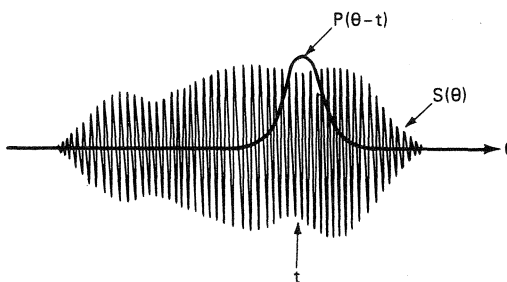


Figure 9.8 Principle of the short-time Fourier transform. It corresponds to taking the Fourier transform of a slice of signal.

## Sec. 9.2 Time-Frequency Signal Analysis

influence of the window width,  $\Delta$ , on the STFT is illustrated in Fig. 9.9 for the case of a chirp signal. The STFT displays a main lobe around the IF,  $f_i(t)$ , and the resolution of the method is determined by the width of this lobe. Figure 9.9 indicates that the resolution is fixed by the parameter  $\delta$  (see Figure 9.9), and therefore by the choice of the width  $\Delta$ . If the width is too large, the main lobe of the STFT is widened to the "larger spectral content" within this slice. On the other hand, if it is too small, the main lobe is also widened as a consequence of the uncertainty relations [1]. The optimum width that corresponds to the best compromise is found graphically to be  $\delta = \sqrt{2}$  corresponding to  $\Delta = \sqrt{T/B}$ . More generally, a nonbiased and accurate analysis requires the window width,  $\Delta$ , to be equal to the relaxation time defined earlier [21], [22]:

$$\Delta = \left| \frac{df_i(t)}{dt} \right|^{-1/2} \quad (9.22)$$

For the FM signal  $|df_i(t)/dt|$  represents the slope of the FM law  $\alpha = T/B$ . The optimal STFT requires, then, an a priori knowledge of  $f_i(t)$ , which can only be obtained after some form of time-frequency analysis. Therefore, any analysis procedure based on the STFT should be iterative.

Another equivalent approach, referred to as the *sonogram*, involves "discretizing" or partitioning the frequency domain, by passing the signal through a bank of

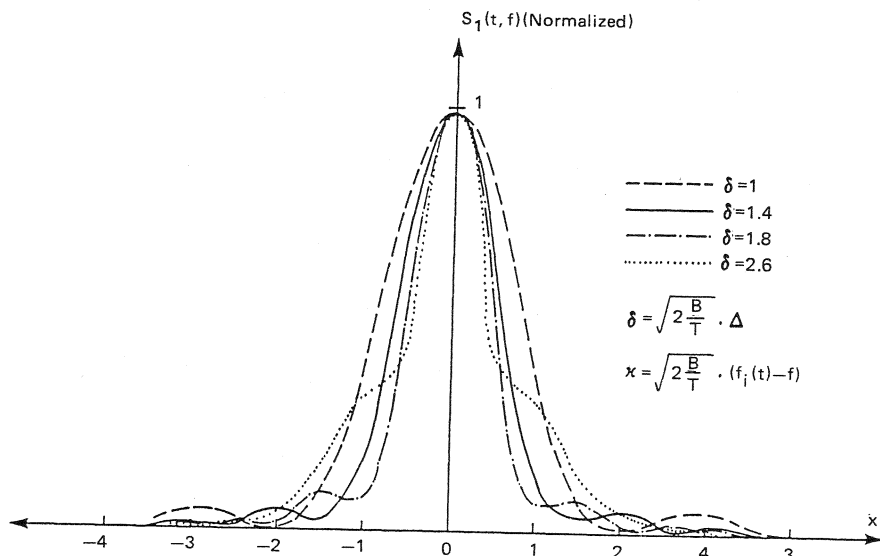


Figure 9.9 Influence of window on resolution of STFT. The window must be neither too large nor too narrow.

adjacent filters centered around frequencies,  $nf_0$  ( $n = 1, \dots, N$ ), and with bandwidth,  $\Delta(f)$ , thereby applying an implicit windowing,  $P(f - f_0)$ , to the Fourier transform,  $S(f)$ , of the signal. This is approximately the processing performed by the human ear. The sonogram is defined as follows:

$$S_2(t, f) = \left| \int_{-\infty}^{\infty} Z(v) P(v - f) e^{j2\pi v t} dv \right|^2. \quad (9.23)$$

These time-frequency representations,  $S_1(t, f)$  and  $S_2(t, f)$ , are equivalent if  $P(f)$  is the Fourier transform of  $p(t)$  [5].

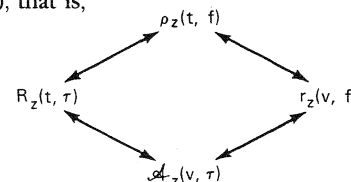
### 9.2.2 A General Class of TFDs

To distribute the energy of a signal in a time-frequency domain, many other time-frequency representations have been proposed by different authors ([4], [1], [23], [19], [10], [17]), each one having its own merits and disadvantages. A unified formulation that generalizes all the previous definitions was proposed by Cohen in 1966 (in a quantum mechanics context [17]) as

$$\rho_z(t, f) = \int_{-\infty}^{+\infty} \int_{-\infty}^{+\infty} \int_{-\infty}^{+\infty} e^{j2\pi v(u-t)} g(v, \tau) z(u + \frac{\tau}{2}) z^*(u - \frac{\tau}{2}) e^{-j2\pi f\tau} dv du d\tau, \quad (9.24)$$

where  $z(t)$  is the analytic signal and  $g(v, \tau)$  is a weighting function that defines the chosen observation mode [17]. An appropriate choice of  $g(v, \tau)$  yields one of the previous particular definitions of time-frequency representation. The formulation was found to be extremely useful by providing a more general framework for the global understanding of any particular method of time-frequency signal analysis and enabling the signal analyst to relate one representation and its properties to the others. All TFDs satisfying some basic properties (see Properties 2–3 and 2–4 later in this section) can be expressed in the general form, and can be considered as a filtered WVD [24]. In fact, any TFD can be written as a linear function of any other TFD.

From (9.24), we can also define by Fourier transforms the time-lag representation  $R_z(t, \tau)$ , the Doppler-frequency representation  $r_z(v, f)$ , and the Doppler-delay representation,  $\mathcal{A}_z(v, \tau)$ , that is,



$\mathcal{A}_z(v, \tau)$  is often referred to as the generalized ambiguity function [24b]. It can be easily shown that

$$\mathcal{A}_z(v, \tau) = g(v, \tau) \cdot A_z(v, \tau), \quad (9.25a)$$

where  $A_z(\phi, \theta)$  is the *Sussman ambiguity function* defined by [25]:

$$A_z(v, \tau) = \int_{-\infty}^{+\infty} z(u + \tau/2) \cdot z^*(u - \tau/2) \cdot e^{+j2\pi vu} du. \quad (9.25b)$$

By taking the Fourier transform of  $g(v, \tau)$ , we obtain

$$G(t, \tau) = \mathcal{F}_{v \rightarrow t}^{-1} [g(v, \tau)], \quad (9.26)$$

where  $\mathcal{F}$  represents the FT. The expression of  $\rho_z(t, f)$  reduces to

$$\rho_z(t, f) = \mathcal{F}_{\tau \rightarrow f} [G(t, \tau) * K_z(t, \tau)], \quad (9.27)$$

where  $K_z(t, \tau) = z(t + \tau/2)z^*(t - \tau/2)$  and  $(*_t)$  denotes the time convolution integral.  $G(t, \tau)$  will henceforth be referred to as the time-lag kernel function, where  $t$  and  $\tau$  are the time and lag variables. The discrete time equivalent of  $G(t, \tau)$  is used later for defining discrete time TFDs (Section 9.2.5).

Both functions,  $g(v, \tau)$  and  $G(t, \tau)$ , characterize the observation mode chosen by the analyst; they determine how the signal energy is distributed in the time-frequency domain. They are analogous to the windows used in spectrum analysis. Choices of  $g(v, \tau)$  and resulting TFDs are shown in Table 9.1 (p. 434).

#### Desirable Properties of a TFD

For a practical and useful analysis, the experimentalist requires from a TFD that it accurately represents the energy distribution of the signal, and therefore desires the following properties:

*Property 2-1.* The TFD must be real to represent the variation in energy, and it is expected to be positive.

*Property 2-2.* Integration of the TFD over both time,  $t$ , and frequency,  $f$ , yields the energy of the signal:

$$\int_{-\infty}^{+\infty} \int_{-\infty}^{+\infty} \rho(t, f) dt df = E, \text{ signal energy.} \quad (9.28)$$

*Property 2-3.* Integration of the TFD over time,  $t$ , yields the spectral density of the signal.

$$\int_{-\infty}^{+\infty} \rho(t, f) dt = |Z(f)|^2, \text{ spectral density.} \quad (9.29)$$

*Property 2-4.* Integration of the TFD over frequency,  $f$ , yields the instantaneous power of the signal.

$$\int_{-\infty}^{+\infty} \rho(t, f) df = |z(t)|^2, \text{ instantaneous power.} \quad (9.30)$$

*Property 2-5.* The first moments of the TFD yield the instantaneous frequency and the time-delay of the signal.

$$\frac{\int_{-\infty}^{+\infty} f \cdot \rho(t, f) \cdot df}{\int_{-\infty}^{+\infty} \rho(t, f) \cdot df} = f_i(t) \quad \frac{\int_{-\infty}^{+\infty} t \cdot \rho(t, f) \cdot dt}{\int_{-\infty}^{+\infty} \rho(t, f) \cdot dt} = \tau_g(f). \quad (9.31)$$

### Constraints on the Window Function $g(v, \tau)$

$\rho_z(t, f)$  is defined if the integral (9.24) converges, yielding the constraint:

$$|g(v, \tau)| \leq 1. \quad (9.32)$$

Property 2-2, described by (9.28) is verified if and only if

$$g(0, 0) = 1. \quad (9.33)$$

Property 2-1 holds ( $\rho_z(t, f)$ ) is real if and only if

$$g(v, \tau) = g^*(-v, -\tau). \quad (9.34)$$

Property 2-5, (9.31), is verified if [27]

$$\frac{\partial g(v, \tau)}{\partial \tau}|_{0,0} = \frac{\partial g(v, \tau)}{\partial v}|_{0,0} = 0, \quad (9.35a)$$

$$g(v, 0) = \text{constant for all } v \quad (9.35b)$$

$$g(0, \tau) = \text{constant for all } \tau.$$

These constraints define a class of TFDs that can be used for a practical analysis. This class  $\{P\}$  is a subclass of Cohen's class [23] and is defined as the ensemble of TFDs for which the characteristic function,  $g(v, \tau)$ , satisfies equations (9.32) to (9.35).

Among the popular TFDs that have been proposed as a possible tool for time-frequency signal analysis, only four TFDs have all the desired properties (apart from the positivity criterion that is discussed in the next section): the Wigner-Ville distribution, the *Rihaczek distribution (RD)*, the *Cohen distribution* (named after Born-Jordan by Cohen in [23]), and the more recently introduced *Choi-Williams distribution* [20].

### Positivity of TFDs

Since the TFD,  $\rho(t, f)$ , expressed in (9.24) is real and its integral yields the energy of the signal, it seems natural to consider attributing to  $\rho(t, f)$  the property of density, and therefore to require that  $\rho(t, f)$  be positive valued. Unfortunately, the positivity characteristic of  $\rho(t, f)$  is incompatible with estimation of the instantaneous frequency,  $f_i(t)$  and time delay  $\tau_g(f)$ , as a moment of the TFD defined by (9.31). The incompatibility is demonstrated in the following equation derived in [27]:

$$m^1 \rho(t) = \frac{\int_{-\infty}^{+\infty} f \rho(t, f) df}{\int_{-\infty}^{+\infty} \rho(t, f) df} = \frac{1}{2\pi} \frac{\int_{-\infty}^{+\infty} G(u - t, 0) \operatorname{Im}\left[\frac{dz}{dt}\right] z^*(u) du}{\int_{-\infty}^{+\infty} G(u - t, 0) |z(u)|^2 du}. \quad (9.36)$$

If  $G(u - t, 0)$  equals  $\delta(u - t)$  as is the case for the WVD, or if  $G(u - t, 0)$  equals a linear combination of  $\delta(u - t)$  (Rihaczek or Cohen), this reduces to  $f_i(t)$ . (However, for positive bilinear TFDs, the function  $g(v, \tau)$  is an ambiguity function and the corresponding  $G(t, \tau)$  is a function without impulses, necessarily implying that the result will always be a smeared version of  $f_i(t)$  [28].)

Recently, Posch and Cohen [29] have defined a new class of positive TFDs that have the desired "mathematical" properties by noting that positive distributions may be included when the kernel  $g(v, \tau)$  is a functional of the signal. Considerable debate has been directed toward the usefulness of these positive bilinear TFDs, especially when it is realized that for any signal, there is an infinite number of them and that they depend on the signal itself. In the light of these factors, it appears that Posch's and Cohen's positive TFDs would be useful for analysis in only very limited and dedicated applications where data dependence of TFDs is considered to be important. In an effort to find a positive distribution to satisfy some mathematical properties, much of the physical interpretability and convenience of TFDs is lost [30].

### 9.2.3 Physical Interpretation of TFDs

Hence, because the TFDs considered for a practical time-frequency signal analysis are not positive definite, they cannot be interpreted as an instantaneous energy spectral density at time,  $t$ , and frequency,  $f$ . To relate  $\rho(t, f)$  to the physical reality of experimentation, it can be considered that  $\rho(t, f)$  is the measure of an energy flow through the spectral window  $(f - \Delta f/2, f + \Delta f/2)$  during the time interval  $(t - \Delta t/2, t + \Delta t/2)$  [5]. The signal energy localized in this time-frequency domain,  $(\Delta t, \Delta f)$ , is then given by:

$$E_{\Delta t, \Delta f} = \int_{t - \Delta t/2}^{t + \Delta t/2} \int_{f - \Delta f/2}^{f + \Delta f/2} \rho(t, f) \cdot dt \cdot df \quad (9.37)$$

provided that  $\Delta t \cdot \Delta f$  satisfies the *Heisenberg uncertainty relation*:  $\Delta t \cdot \Delta f \geq 1/4\pi$ . Note that because it is a gradient of energy, the TFD may have positive and negative values, but the integral over any domain  $(\Delta t, \Delta f)$  wider than the minimum Heisenberg's area is in general positive valued for the class of signals considered [31], [32], [33]. This question is discussed in detail in [30b]. In practice, the domain  $(\Delta t, \Delta f)$  corresponds to the elementary cell defined in Section 9.1.3, of size  $[T_r(t), B_d(f)]$ .

The interpretation of a TFD as an energy gradient representation is particularly clear in the case of Page's distribution (Table 9.1), it being defined as the gradient of the running spectrum.

#### 9.2.4 Comparison of TFDs

One measure for the performance of a signal analysis tool based on TFDs is the resolution and accuracy provided by that TFD when used for determination of the frequency modulation law of a monocomponent signal. The best TFD may be considered as the one that allows the best and simplest estimation of this law. Such a tool is also expected to track the multiple laws of a multicomponent signal accurately, such as, for example, the linear combination of several FM signals. It should also be possible to determine easily the time-varying nature of the impulse response of a system with deterministic or stochastic excitation. Additionally, it is desirable that the chosen method be robust when the signals under analysis are observed with additive noise.

A signal well suited for this comparison is the chirp signal of (9.5), as this signal is a good model for a large number of natural signals, and allows explicit calculations. It belongs to the class of asymptotic signals (if  $BT$  is large, as is the case with most natural applications of this signal) and its frequency modulation law is given by its instantaneous frequency,  $f_i(t)$ . It is commonly used in radar, sonar and seismic surveying. In the latter case, it is referred to as a *Vibroseis signal*. It is a generally accepted view that any TFD that does not perform well for such a signal is of little use to a signal analyst.

##### Example:

The analytic signal associated with the chirp is expressed as

$$z(t) = \Pi_T(t - T/2) e^{j\phi(t)} \quad (9.38)$$

where

$$\phi(t) = 2\pi(f_c \cdot t + \alpha \cdot t^2/2).$$

In this case, the instantaneous frequency is given by

$$f_i(t) = f_c + \alpha t; B = \alpha \cdot T.$$

Figure 9.10 shows that the WVD exhibits an amplitude concentration along a curve representing the instantaneous frequency law of the signal, that is, its frequency modulation law. The degree of energy concentration about this curve is proportional to the

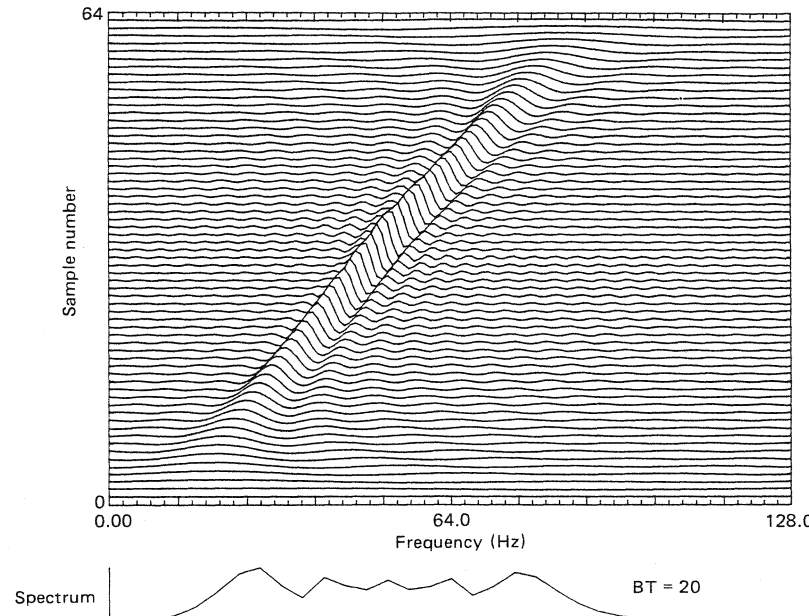


Figure 9.10 WVD of a chirp signal.

value of the  $BT$  product [34]. (See Fig. 9.6.) A sufficiently good resolution is obtained for  $BT > 5$  [8]. On the other hand, Rihaczek's TFD, defined as [10]

$$R_z(t, f) = \text{Re}[z(t)Z^*(f)e^{-j2\pi ft}], \quad (9.39)$$

does not exhibit directly the instantaneous frequency law of the signal, but shows numerous oscillations that render the reading of the representation very difficult and almost impossible if the analyzed signal is disturbed by noise [5]. (See Fig. 9.11.)

In both cases, though, the first-order moments will yield  $f_i(t)$  and  $\tau_g(f)$ . This is explained by the fact that in both cases, the TFD has *stationary phase* around the curve,  $f = f_i(t)$  [5]; that is, the TFD is highly oscillatory everywhere in the time-frequency domain except about the IF law of the signal — if the TFD is integrated, the contributions will be zero everywhere except where the stationarity occurs. For a practical analysis, the WVD is preferred to Rihaczek's TFD since it allows the estimation of the instantaneous frequency by simple peak detection, and provides at least a good initial indication of the time-frequency behavior of the signal under analysis.

If the WVD is compared with the STFT defined in (9.21), we find that, as indicated in Section 9.1, any analysis procedure based on the latter should be iterative. (Note the poor performance in Fig. 9.12 for long windows.) The analysis pro-

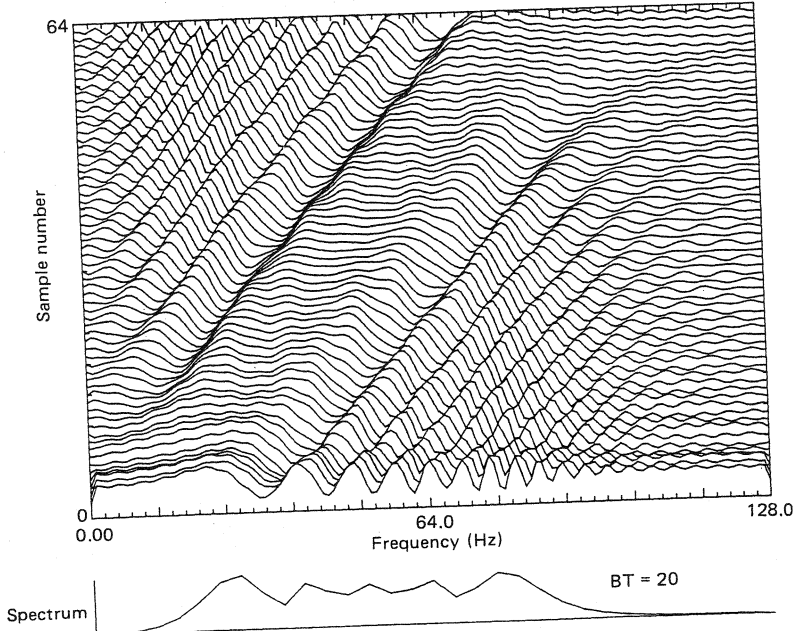


Figure 9.11 Rihaczek distribution of a chirp signal.

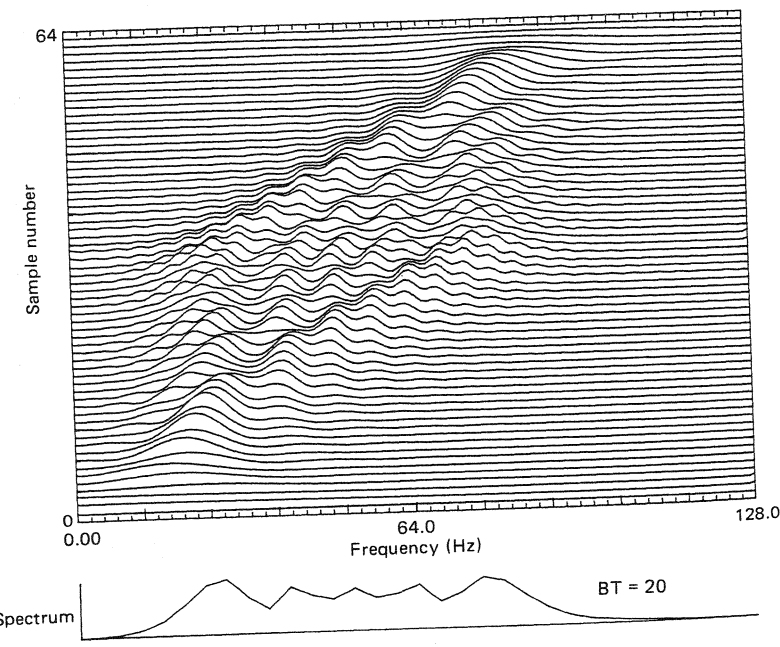


Figure 9.12 STFT of a chirp signal with large window.

cedure also introduces a bias on the estimation of the time-frequency laws of the signal [8]. Even in the optimum case (shown in Fig. 9.13), the STFT energy concentration remains inferior to that of the Wigner-Ville distribution [8]. The filtering operation needed to be performed on the WVD to obtain an STFT results in this case in a smearing and degraded resolution capability.

The Cohen representation displayed in Fig. 9.14 correctly concentrates the energy about the  $f_i(t)$  law, both by visual inspection and through its first moment, but the concentration is significantly poorer than with the WVD (i.e., compare Fig. 9.14 with Fig. 9.10). Similarly, the Choi-Williams distribution, which was introduced largely because of its good performance on multicomponent signals, yields accurately the time-frequency laws (see Fig. 9.15), but does not provide concentration comparable with the WVD.

The preceding comparison suggests that among the TFDs considered, the WVD is the most desirable tool for time-frequency analysis, at least for the class of asymptotic signals. It is not ideal, but it is the closest to the intuitive idea that signal analysts have of a time-frequency distribution, and is therefore currently the best available time-frequency analysis tool for the class of signals of interest. (For multicomponent signals, the Choi-Williams Distribution provides a good compromise between component separability and concentration [20]). In considering the general usefulness of

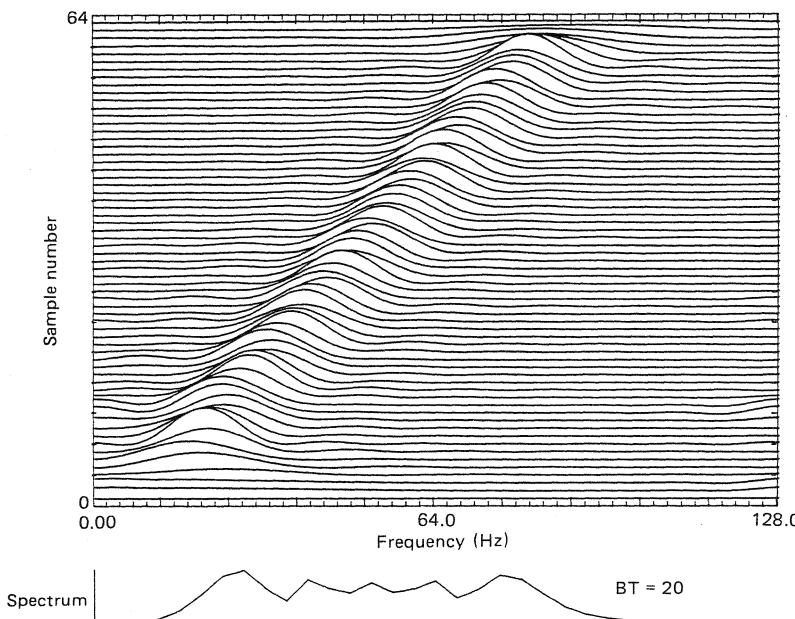


Figure 9.13 STFT of a chirp signal with optimal window.



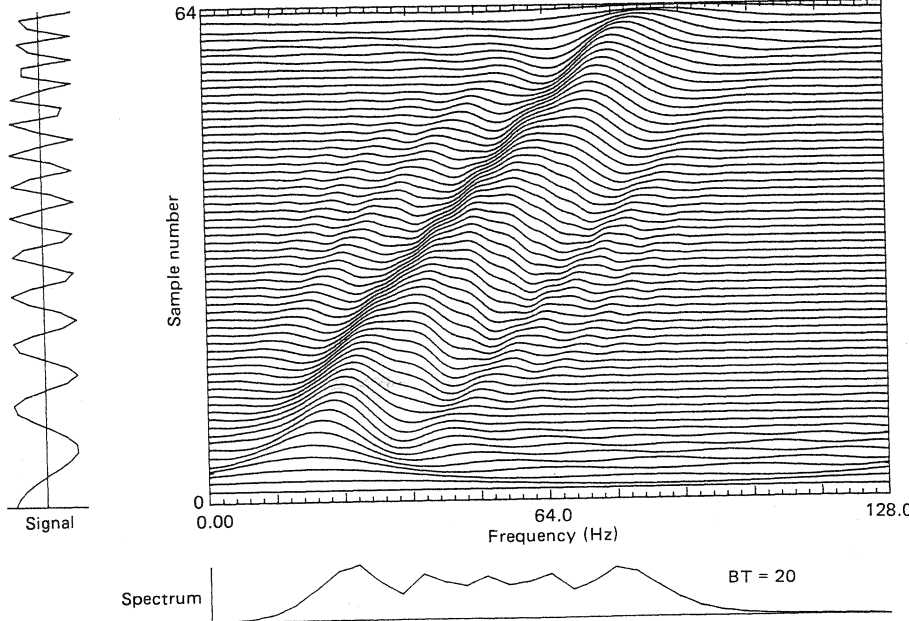


Figure 9.14 Cohen distribution of a chirp signal (also referred to as Born-Jordan).

the WVD, however, it is important to look at the properties of discrete-time TFDs and their ease of implementation. This is dealt with next.

### 9.2.5 Discrete-Time TFDs: Implementation, Comparison, and Choice

This section examines discrete implementation of Cohen's class of TFDs. The discrete-time definition equivalent to the time-lag definition given in (9.27) leads to the easiest implementation of a TFD and is expressed as

$$\rho_z(n, k) = \mathcal{F}_{m \rightarrow k} [G(n, m)]_n^* K_z(n, m), \quad (9.40)$$

which can be expressed as

$$\rho_z(n, k) = \sum_{m=-M}^M \sum_{p=-M}^M G(p-n, m) z(p+m) z^*(p-m) e^{-j4\pi mk/N}, \quad (9.41)$$

where  $\rho_z(n, k)$  denotes the discrete time convolution.

The discrete real signal,  $s(n\Delta t)$ , is formed by sampling  $s(t)$  at frequency  $f_s =$

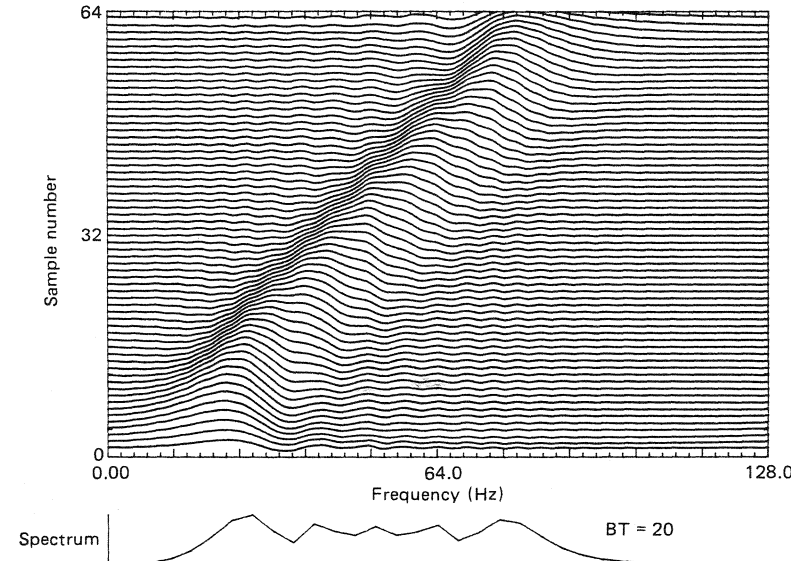


Figure 9.15 Choi-Williams distribution of a chirp signal.

$1/\Delta t$ , such that  $t = n \cdot \Delta t$  and  $f = k \cdot \Delta f = k \cdot f_s/N$ ,  $N$  = signal length, and  $M = (N - 1)/2$ ;  $G(n, m)$  represents the sampled  $G(t, \tau)$ . For simplicity and without any loss of generality, it is assumed that  $\Delta t = f_s = 1$ .

Equations (9.40) and (9.41) indicate that the implementation of a TFD requires three steps:

1. Formation of the bilinear product  $K_z(n, m) = z(n + m)z^*(n - m)$ .
2. Discrete convolution in the  $n$  (time) direction.
3. Discrete FT with respect to  $m$ .

The WVD is the only TFD that does not require step 2 because its determining function  $G(n, m)$  equals  $\delta(n)$ .

#### Desirable Properties of Discrete TFDs

To be useful as a tool for time-frequency signal analysis, a discrete-time TFD must preserve the desirable properties of TFDs listed previously. The constraints on  $G(n, m)$  are derived from those on  $g(v, \tau)$  and (9.28) to (9.35) become [35]:

*Property 2–6.* The TFD must be real-valued; this imposes the condition

$$G(n, m) = G^*(-n, -m). \quad (9.42)$$

*Property 2–7.* The marginals of the distribution should be equal to the spectrum and instantaneous power:

$$\sum_{n=0}^{N-1} \rho_z(n, k) = |Z(k)|^2 \quad (9.43)$$

$$\sum_{k=0}^{N-1} \rho_z(n, k) = |z(n)|^2 \quad (9.44)$$

This is obtained if

$$G(n, 0) = \delta(n) \quad \text{and} \quad \sum_{n=0}^{N-1} G(n, m) = 1, \quad (9.45)$$

where  $\delta(n)$  is the discrete-time delta function.

*Property 2–8.* The representation should be zero outside the time and frequency regions where the signal is present:

$$\rho_z(n, k) = 0 \text{ when}$$

$$z(n) = 0 \text{ for } n < n_1 \text{ and } n > n_2, \quad (9.46)$$

$$Z(k) = 0 \text{ for } k < k_1 \text{ and } k > k_2.$$

This requires that

$$G(n, m) = 0 \text{ for } |n| > |m|. \quad (9.47)$$

*Property 2–9.* The normalized periodic first moment in frequency of the TFD should yield the instantaneous frequency (for the discrete IF as defined in Section 9.4.1). This imposes the conditions

$$G(n, 0) = \delta(n) \quad \text{and} \quad G(n, 1) = \delta(n) \quad (9.48)$$

TFDs for which Properties 2–6 to 2–9 are verified are said to be members of the class  $\mathcal{P}$ .

### Butterfly Functions

Accounting for all the constraints on the shape and magnitude of the kernel, the shaded section of Fig. 9.16 indicates the region in the time-lag plane where the kernel function must be zero. The  $G(n, m)$  functions describing the TFDs which are members of  $\mathcal{P}$  will be referred to as the Butterfly functions, since the time-lag kernel represents a butterfly pattern in the time-lag plane. These functions are also referred to as cone-shaped kernel in [35b], where a detailed discussion is given. Table 9.2 lists  $G(n, m)$  for the most common TFDs. Each  $G(n, m)$  is plotted in Figs. 9.17(a)–(f). The concept is useful because many qualitative characteristics of TFD behavior can be inferred directly from  $G$ , as illustrated.

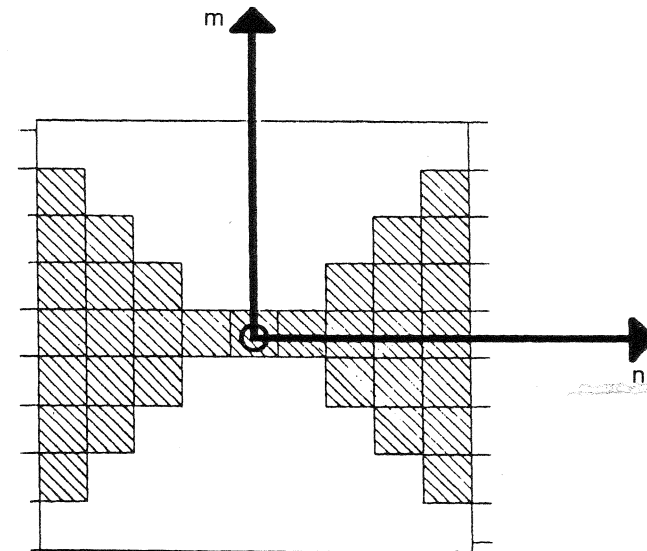


Figure 9.16 Shape of time-lag kernel functions satisfying the desirable properties of a discrete TFD.

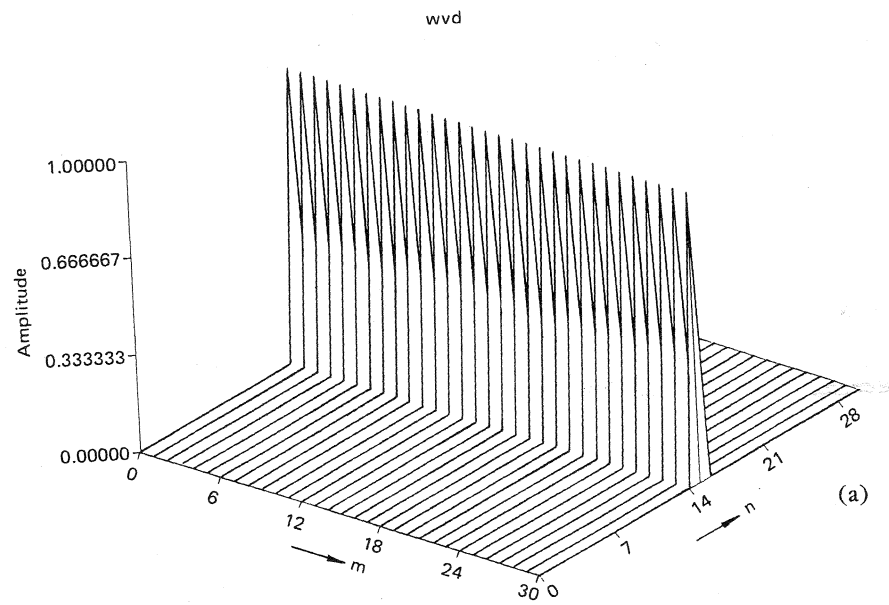
TABLE 9.2 Popular TFDs and  $G(n, m)$ .

Time-Frequency Representation	$G(n, m)$
Windowed discrete WVD	$\delta(n), m \in [-(M-1)/2, (M-1)/2]$ 0, otherwise
Smoothed WVD using a rectangular window of odd length $P$	$\frac{1}{P}, n \in [-(P-1)/2, (P-1)/2]$ 0, otherwise
Rihaczek-Margenau	$\frac{1}{2} [\delta(n+m) + \delta(n-m)]$
STFT using a rectangular window of odd length $P$	$\frac{1}{P},  m+n  \leq (P-1)/2$ 0, otherwise
Cohen	$\frac{1}{ m +1},  m  \leq  n $ 0, otherwise
Choi-Williams (with parameter $\sigma$ )	$\frac{\sqrt{\sigma/\pi}}{2m} e^{-\sigma n^2/4m^2}$

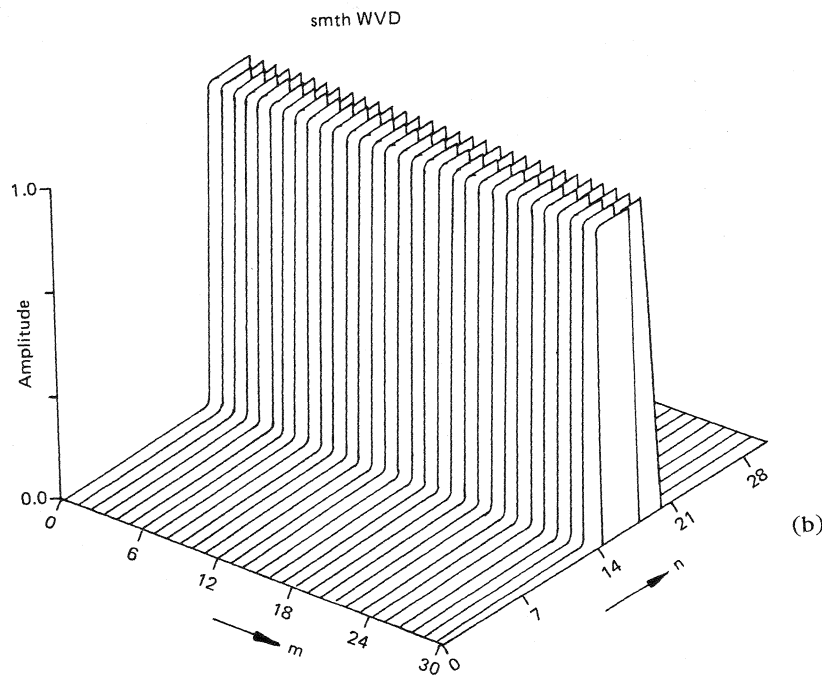
## Sec. 9.2 Time-Frequency Signal Analysis

448

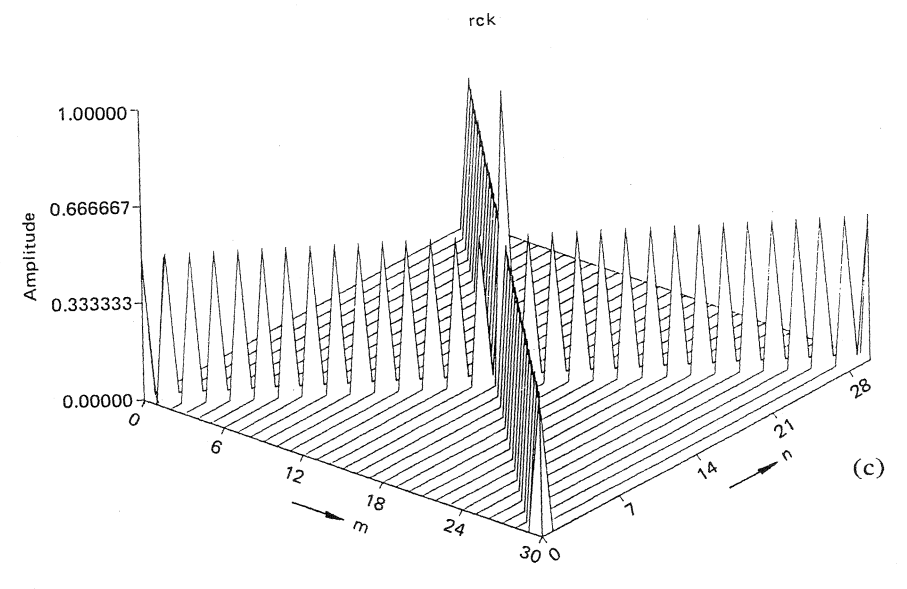
## Time-Frequency Signal Analysis Chap. 9



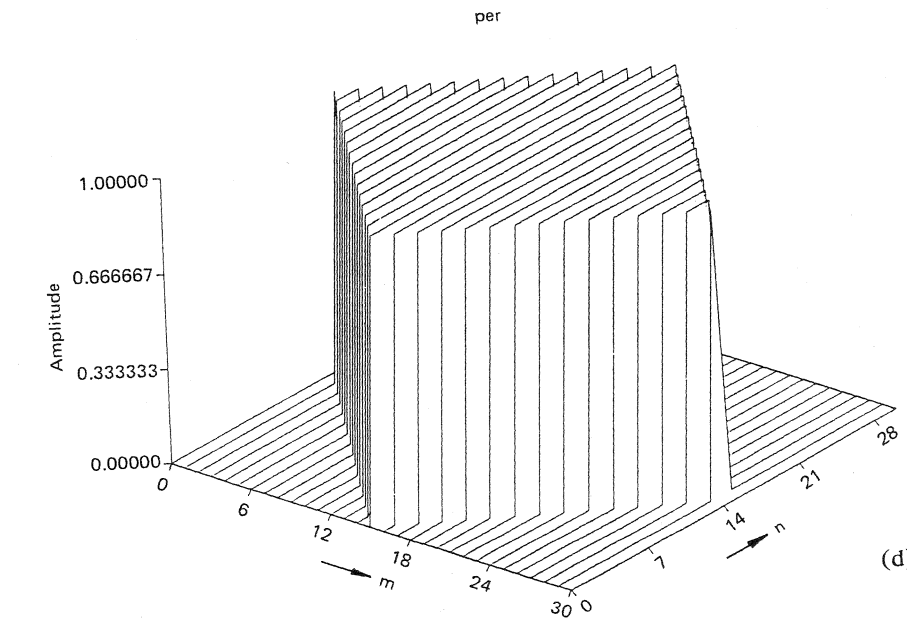
(a)



(b)



(c)



(d)

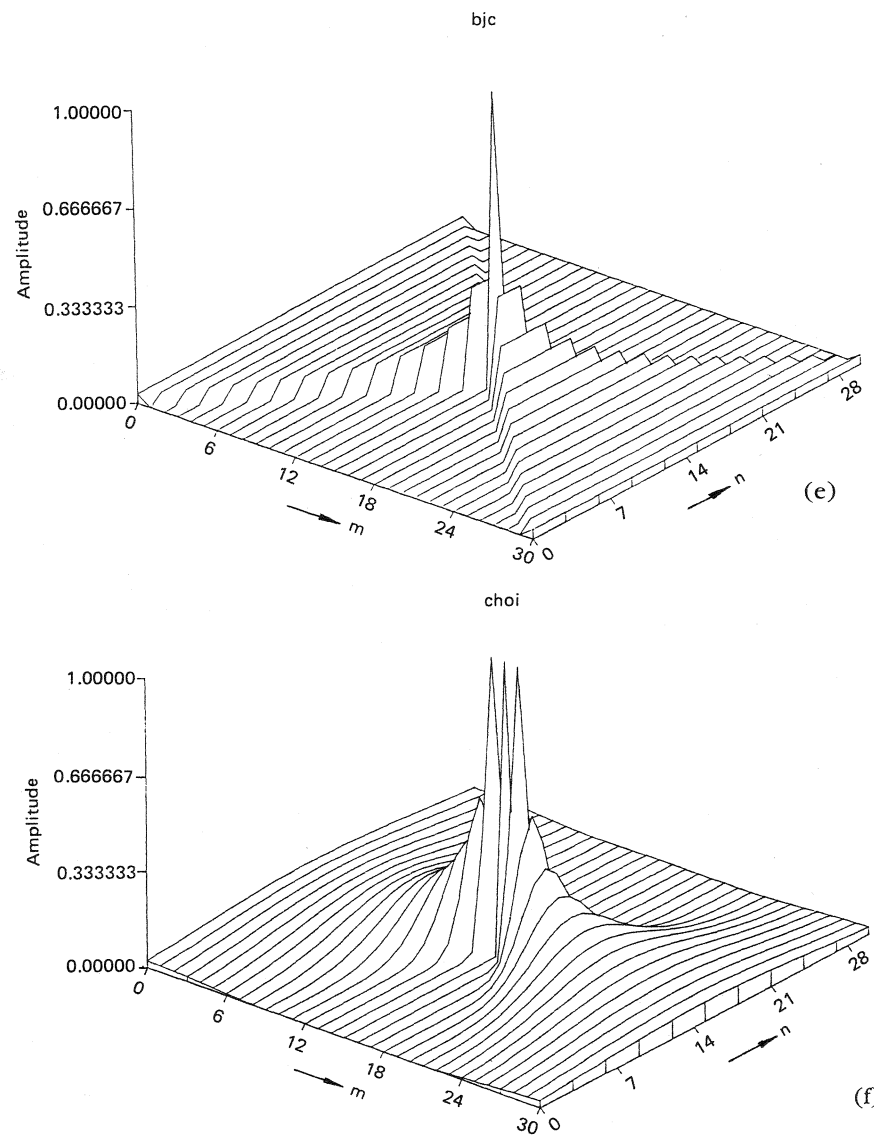


**Figure 9.17** Plots of the time-lag kernel functions  $G(n, m)$  for various discrete TFDs. (a) Windowed WVD, (b) smoothed windowed WVD, (c) Rihaczek, (d) STFT, (e) Cohen (Born-Jordan), (f) Choi-Williams.

**1. Energy Concentration.** For the distribution to exhibit a high-energy concentration about the IF law of a signal, the kernel function must be concentrated about the  $n = 0$  axis. The kernel function of the discrete WVD is only nonzero along this axis, so it will exhibit this property. The Choi-Williams distribution will also give high concentration for large values of the  $\sigma$  parameter.

**2. Artifacts.** The shape of the artifacts of TFDs is given by the cross section of  $G(n, m)$  in the  $n$  direction (with a constant value of  $m$ ). This occurs only when the discrete kernel function  $g(\ell, m)$  corresponding to  $g(v, \tau)$  is a product kernel, that is, when  $g(\ell, m)$  is a separable function in  $\ell$  and  $m$ , such as  $g(\ell, m) = g_1(\ell)g_2(m)$ .

The discrete WVD, Cohen, and Choi-Williams distributions artifact shapes will all be given by the cross section of the kernel function. The artifacts of the STFT, for which the kernel function  $g(v, \tau)$  or  $g(\ell, m)$  shown in Tables 9.1 and 9.2, is not a product kernel, must be calculated differently [9]. The STFT artifacts are superimposed on the true spectral components and cause them to oscillate or jitter slightly; they are much smaller in magnitude than are the true components [15].

The preceding discussion implies that there is necessarily a trade-off between energy concentration (mainlobe width) and artifact magnitude. (see Fig. 9.17).

#### The Choice of a Discrete TFD for Time-Frequency Signal Analysis

The shape of  $G(n, m)$  allows the properties of a TFD to be predicted. The desirable Properties 2-6 to 2-9 are verified if  $G(n, m)$  is a desirable Butterly function. Other properties, such as energy concentration and artifact shape (for product ambiguity kernel functions) may also be found from  $G(n, m)$ .

The only discrete TFDs that satisfy all Properties 2-6 to 2-9 are the windowed discrete WVD and the Choi-Williams distribution (for large  $\sigma$ ). Although the Cohen distribution gives the IF law exactly in the continuous case, the discrete Cohen distribution does not satisfy Property 2-9 exactly, if the *central finite difference* (see Section 9.4.1) estimator of the discrete instantaneous frequency is used; its periodic first moment in frequency will give a smoothed (three-point moving average filtered) version of the true IF law.

In the case of a monocomponent signal, the WVD gives the greatest energy concentration about the frequency law. In the case of multicomponent signals, the Choi-Williams distribution or Cohen distribution might be a better choice because they have reduced artifacts, but they exhibit poor energy concentration. In some applications it might be acceptable to tolerate a certain degradation in energy concentration. In this case the Choi-Williams distribution could be advantageous. The standard approach is to use the STFT to help separate the different components of the multicomponent signal and then to use the WVD.

Another method of reducing artifacts is to use windowed versions of TFDs. The analysis window limits the extent to which a TFD is affected by occurrences in the signal, both in the future and distant past, and thus reduces or eliminates the artifacts that arise between components at different times.

### 9.3 THE WIGNER-VILLE DISTRIBUTION

#### 9.3.1 Definition and Properties

Letting  $g(v, \tau) = 1$  in (9.24) defines the WVD of a signal  $s(t)$  as follows:

$$W(t, f) = \int_{-\infty}^{+\infty} z(t + \tau/2) z^*(t - \tau/2) e^{-j2\pi f\tau} d\tau, \quad (9.49)$$

where  $z(t)$  represents the analytic signal associated with  $s(t)$ . The WVD can also be expressed from the spectrum of the signal under analysis, as follows:

$$W(t, f) = \int_{-\infty}^{\infty} Z(f + v/2) \cdot Z^*(f - v/2) e^{j2\pi vt} dv. \quad (9.50)$$

The interesting properties of the WVD with regard to time-frequency signal analysis are summarized below:

*Property 3-1.*  $W(t, f)$  is a member of Cohen's class.

*Property 3-2.*  $W(t, f)$  is real for all values of  $t$  and  $f$  and can therefore represent the variations in energy. (Note that the ambiguity function is complex even for real signals.)

*Property 3-3.*  $W(t, f)$  satisfies the marginals (see (9.29) and (9.30)). Some TFDs like the spectrogram can at best only evaluate smeared versions of the true quantities.

*Property 3-4.* The first moments of the WVD yield directly the instantaneous frequency,  $f_i(t)$ , and the time delay,  $\tau_g(f)$ , of the signal. The WVD estimator of  $f_i(t)$  is independent of the windowing applied to the WVD, assuming that some nonrestrictive conditions on the window are met [36]. This property was used in the work reported in [22].

*Property 3-5.* The WVD directly displays the instantaneous frequency,  $f_i(t)$  and time delay,  $\tau_g(f)$ , by exhibiting a range of peaks along the curve described by  $f_i(t)$  and  $\tau_g(f)$  [5]. This property was used in [37], [38].

*Property 3-6.* The spectral extent of the WVD reflects the bandwidth of the signal. The maximum frequency,  $f_m$ , of the signal can be localized in time as the maximum frequency at that time instant, and one can follow the fluctuations of  $f_m$  with time in the WVD time-frequency plane. This property was used in [22].

*Property 3-7.* The time-frequency support of  $W(t, f)$  is given by the spectral bandwidth and the duration of the asymptotic signal:

If  $z(t) = 0$  for  $t < T_1$  and  $t > T_2$ , then  $W(t, f) = 0$  for  $t < T_1$  and  $t > T_2$ . (9.51)

If  $Z(f) = 0$  for  $f < f_1$  and  $f > f_2$ , then  $W(t, f) = 0$  for  $f < f_1$  and  $f > f_2$ .

*Property 3-8.* The WVD is time and frequency invariant, so that similar shifts to those in the signal are introduced in the WVD:

$$\begin{aligned} \text{If } x(t) = z(t - t_0), \text{ then } W_X(t, f) &= W_Z(t - t_0, f). \\ \text{If } x(t) = z(t) \cdot e^{j2\pi f_0 t}, \text{ then } W_X(t, f) &= W_Z(t, f - f_0) \end{aligned} \quad (9.52)$$

*Property 3-9.* Time convolution of two signals results in time convolution in the Wigner-Ville plane,

$$\begin{aligned} \text{If } y(t) = z(t) * b(t), \text{ then } W_Y(t, f) &= W_Z(t, f) \underset{(t)}{*} W_B(t, f), \\ \text{where } \underset{(t)}{*} \text{ denotes convolution in the continuous time domain.} \end{aligned} \quad (9.53)$$

*Property 3-10.* There is a similar relation for modulation:

$$\begin{aligned} \text{If } y(t) = m(t) \cdot z(t), \text{ then } W_Y(t, f) &= W_Z(t, f) \underset{(f)}{*} W_M(t, f), \\ \text{where } \underset{(f)}{*} \text{ denotes convolution in the continuous frequency domain.} \end{aligned} \quad (9.54)$$

Properties 3-9 and 3-10 show that use of the WVD is compatible with linear filtering theory.

*Property 3-11. Invertibility of the WVD.* Given the WVD,  $W(t, f)$ , of a signal,  $z(t)$ , it may be shown that [39]

$$\int_{-\infty}^{\infty} W_Z(t/2, f) e^{j2\pi ft} df = z(t) z^*(0). \quad (9.55)$$

The signal may be uniquely recovered, to within a complex scaling factor  $z^*(0)$ , from the WVD. This shows that the WVD contains and conveys all the information carried by the signal. No information is lost. This property is useful for signal synthesis in the WVD plane (see Section 9.7).

*Property 3-12.* The two-dimensional FT of the WVD of a signal is its Sussman ambiguity function [25]. This is a consequence of (9.25):

$$W_Z(t, f) \xleftrightarrow[t]{\quad} A_Z(v, \tau) \xleftrightarrow[f]{\quad} \quad (9.56)$$

#### 9.3.2 Instantaneous Frequency, Average Frequency, and the WVD

In this section, it is intended to provide further insight into the physical meaning of instantaneous frequency and to try to relate it to more traditional concepts. Consider a basic waveform,  $s(t)$ , with constant frequency,  $f_0$ , such that

$$s(t) = \cos(2\pi f_0 t + \Psi) = \cos \phi(t), \quad (9.57)$$

where  $\Psi$  is a constant and  $\phi(t)$  is the phase of the signal. The carrier frequency,  $f_0$ , of  $s(t)$  is usually defined by

$$f_0 = \frac{\int_0^{+\infty} f |S(f)|^2 df}{\int_0^{+\infty} |S(f)|^2 df}, \quad (9.58)$$

where  $|S(f)|^2$  is the energy density spectrum of  $s(t)$ . Property 3-4 stipulates that the expression of  $f_i(t)$  given in (9.7) can be evaluated by a direct extension of (9.58). This is achieved by replacing  $|S(f)|^2$  with  $W_z(t,f)$  when the signal has a "time-varying frequency content" that is denoted by  $f_i(t)$ ; that is,

$$f_i(t) = \frac{\int_0^{\infty} f W_z(t,f) df}{\int_0^{\infty} W_z(t,f) df}. \quad (9.59)$$

Considering the signal of (9.57), it can be easily derived that  $W_z(t,f) = \delta(f - f_0)$ . Application of (9.59) gives  $f_i(t) = f_0$ , and in this case (9.58) and (9.59) represent the same quantity. If another signal that has a "time-varying frequency content" is chosen, such as FM signals, then (9.58) is not as revealing and one should use (9.59) to obtain an accurate time-varying spectral representation of the signal. Property 3-4 and (9.59) suggest that the instantaneous frequency of the signal,  $s(t)$ , can be interpreted as the frequency of a monochromatic waveform that fits locally at time,  $t$ , the time-varying signal under consideration.

This parameter,  $f_i(t)$ , plays a major role in many engineering applications. It can be seen from the above-mentioned properties that it has meaning only for asymptotic monocomponent signals. It will be seen in Section 9.7, however, that the WVD can be used for breaking up a multicomponent signal as a combination of monocomponent signals, each one characterized by its own instantaneous frequency [9].

### 9.3.3 The Analytic Signal: A Necessity

The Wigner distribution (WD) should always be used in conjunction with the analytic signal for an effective time-frequency analysis of signals [40]. To see the importance of using the analytic signal, consider the WD defined by

$$W_s(t,f) = \int_{-\infty}^{+\infty} s(t + \tau/2) s^*(t - \tau/2) e^{-j2\pi f\tau} d\tau, \quad (9.60)$$

where  $s(t)$  is the real signal to be analyzed. This distribution differs from the Wigner-Ville distribution by its use of the real signal,  $s(t)$ , instead of the analytic signal,  $z(t)$ .

The relationship between the Wigner distribution and Wigner-Ville distribution is [40]:

$$W_s(t,f) = \frac{1}{4} [W_z(t,f) + W_z(t,-f)] + \gamma(t,f), \quad (9.61)$$

where  $\gamma(t,f)$  represents the interaction terms between positive and negative frequencies as given in [40] and is oscillatory in nature. For example, if  $s(t)$  is the chirp signal of (9.5), then [5]

$$\gamma(t,f) = \frac{1}{\sqrt{2\alpha}} \cdot \Pi_T(t) \cdot \Pi_{B'}(f) \cdot \cos 2\pi \left( \frac{f^2}{\alpha} - 2f_0 t - \alpha t^2 - \frac{1}{8} \right), \quad (9.62)$$

where  $B' = B(1 - 2|t|/T)$  and  $\alpha = B/T$ .

The WD of a linear FM (Fig. 9.18a) exhibits a pattern that is characteristic of the frequency modulation law of the signal, plus another oscillatory pattern located lower in the spectral domain. Figure 9.18(b) represents the WVD of the same signal. It contains only the one pattern that is of interest, the one that contains the useful information.

The low-frequency artifacts appearing in the WD have no physical meaning in themselves and should be removed [40]. The same comment applies to Fig. 9.18(c) and Fig. 9.18(d), which show the WD and WVD of an hyperbolic FM signal. It is therefore recommended that the original formulation proposed by Ville in 1948 [4] be used to avoid unnecessary distortion effects. Another reason for retaining the analytic signal in Ville's formulation of the WVD is that it avoids the need for oversampling, as would be required for the real signal [40], [41].

### 9.3.4 Implementation of the Discrete WVD

Equation (9.49) defining the WVD indicates that evaluation of the WVD is a noncausal operation, as is the evaluation of the Fourier transform or Hilbert transform. Since the signals considered have a finite duration, this problem is easily overcome by introducing a delay. If the delay acceptable to the analyst is much smaller than the duration of the signal, then an estimation procedure can be defined by applying the WVD to a windowed version of the signal,  $z(t)$ , at time,  $t_0$ , such that

$$z_w(t, t_0) = z(t)w(t - t_0). \quad (9.63)$$

This is equivalent to applying a positive, real window function,  $g(\tau)$ , of finite length,  $\Delta$ , to the bilinear term in the integrand and the resultant time-frequency representation will be denoted the windowed WVD (sometimes called the pseudo-Wigner distribution). If the window length is denoted by  $\Delta$ , then  $g(\tau) > 0$  for  $\tau \in (-\Delta/2, +\Delta/2)$  and zero elsewhere. The windowed WVD is suitable for real-time processing, since it is only necessary to know  $z(t)$  within the window. Another advantage of the windowing is that nonrectangular windows (such as the Hamming window) can be used to reduce sidelobe level and improve interpretation. The window is given by [42]

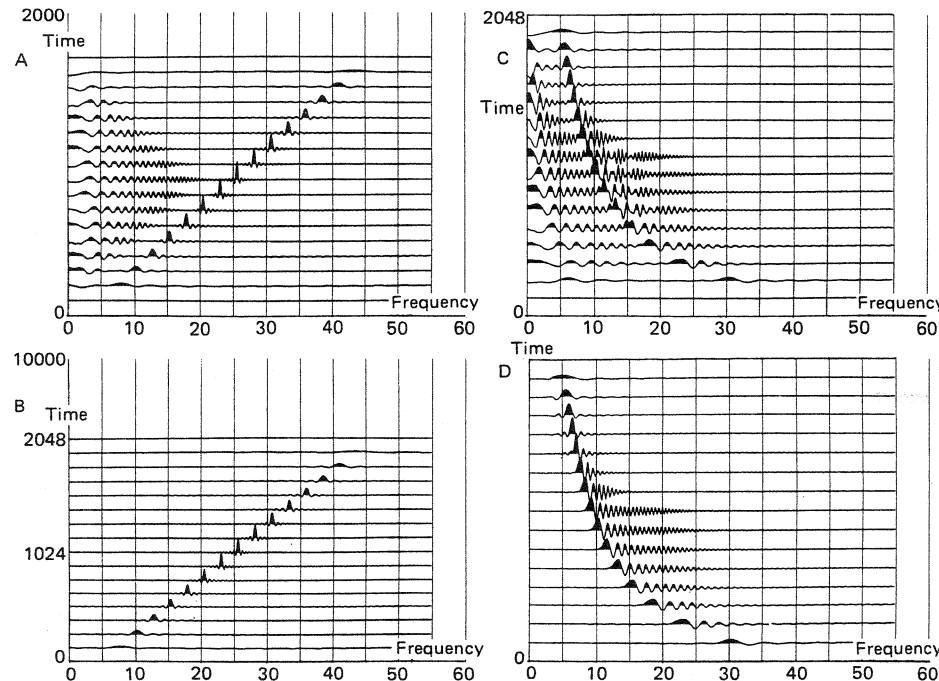


**Figure 9.18** Importance of using the analytic signal in the Wigner-Ville distribution. (a) A chirp signal, without analytic signal; (b) a chirp signal, with analytic signal; (c) a hyperbolic FM signal, without analytic signal; (d) a hyperbolic signal, with analytic signal.

$$g(\tau) = w(\tau/2)w^*(-\tau/2), \quad (9.64)$$

where  $w(\tau)$  is also of length,  $\Delta$ , and corresponds to the actual window applied to  $z(t)$ . The term  $g(\tau)$  is called the effective window since the resulting frequency resolution is directly related to the spectrum of  $g(\tau)$ . Using the concept of effective window, the wealth of knowledge on window functions for Fourier spectral analysis may be directly applied to the windowed WVD [43], [44].

#### Continuous Windowed WVD

The continuous form of the windowed WVD of a finite-energy real signal,  $s(t)$ , is defined by

$$W_z(t, f) = \int_{-\Delta/2}^{+\Delta/2} g(\tau)z(t + \tau/2)z^*(t - \tau/2)e^{-j2\pi f\tau} d\tau, \quad (9.65)$$

where  $g(\tau)$  is the positive real window function of length  $\Delta$  such that  $g(\tau) > 0$  for  $\tau \in [-\Delta/2, +\Delta/2]$  and zero elsewhere. The windowed WVD is also referred to as the pseudo WVD.

The kernel,  $K_z$ , has previously been defined as  $K_z(\tau) = z(t + \tau/2)z^*(t - \tau/2)$ . The WVD at any point in time is evaluated by shifting the analytic signal,  $z(t)$ , so that the window is centered about  $t = 0$ . Therefore, the WVD computation reduces to the evaluation of

$$W_z^0(t = 0, f) = \int_{-\Delta/2}^{+\Delta/2} K_z(\tau)g(\tau)e^{-j2\pi f\tau} d\tau, \quad (9.66)$$

which defines  $W_z^0$  as an approximation of  $W_z$  and where  $\Delta$  represents the effective window width. Hence, the estimation of the WVD reduces to the computation of the FT of a signal,  $K_z(\tau)$ , with analysis window,  $g(\tau)$ , which is a classical problem of signal analysis. The discrete-time equivalent forms for the WVD and windowed WVD are defined below.

#### Discrete WVD

The *Discrete Wigner-Ville distribution (DWVD)* with discrete frequency variable is defined for a discrete time signal of length,  $N'$ , band-limited to  $f_m$  by

$$W(n, k) = 2 \sum_{m=-(N-1)/2}^{(N-1)/2} z(n+m) z^*(n-m) e^{-j4\pi mk/N} \quad (9.67)$$

where  $N = N'$  for  $N'$  odd and  $N = N' + 1$  for  $N'$  even;  $0 \leq n \leq N'$ ,  $0 \leq k \leq N$ ,  $-(N-1)/2 \leq m \leq (N-1)/2$ ; and  $n$ ,  $k$ , and  $m$  are the discrete variables corresponding to the continuous variables  $t$ ,  $f$ , and  $\tau$ .

The discrete-time quantities can be converted to the corresponding continuous-time quantities by the following transformations:

$$f = \frac{f_s k}{2N}, \quad t = \frac{n}{f_s}, \quad \text{and } \tau = \frac{m}{f_s}, \quad (9.68)$$

where  $f_s$  is the sampling frequency which must be at least  $2f_m$  to satisfy the Nyquist criterion, where  $f_m$  is the maximum global frequency of the signal.

The quantity  $N$  represents the number of frequency samples in the distribution for each time  $n$ . Thus the DWVD may be represented by an  $N'$  by  $N$  real matrix. A windowed DWVD can be defined by applying a discrete window,  $g(m)$ , of odd length,  $M$ , to the bilinear term in the summand, such that

$$g(m) = w(m)w^*(m), \quad (9.69)$$

where  $w(m)$  is of length  $M$ .

#### Windowed DWVD

The windowed DWVD with discrete frequency variable is defined for a discrete-time signal of length  $N'$  band-limited to  $f_m$  by

$$W^g(n, k) = 2 \sum_{m=-(M-1)/2}^{(M-1)/2} g(m)z(n+m) z^*(n-m) e^{-j4\pi mk/M}, \quad (9.70)$$

where  $g(m)$  is a positive, real window function of odd length  $M$ . The other variables are the same as in (9.67). The discrete-time quantities can be converted to the corresponding continuous time quantities through the following relationships:

$$f = \frac{f_s k}{2M}, \quad t = \frac{n}{f_s}, \quad \text{and } \tau = \frac{m}{f_s}.$$

The quantity,  $M$ , represents the number of frequency samples in the distribution for each time,  $n$ . Thus the DWVD may be represented by an  $N$  by  $M$  real matrix. The windowed DWVD at time  $t = n/f_s$  is calculated by forming the DFT operating on the  $m$  variable of the  $M$ -point function,  $c(n, m)$ , defined by

$$c(n, m) = g(m)z(n + m)z^*(n - m), \quad 0 \leq m \leq M/2 \quad (9.71)$$

and

$$c(n, m) = g(m - M)z(n + m - M)z^*(n - m + M), \quad M/2 < m \leq M - 1. \quad (9.72)$$

The windowed DWVD only represents the positive frequencies of the corresponding windowed WVD. The negative frequency components are assumed to be zero because the analytic signal is used. This assumption causes no problems when larger analysis window lengths are used. However, with very small analysis windows, say,  $M = 17$ , the negative components can become significant and introduce aliasing errors. This problem may also occur in the nonwindowed DWVD when analyzing very short signals. Under these circumstances,  $z(n)$  can be interpolated or oversampled to reduce the problem.

As the window  $g(m)$  is real and even, the product  $g(m)z(n + m)z^*(n - m)$  presents the Hermitian symmetry that is used to reduce the storage and computational load by one-half [42]. The analytic signal,  $z(n)$ , is calculated either in the time domain using an FIR filter, or in the frequency domain as follows:

1. Take the  $N$ -point DFT of  $s(n)$  to give  $S(k)$ ,  $k = 0, N - 1$ .
2. Define

$$Z(k) = \begin{cases} S(k), & k = 0 \\ 2S(k), & k = 1, \frac{N}{2} - 1 \\ 0, & \text{otherwise.} \end{cases}$$

3. Calculate  $z(n) = \text{IDFT}[Z(k)]$ , IDFT = inverse DFT

The flowchart of the WVD implementation described in [42] is shown in (Fig. 9.19a). An alternative approach is to implement equation 9.50, i.e. calculate the WVD from its spectrum.

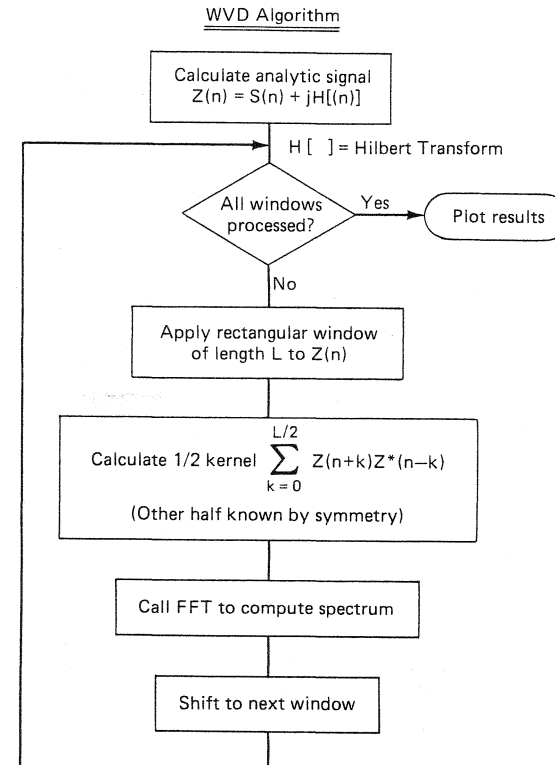


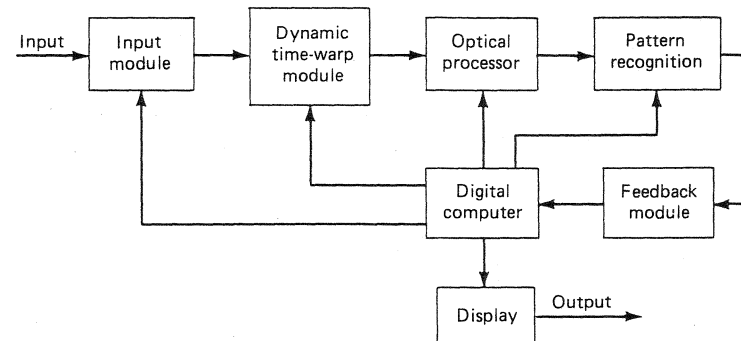
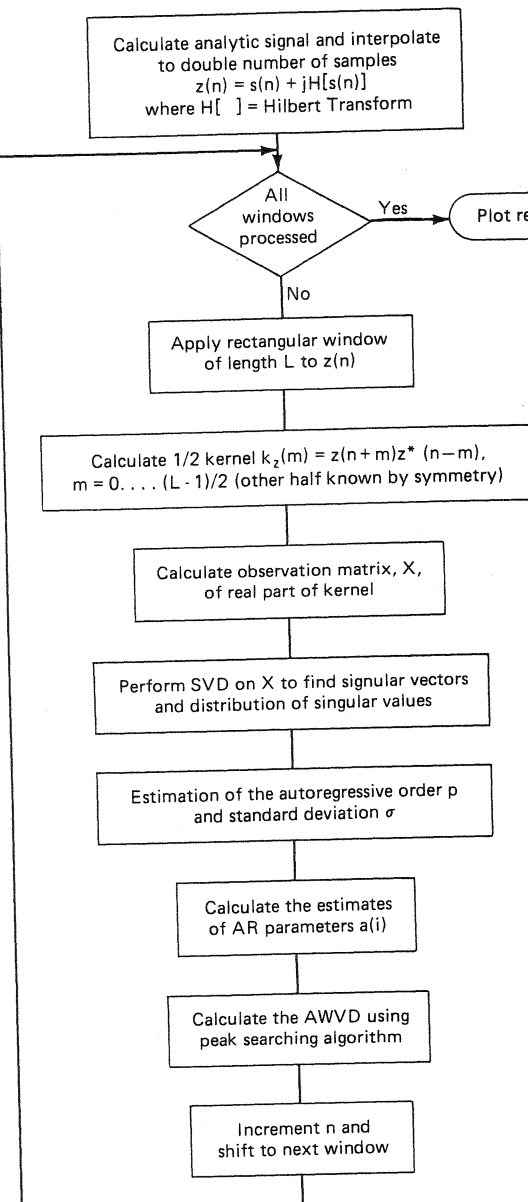
**Figure 9.19** (a) Flowchart of an algorithm implementing the WVD. (From B. Boashash and P. Black, "An Efficient Real Time Implementation of the Wigner-Ville Distribution," *IEEE Trans. Acoustics, Speech, and Signal Processing* 35:11, November 1987, pp. 1611–1618.)

### High-Accuracy WVD

For certain signals (such as FM signals), an improvement in accuracy is obtained by replacing the FT of the bilinear kernel by a high-resolution spectral analyzer such as Burg's algorithm and other autoregressive methods or any algorithm based on autoregressive modeling. The parametric WVD thus defined may achieve in some cases a highly accurate time-frequency analysis that demonstrates an enormous potential for a variety of applications, despite its computational load [45], [46], [47]. The flowchart of an autoregressive high-accuracy WVD implementation is shown in Fig. 9.19(b).

### Optical Implementation of the WVD

A digital/optical hybrid pattern recognition system, shown in Fig. 9.19(c) incorporates a high-speed optical Wigner-Ville analyser. The optical processor uses acoustooptic refractive devices and imaging optics to produce a two-dimensional spatially modulated light distribution. By use of a spatial filter of a rotated kernel of the WVD is



obtained. One-dimensional Fourier transformation of this filtered light distribution in the appropriate direction will produce the WVD. The resultant WVD is then used to correlate a reference pattern optically in real time. These correlation values are then relayed to the digital computer for estimation processing [48]. The need for such a processor arises in applications such as radar imaging. An alternative implementation was proposed by Szu in [81].

## 9.4. DISCRETE INSTANTANEOUS FREQUENCY ESTIMATION

### 9.4.1 Discrete Instantaneous Frequency

The *discrete-time analytic signal*,  $z(n)$ , associated with the real discrete time signal,  $s(n)$ , is given by

$$z(n) = s(n) + j\mathcal{H}[s(n)], \quad (9.74)$$

where  $\mathcal{H}[ ]$  is the *discrete-time Hilbert transform* defined by

$$\mathcal{H}[s(n)] = \sum_{m=-\infty}^{+\infty} \frac{2s(n-m)}{m\pi}, \quad (m \text{ odd}). \quad (9.75)$$

This definition of  $\mathcal{H}$  given in [43] describes the ideal case, but the corresponding filter is not realizable. However, realizable approximations are easily obtainable [44].

Let  $s(t)$  be a continuous-time real signal, with  $z(t)$  its corresponding analytic signal. Then the *continuous-time instantaneous frequency* of  $s(t)$  is defined by the derivative of the phase of  $z(t)$ , as shown in (9.7) and can be rewritten as

$$f_i(t) = \lim_{\delta t \rightarrow 0} \frac{1}{4\pi\delta t} (\arg[z(t + \delta t)] - \arg[z(t - \delta t)]) \bmod 2\pi, \quad (9.76)$$

where the notation mod. $2\pi$  represents a modulo  $2\pi$  operation to account for  $\arg[z(t)]$  being defined on  $[-\pi, +\pi]$ . The concept of instantaneous frequency may be extended to discrete-time signals by using the central finite difference of the phase of a discrete-time analytic signal.

Let  $s(n)$  be a discrete sequence formed by sampling the continuous time signal,  $s(t)$ , at frequency  $f_s$ . Then the *discrete instantaneous frequency (DIF)* of  $s(n)$  is defined by the central finite difference [41]:

$$f_i(n) = \frac{f_s}{4\pi} (\arg[z(n+1)] - \arg[z(n-1)]) \text{ mod.}2\pi. \quad (9.77)$$

For a noisy signal,  $\hat{s}(n) = s(n) + \epsilon(n)$ , where  $\epsilon(n)$  is a random noise sequence corrupting  $s(n)$ , we may estimate the IF of  $s(n)$  by using the DIF estimator defined by

$$\hat{f}_i(n) = \frac{f_s}{4\pi} (\arg[\hat{z}(n+1)] - \arg[\hat{z}(n-1)]) \text{ mod.}2\pi, \quad (9.78)$$

where  $\hat{z}(n)$  is the analytic signal associated with  $\hat{s}(n)$ .

The statistical properties of this estimator can be derived using expressions of periodic moments given in [49]. A flowchart of the algorithm for implementing the discrete instantaneous frequency is shown in Fig. 9.20.

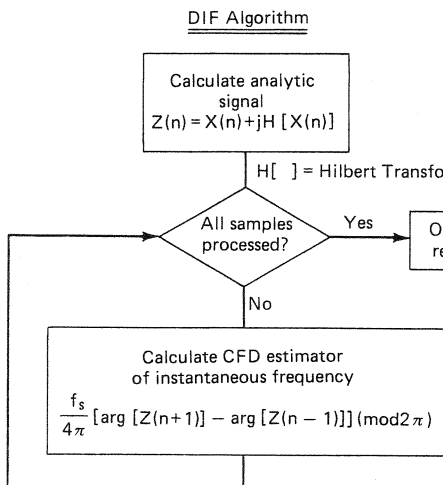


Figure 9.20 Flowchart of an algorithm implementing the discrete instantaneous frequency.

#### 9.4.2. Estimation Using the First Moment of the WVD

Discrete-time TFDs are periodic in the frequency variable, and this must be taken into account when calculating the IF as the first moment of a TFD with respect to frequency [35]. Determining the moments of this periodic function is equivalent to

finding a sensible way of averaging circular or angular data problem presented in [49].

Let  $\rho(n, k)$  be a discrete TFD from Cohen's class which may be represented by an  $N$  by  $M$  matrix. Then the periodic first moment of  $\rho(n, k)$  with respect to frequency is defined by

$$m_p^1(n) = \frac{M}{2\pi} \left\{ \arg \left[ \sum_{k=0}^{M-1} e^{j2\pi k/M} \rho(n, k) \right] \right\} \text{ mod.}2\pi \quad (9.79)$$

In the special case where  $\rho(n, k)$  is the discrete windowed WVD,  $W^g(n, k)$  defined in (9.70), the normalized periodic first moment equals the DIF estimator [35]:

$$\hat{f}_i(n) = \frac{f_s}{2M} m_w^1(n). \quad (9.80)$$

*Proof*

Let

$$m_w^1(n) = \frac{M}{2\pi} \arg \left[ \sum_{k=0}^{M-1} e^{j2\pi k/M} W^g(n, k) \right] \text{ mod.}2\pi. \quad (9.81)$$

Now taking the inverse Fourier transform of the  $W^g(n, k)$  as defined in (9.70), we obtain:

$$\sum_{k=0}^{M-1} e^{j2\pi mk/M} W^g(n, k) = 2g(m)z(n+m)z^*(n-m). \quad (9.82)$$

Combining these two equations with  $m = 1$  and  $0 < g(1) \in \mathcal{R}$  yields

$$m_w^1(n) = \frac{M}{2\pi} \{\arg[z(n+1)] - \arg[z(n-1)]\} \text{ mod.}2\pi. \quad (9.83)$$

*Q.E.D.*

The conventional linear definition of the first moment of the WVD can also be used as an estimator of IF. Simulations show that this estimator performs no better than the direct definition given in (9.77) [50]. Additionally, this estimator is in general biased—the equality in (9.80) no longer holds because of the fact that the discrete WVD is periodic in  $f$ , extending to  $\infty$  in the frequency domain. By using the periodic definition, we may account for the repetitive nature of the information in the frequency direction. In practice, if the signal is properly sampled, there is little or very-narrow-band noise, and the signal has very little low-frequency or high-frequency energy, then the linear moment closely approaches the periodic moment. Where these criteria are not met, low- and high-frequency truncation effects can introduce unacceptable bias into the linear moment.

### Time-Frequency Filtering and IF Estimation

Indeed, the previous result, and computer simulations have shown that estimating the IF as the periodic first moment of the discrete WVD is exactly equivalent to implementing the central finite difference of the phase of the analytic signal [41]. However, the influence of noise on the WVD-based IF estimate will decrease if the integration is performed over a selective region of the time-frequency plane. This uses the full potential of time-frequency signal analysis. In that sense, the IF estimated as the first moment of the WVD can perform better than the direct implementation, when the signals under analysis are time varying. For example, consider the problem of estimating the IF of the linear FM signal (9.5) distorted by 3-db white Gaussian noise. Figure 9.21a shows the IF law estimated using the direct definition of (9.7), while Fig. 9.21b shows the IF law estimated by using the moment of the WVD after a time-frequency window has been applied. It is clear that this method for estimating the IF could be potentially very useful. In a practical situation we could start by obtaining a rough estimate of the IF law, then window about this region of time-frequency concentration, and finally obtain the improved IF estimate. We could also use signal synthesis to obtain a time-domain signal from the windowed WVD, and then form the DIF from this filtered signal.

#### 9.4.3 Relationship Between Smoothed DIF and TFD IF Estimators

In this section, we describe IF estimators that are calculated by applying a time-averaging or smoothing window to the DIF estimator. As shown in (9.36), in the continuous-time case, the first moment of a TFD is in general a smeared version of the IF. If the denominator of (9.36) is constant, that is, if the signal magnitude is constant, then it is clear that

$$m_p^1(t) = f(t) \underset{(\cdot)}{*} G(t, 0). \quad (9.84)$$

A similar relation exists for the discrete-time case. Since the DIF estimator is periodic in value with frequency modulo  $f_s/2$  and a linear function of time, the smoothed estimator cannot simply be calculated by linear convolution with a smoothing function. Instead, modulo convolution is used, defined as follows.

Let the IF sequence be  $f(n)$  (modulo  $A$ ); if  $f(n)$  is convolved with window  $b(n)$  of odd length  $P = 2Q + 1$ ,  $b \in \mathcal{R}$ , then the *modulo A convolution operation* defined by

$$[f(n) * b(n)] \text{ mod } A = \frac{A}{2\pi} \left\{ \arg \left[ \sum_{p=-Q}^Q b(p) e^{j2\pi f(n-p)/A} \right] \text{ mod. } 2\pi \right\} \quad (9.85)$$

must be used [35]. This definition ensures that values of  $f(n)$  are averaged sensibly to reflect their periodic nature and is effectively the argument of a phasor sum.

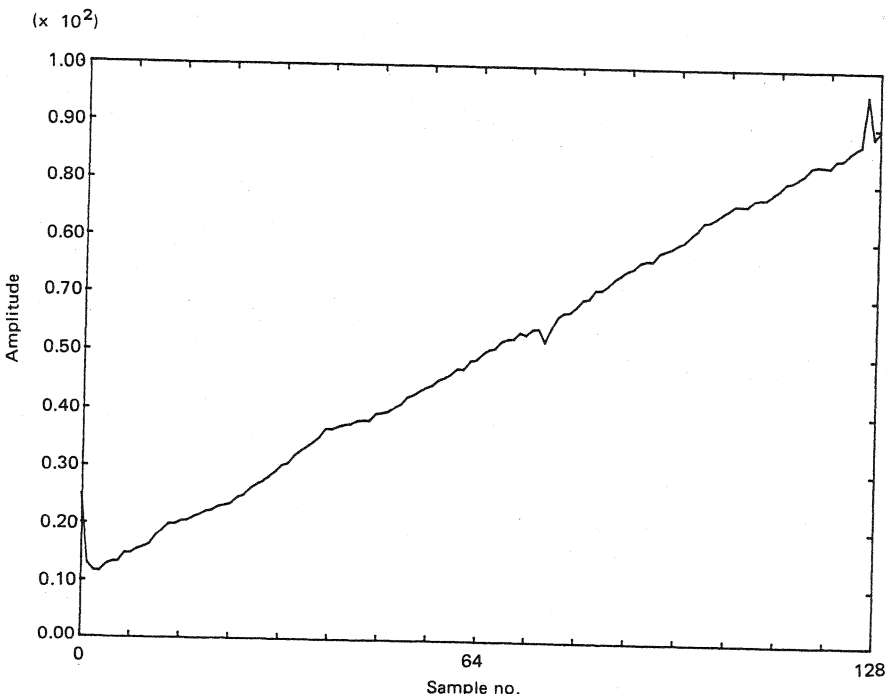
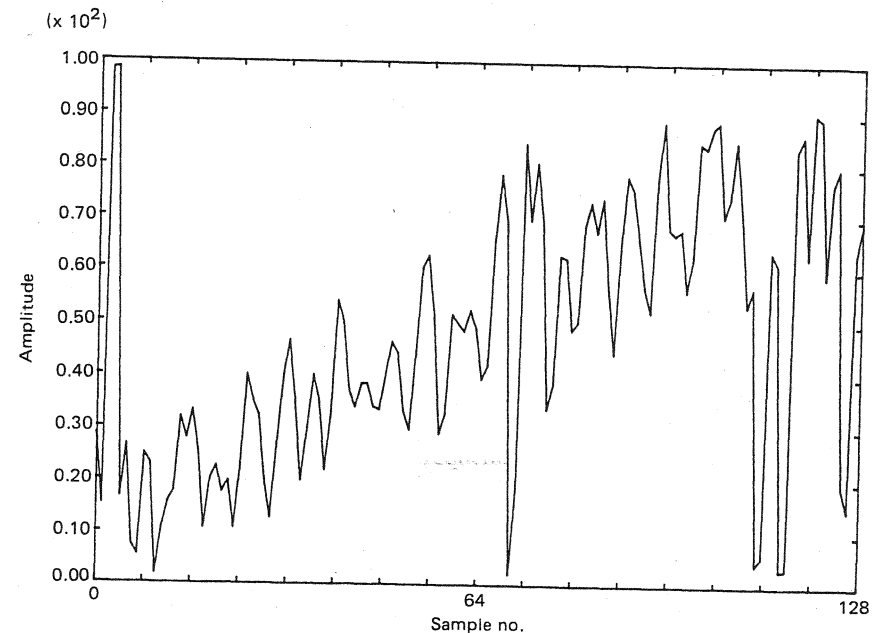


**Figure 9.21** Estimation of the instantaneous frequency of a chirp signal in noise (a) using the direct definition, (b) using the first moment of the WVD and time-frequency filtering.

Let  $\hat{f}_i(n)$  denote the DIF estimator that is modulo  $f_s/2$ , and let  $b$  be a smoothing function of odd length  $P$ . Then the *smoothed DIF estimator* is defined by

$$\hat{f}_i^s(n) = [\hat{f}_i(n) * b(n)] \bmod f_s/2. \quad (9.86)$$

The function  $b(n)$  that makes  $\hat{f}_i^s(n)$  correspond approximately to an IF estimate calculated as the first moment of a TFD from Cohen's class is now determined as follows. The normalized periodic first moment of a TFD as given in (9.79) becomes

$$\hat{f}_i^c(n) = \frac{f_s}{4\pi} \left\{ \arg \left[ \sum_{p=-\lfloor (N-1)/2 \rfloor}^{\lfloor (N-1)/2 \rfloor} G(p, 1) z(n-p+1) z^*(n-p-1) \right] \right\} \bmod 2\pi. \quad (9.87)$$

Substituting

$$|z(n-p+1)z^*(n-p-1)| e^{j4\pi\hat{f}_i(n-p)/f_s} \quad (9.88)$$

for  $|z(n-p+1)z^*(n-p-1)|$  in (9.87), it is found that, apart from the  $|z(n-p+1)z^*(n-p-1)|$  multiplier term, (9.87) is of the form of a modulo convolution. As in the continuous case, if high-SNR and constant signal amplitude are assumed within the window defined by  $G(n, 1)$ , then this multiplier term is constant and the following approximation may be obtained:

$$\hat{f}_i^c(n) \approx [\hat{f}_i(n) * G(n, 1)] \bmod f_s/2. \quad (9.89)$$

Thus the IF estimate calculated as the first moment of any TFD is approximately equivalent to a smoothed DIF estimator with window function,  $b(n)$ , approximately equal to  $G(n, m)$ , evaluated at  $m = 1$ . In fact, the smoothed DIF estimator will always have a dispersion parameter slightly less than the corresponding estimator calculated as the first moment of a TFD due to variations in  $|z(n-p+1)z^*(n-p-1)|$  from noise. In other words, the approximation in (9.89) is rough (unless the SNR is high), but it is nonetheless useful since it provides insight into the physical meaning of the results obtained in the estimation of the IF.

Since  $b(n) = \delta(n)$  for the discrete WVD, the IF estimator derived from the periodic first moment of the WVD is identical to the unsmoothed DIF estimator as seen previously. If  $\rho(n, k)$  is a *general* member of Cohen's class, the normalized periodic first moment of (9.79) may yield an IF estimator with excessive bias [35].

#### Instantaneous Bandwidth and Spread of IF

The concept of instantaneous bandwidth could be related to that of instantaneous frequency in an analogy to the classical bandwidth-frequency relationship. It is a measure of the signal concentration about its IF and an approximate value can be determined graphically on the signal's time-frequency representation. There is, however, no known theoretical formulation of the concept as yet. (The second moment of the WVD has been proposed to this effect, but often gives unexpected results.)

Work is in progress in several places to establish theoretical foundations for this concept [9], [51].

#### Statistical Properties of IF Estimators

The estimation problem for the IF when this quantity is a random process is addressed in [51b], [51c] and [51d]. At the time of proofchecking this manuscript, the author became aware of important results contained in two new papers by Rao and Taylor [51e] and Wong and Jin [51f]. In [51e], it is shown that the IF estimator based on the peak of the WVD is optimal for chirp signals at high to moderate signal to noise ratio. Cramer-Rao bounds for the estimation of the instantaneous frequency are provided in [51f].

### 9.5. THE WIGNER-VILLE DISTRIBUTION OF MODULATED SIGNALS

In this section a detailed study of the behavior of the WVD for typical signals is described. This is particularly important in experimental applications, so that proper interpretation of time-frequency signal analysis results can be made. For instance, it is essential when we interpret the results of an analysis that it be possible to discriminate between oscillations created by the method and those inherent to the signal under analysis.

#### 9.5.1 WVD of Monocomponent FM Signals

In the case of monocomponent signals (defined in Section 9.1.3), the WVD exhibits the frequency modulation law of the signal in the time-frequency domain, simply by direct observation of the maximum amplitude curve [37]; this result is a consequence of Property 3-5 of the WVD, and is illustrated by the following examples.

##### Example: WVD of a Linear FM Signal

Substituting the chirp signal in the definition of the WVD yields

$$W(t, f) = \Pi_T(t) \cdot \frac{\sin 2\pi\{(T - 2|t|)(f - f_i(t))\}}{\pi[f - f_i(t)]}, \quad (9.90)$$

where  $f_i(t) = f_0 + \alpha t$ . This result can also be expressed as

$$W(t, f) = 2\Pi_T(t)(T - 2|t|) \cdot \sin \{(T - 2|t|)[f - f_i(t)]\}. \quad (9.91)$$

The result of the simulation for a linear FM chirp is shown in Fig. 9.22 with the following signal parameters:  $B = 80$  Hz,  $T = 2s$ ,  $f_0 = 50$  Hz.

This type of signal, for example, may represent the Vibroseis signal used in seismic surveying. The representation exhibits an energy concentration along a line that describes the instantaneous frequency law of the signal. This concentration increases with the parameter,  $BT$  [5]. This is seen by comparing figures 9.22 and 9.10.

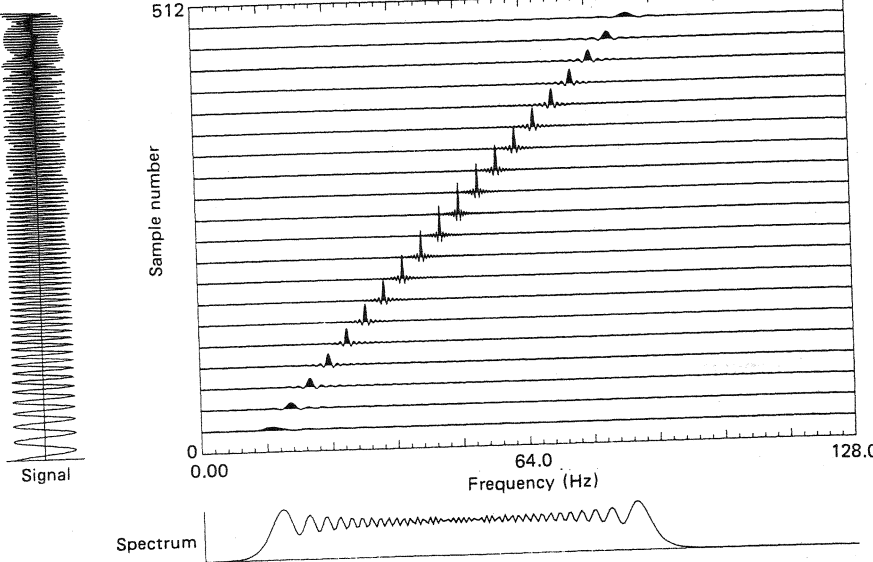


Figure 9.22 WVD of a chirp signal.

**Example: WVD of an Hyperbolic FM Signal**

For this example, the signal is expressed in the form  $z(t) = a(t)e^{j\phi(t)}$ . Consider a signal characterized by:

$$\begin{aligned}\phi(t) &= \frac{2\pi f_0}{\alpha} \log |1 + \alpha t|, \\ a(t) &= \Pi_T(t),\end{aligned}\quad (9.92)$$

$$f_i(t) = \frac{f_0}{1 + \alpha t} \quad B = \frac{f_0 \alpha T}{1 + \alpha T}$$

This signal is typical of some sonar signals emitted by some bats [52]. It is assumed that the signal is narrow band, in order to represent the real signal, that is,  $B \ll f_0$ . The resulting WVD is [5]:

$$W(t, f) = 2 \cdot \Pi_T(t) \cdot (T - 2|t|) \cdot \text{sinc}\{(T - 2|t|)[f - f_i(t)]\}. \quad (9.93)$$

In the general case, where the signal is not narrow band, the result becomes

$$W(t, f) = A_t \left\{ \left[ \frac{4\pi f_0}{\alpha} \right]^{2/3} \left[ \frac{f}{f_i(t)} - 1 \right] \right\}, \quad (9.94)$$

where  $A_t(\cdot)$  is the *Airy function* defined as follows [53]:

$$A_t(x) = \int_{-\infty}^{\infty} e^{j(xu - \frac{u^3}{x})} du. \quad (9.95)$$

Consider the signal with the following parameters:  $a(t) = \Pi_T(t - T/2)$  and  $T = 1 \text{ ms}$ ;  $B = 90 \text{ kHz}$ ;  $f_0 = 100 \text{ kHz}$ ;  $BT = 90$ . Figure 9.23 is a plot of the WVD of this signal whose parameters are defined above. The hyperbolic FM law for this signal is approximated by the curve of the maximum values of the WVD plot. The oscillations that appear on the side of this curve (past its peak) can be reduced by a proper selection of an analysis window  $g(\tau)$ .

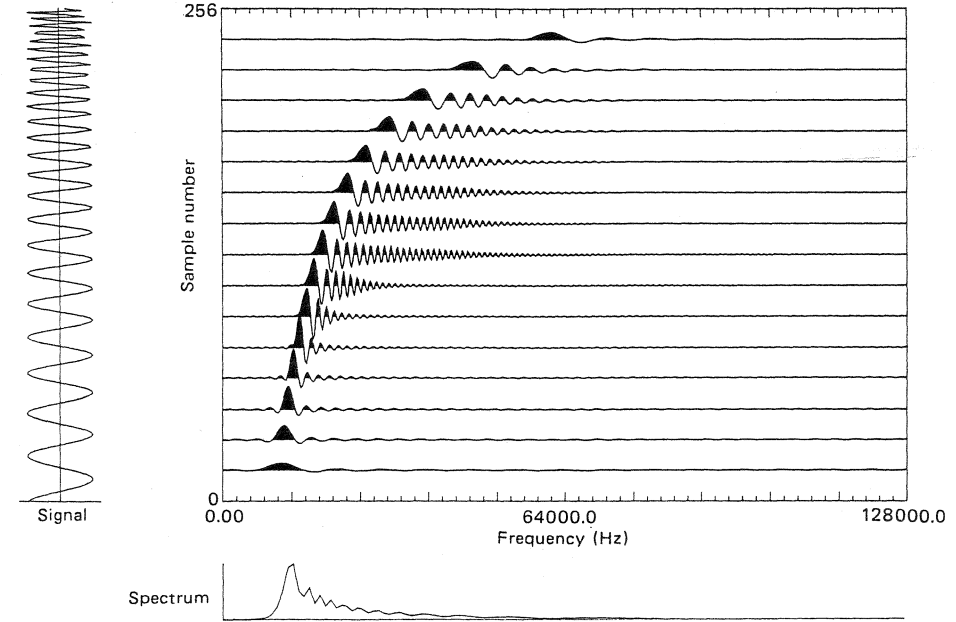


Figure 9.23 WVD of a hyperbolic FM signal.

**9.5.2 WVD of Multicomponent Signals****Example 1: WVD of a Bicomponent Signal Composed of Two-Crossed Linear FMs**

Such a signal is expressed as

$$s(t) = x_1(t) + x_2(t)$$

where

$$x_1(t) = \Pi_T(t) \cos 2\pi(f_0 t + B/2T t^2) \quad (9.96a)$$

$$x_2(t) = \Pi_T(t) \cos 2\pi(f_0 t - B/2T t^2) \quad (9.96b)$$

Assuming that  $BT \gg 1$ , we get the WVD:

$$W_s(t, f) = W_{z_1}(t, f) + W_{z_2}(t, f) + 2 \cdot \text{Re} [W_{z_1 z_2}(t, f)] \quad (9.97)$$

where  $W_{z_1 z_2}(t, f)$  is defined as the cross-WVD of  $z_1(t)$  and  $z_2(t)$ . It is expressed as follows [5]:

$$W_{z_1 z_2}(t, f) = \Pi_{B'}(t) \cdot \Pi_T(t) e^{j\pi/4} e^{j2\pi B T [(t/T)^2 + (f - f_0)^2/B^2]} \quad (9.98)$$

where  $B' = B/2 - B/T|t|$ .

If the signal is defined over the interval  $(0, T)$ , it is sufficient simply to substitute  $t - T/2$  for  $t$  (property of time invariance). The condition  $BT \gg 1$  yields a rapidly oscillating exponential versus time,  $t$ , and frequency,  $f$ , for the cross term. The WVD of  $s(t) = [x_1(t) + x_2(t)]$  is then obscured by these oscillations due to the time-frequency interaction.

**Result of the Simulation.** Consider the signal  $s(t) = x_1(t) + x_2(t)$  defined above with  $B = 100$  Hz,  $T = 2$  s and  $f_0 = 50$  Hz. It is observed that the maxima of the WVD of  $s(t)$  are located along two line secants at  $f = f_0$  and  $t = T/2$  and with opposite slopes (Fig. 9.24). These lines, respectively, characterize the frequency modulation laws of  $x_1(t)$  and  $x_2(t)$ . The effects of the WVD interaction are stronger nearby  $t = T/2$ , as predicted by the analytical result. A similar result is obtained when dealing with the analysis of the sum  $s(t) = x_1(t) + x_3(t)$ , where  $x_3(t)$  is now an FM signal with an hyperbolic law (Fig. 9.25).

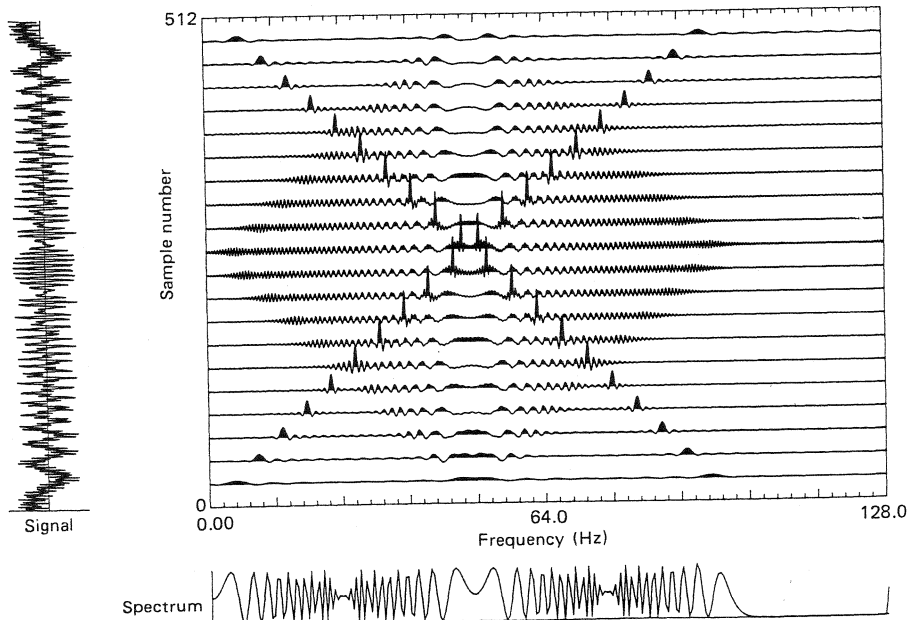


Figure 9.24 WVD of the sum of two chirp signals.

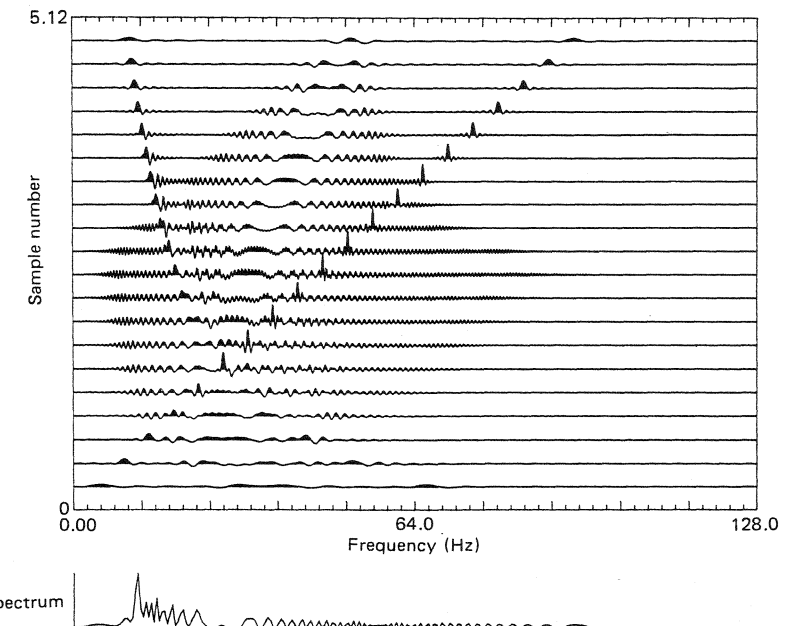


Figure 9.25 WVD of the sum of a chirp signal and a hyperbolic FM signal.

#### Example 2: WVD Analysis of a Multicomponent (Parallel) Linear FM Signal

Consider the signal  $s(t) = x_1(t) + x_2(t)$ , defined by

$$x_1(t) = \Pi_T(t - T/2) \cos 2\pi(f_1 t + \alpha t^2/2) \quad (9.99a)$$

and

$$x_2(t) = \Pi_T(t - T/2) \cos 2\pi(f_2 t + \alpha t^2/2) \quad (9.99b)$$

where  $\alpha = B/T$  and  $BT \gg 1$ . The corresponding WVD is

$$W_s(t, f) = W_{z_1}(t, f) + W_{z_2}(t, f) + 2 \operatorname{Re}[W_{z_1 z_2}(t, f)]. \quad (9.100)$$

Using the stationary phase method, it is shown that in the time-frequency domain, the stationary points of the WVD are contained on the three following curves [26], [33], [5]:

$$f_1(t) = f_1 + \alpha t = f_{i_1}(t) \quad (9.101a)$$

$$f_2(t) = f_2 + \alpha t = f_{i_2}(t) \quad (9.101b)$$

$$f_3(t) = \frac{f_1 + f_2}{2} + \alpha t. \quad (9.101c)$$

The functions,  $f_1(t)$  and  $f_2(t)$ , characterize, respectively, the frequency modulation laws of  $x_1(t)$  and  $x_2(t)$ . The ghost law,  $f_3(t)$ , is introduced by the WVD and is due to the bilinearity [5]. To discriminate the “real laws” from the “ghost law,” it suffices to note that the maximum values of  $W(t, f)$  along the “ghost law” are alternatively positive and negative [33], [54]. The next example illustrates this point.

### Example 3: Simulation of a Multicomponent Signal

The multicomponent signal simulated is described in Fig. 9.26. The result of the numerical WVD computation clearly shows the “ghost” curves and real curves of the WVD in the time-frequency domain. Curves 1, 2, 3, 4, and 5 are “ghost laws” because they are situated exactly equidistant between a pair of the curves 6, 7, 8, and 9. Note that the peaks along these curves are alternatively positive and negative.

*Comment.* As previously indicated, the analysis of multicomponent signals represent a major problem of the WVD, since the two-dimensional windowing necessary to separate the signal subcomponents could be difficult to define in the case where there are many of them and where cross-terms are significant. To improve the performance of WVD analysis for these signals, it is frequently proposed to apply a two-dimensional filtering (smoothing) to the WVD [55]. In fact, it is known that a proper linear transformation will result in the spectrogram of the signal, which is known to be a less accurate TFD, to be positive, and not to suffer from cross-terms. A compromise between the high accuracy of the WVD and the positivity (= absence of cross-terms) can be achieved by an intermediate transformation, such as the one that

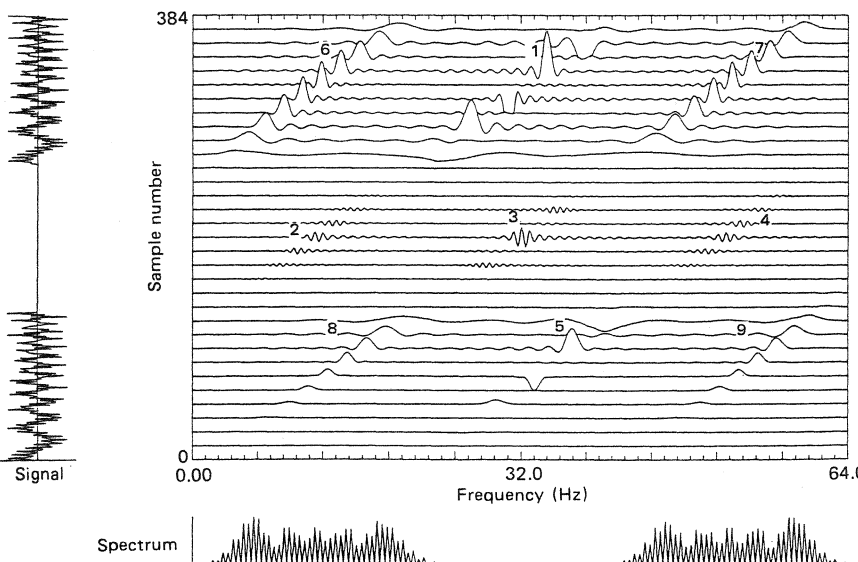


Figure 9.26 WVD of a multicomponent signal composed of four chirp signals.

results in a function that controls the level of artifact reduction as proposed by Choi and Williams [20]. The Choi-Williams distribution has the property that it contains as much information as the WVD, while the spectrogram does not. Then, the proper selection of a two-dimensional windowing can be used to separate subcomponents.

## 9.6. WIGNER-VILLE ANALYSIS OF RANDOM SIGNALS

### 9.6.1 Formulation

Let  $z(t)$  be an analytic, harmonizable, random, zero-mean Gaussian process [56] with autocorrelation,  $R_z(t, \tau) = E[z(t + \tau/2)z^*(t - \tau/2)]$ , where  $E$  denotes the expectation operator. If  $z(t)$  is stationary, it allows us to use a spectral representation,  $S_z(t, f)$ , given by the Fourier transform of its autocorrelation function, operating on the variable  $\tau$ , that is,

$$S_z(f) = \int_{-\infty}^{+\infty} R_z(\tau) e^{-j2\pi f\tau} d\tau. \quad (9.102)$$

Under these conditions,  $S_z(f)$  has the property that it is independent of  $t$ , and it is referred to as the *power spectral density* of  $z(t)$ . However, if  $z(t)$  is not stationary, this property no longer holds. In this case,  $S_z(t, f)$  is called the *evolutive spectrum*. Its relation to the “evolutionary spectrum” of Priestly [56b] was studied in [56c]. By substituting  $R_z(t, \tau)$  with its definition, (9.102) yields

$$S_z(t, f) = \int_{-\infty}^{+\infty} E[z(t + \tau/2)z^*(t - \tau/2)] e^{-j2\pi f\tau} d\tau. \quad (9.103)$$

Interchanging the operators “expectation value” and “integration” gives

$$S_z(t, f) = E \left\{ \int_{-\infty}^{+\infty} z(t + \tau/2)z^*(t - \tau/2) e^{-j2\pi f\tau} d\tau \right\}, \quad (9.104)$$

the integral being defined in the mean square sense. Equation (9.104) shows that the *evolutive spectrum* (ES) of the signal,  $z(t)$ , equals the expectation of  $W_z(t, f)$ , the WVD of the signal, as shown by

$$S_z(t, f) = E[W_z(t, f)]. \quad (9.105)$$

This expression shows that the evolutive spectrum (or Wigner-Ville spectrum) of a random process represents a time-varying power spectrum, and it can therefore be regarded as being the average of the WVD of the individual signal samples of the process. The evolutive spectrum of a random signal,  $s(t)$ , will be used to denote its time-frequency representation estimated as the expectation of the WVD.

**Example. Evolutive Spectrum of a Deterministic Signal in Additive Noise**

Consider the random signal:  $v(t) = z(t) + n(t)$ , where  $z(t)$  is an analytic deterministic signal and  $n(t)$  is a stationary zero-mean colored noise. A realization is represented in the WVD, time-frequency domain by:

$$W_v(t, f) = W_z(t, f) + W_n(t, f) + 2 \operatorname{Re}[W_{zn}(t, f)]. \quad (9.106)$$

It can easily be shown that

$$S_v(t, f) = W_z(t, f) + S_n(f) \quad (9.107)$$

where  $S_n(f)$  defines the spectral density function of  $n(t)$ . If the noise is assumed to be a band-limited white noise, in the band of the signal  $z(t)$ , we get

$$S_v(t, f) = W_z(t, f) + S_0, \quad (9.108)$$

where  $S_0$  is a constant representing the spectral level of the noise.

This expression illustrates the potential of the WVD for the detection of signals in noise. The signal  $s(t)$  is concentrated around a time-frequency law in a particular sector of the time-frequency plane, while the noise being spread all over the surface, will have a minor contribution to the signal sector [57]. A simple time-frequency filtering can thus drastically improve signal-to-noise ratio.

**Example: WVD of Signals Corrupted by Noise**

The WVD of a signal distorted by noise is shown so as to illustrate the robustness of the method as a function of the SNR. The signal is a linear FM signal and  $n(t)$  is a white Gaussian noise in the spectral band of  $s(t)$ . The result is shown in Fig. 9.27. This demonstrates the interest in such an analysis tool since the energy of the noise is distributed over the entire time-frequency plane, while the signal itself is concentrated along one

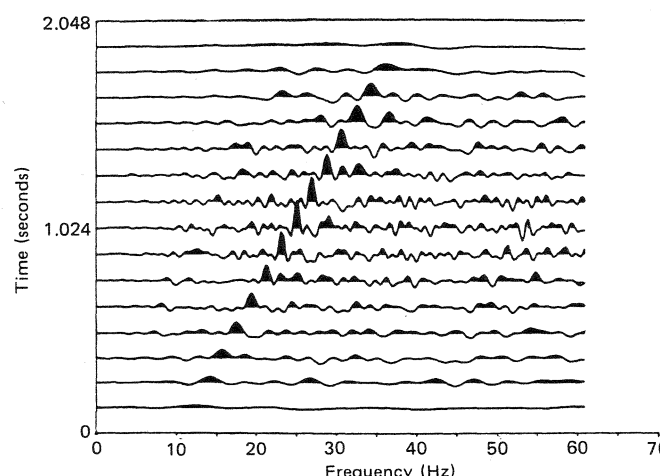


Figure 9.27 WVD of a chirp signal in additive noise.

single line. The SNR along this line will be greatly improved. This will be discussed in the next section.

### 9.6.2 Estimation Procedure

Since in practice, analysts seldom have access to the numerous realizations of the process needed to perform the ensemble averaging, as required by (9.103) or (9.105), an estimation procedure based on this method is impossible to implement. When only one realization is available, analysts generally approach the problem by assuming an interval of local ergodicity,  $\Delta(t)$ , and replacing the ensemble averaging by a time averaging over this interval. The estimator,  $S^0(t, f)$ , of  $S(t, f)$  is defined as

$$S_z^0(t, f) = \frac{1}{\Delta(t)} \int_{t-\lambda}^{t+\lambda} W_z^0(\theta, f) d\theta, \quad (9.109)$$

where  $\lambda = \Delta(t)/2$  and  $W_z^0(t, f)$  is defined by (9.66). Equation (9.109) shows that to estimate  $S(t, f)$ , it is necessary to apply two windowing procedures, one corresponding to the analysis window,  $g(\tau)$ , and the other corresponding to the averaging window of length,  $\Delta(t)$ , that is denoted by  $b(t)$ . The averaging window can be a rectangular window as in (9.109) or of another shape. This generalizes (9.109) as follows:

$$S_z^0(t, f) = W_z(t, f) \stackrel{\leftrightarrow}{f} V(t, f) \quad (9.110)$$

where  $V(t, f) \stackrel{\leftrightarrow}{f} g(\tau) \cdot b(t)$ . ( $\stackrel{\leftrightarrow}{f}$  denotes an inverse Fourier transform operation).

Combined windowing procedures result in a two-dimensional convolution, resulting in possible distortion in both time and frequency directions. The choice of optimal windows to use for the analysis is given in [36], [58], [59].

The design philosophy for the specification of estimators of the evolutive spectrum relies on a numerical procedure for determining the one-dimensional probability density functions in the Gaussian case [15], [56b]. The chosen class of estimators are members of Cohen's class of TFDs, as is evident from (9.110) with  $V(t, f)$  being any admissible two-dimensional window function. The design procedure is as follows [60]:

1. Obtain a segmentation of the signal record into approximately stationary intervals using the method outlined in [61]. These methods involve a statistical significance test on the difference between autoregressive coefficients derived from successive sections of the signal, to detect changes in the signal structure.
2. Determine the usual stationary biased covariance lag estimator on each interval.

3. Use these covariance estimates to obtain a *Karhunen-Loeve expansion* (KLE) for the process on each interval. The eigenvectors of the covariance estimates matrices are used to determine a principal component decomposition for the ES estimator on each interval and may be used to derive the relevant PDFs.
4. By use of these PDFs, the shape of the chosen window may be altered according to given criteria [15], [60].
5. The product is iterated until the desired bias-variance-resolution trade-offs are satisfactory for the task at hand.

Another approach proposed recently is to start the estimation procedure in the time-lag domain using (9.103) and replacing the Wigner-Ville kernel by a TFD kernel that is the convolution between  $K_z(t, \tau)$  and a desirable time-lag kernel function as seen in Section 9.2.5. [59], [58]. A requirement of the time-varying nature of the signals is to use fewer samples to estimate the autocorrelation lags that correspond to a short stationary interval [58].

These methodologies for obtaining a smoothed version of the ES of a signal provide the analyst with an estimate of the power spectrum of the signal as a function of time and specifies the best averaging to use for a particular application.

### 9.6.3 Coherence Estimation for Nonstationary Signals

In this section the notion of evolutive spectrum is extended to provide a theoretical framework for cross-analysis of nonstationary random signals [15], [61b]. The *time-frequency coherence* is a natural generalization of the stationary coherence function. It is defined by

$$C_{xy}(t, f) = \frac{S_{xy}(t, f)}{\sqrt{S_x(t, f) S_y(t, f)}}, \quad (9.111)$$

where  $S_{xy}$  is the cross evolutive spectrum (or Wigner-Ville spectrum), defined by

$$S_{xy}(t, f) = \int_{-\infty}^{+\infty} E \{ x(t + \tau/2) y^*(t - \tau/2) \} e^{-j2\pi f\tau} d\tau \quad (9.112)$$

$$S_x(t, f) = S_{xx}(t, f) \text{ and } S_y(t, f) = S_{yy}(t, f).$$

**Properties** The time-frequency coherence has the following properties [15].

*Property 6-1.*  $0 \leq |C_{xy}(t, f)| \leq 1$ .

*Property 6-2.* If  $x$  and  $y$  are uncorrelated at time  $t$ ; that is,  $R_{xy}(t + \tau/2, t - \tau/2) = 0$ , for all  $\tau$ , then  $C_{xy}(t, f) = 0$ .

*Property 6-3.* Let  $x(t)$  and  $y(t)$  be derived from a harmonizable process,  $q(t)$  by linear-shift invariant filterings  $H_1$  and  $H_2$ , respectively. Then

$$C_{xy}(t, f) = \frac{S_q(t, f) * W_{b_1 b_2}(t, f)}{[S_q(t, f) * W_{b_1}(t, f)]^{1/2} [S_q(t, f) * W_{b_2}(t, f)]^{1/2}} \quad (9.113)$$

where  $*$  represents convolution in time and frequency and

$$W_{b_1 b_2}(t, f) = \int_{-\infty}^{+\infty} b_1(t + \tau/2) b_2^*(t - \tau/2) e^{-j2\pi f\tau} d\tau \quad (9.114)$$

is the cross WVD of the filter impulse responses. The auto WVDs are analogously defined. If  $q(t)$  is semistationary with correlation width exceeding the duration of the filter impulse responses, then the ES of  $q(t)$  is approximately constant in time over the duration of the impulse response WVDs and  $|C_{xy}(t, f)|$  is approximately unity.

These properties show that the time-frequency coherence between two semistationary, harmonizable processes may be interpreted in a manner similar to that of the stationary coherence function. If the processes are not semistationary, then the time-frequency coherence represents the degree of bidirectional linear relationship averaged over the filter durations.

The estimation of the time-frequency coherence is based on the class of evolutive spectrum estimators previously considered. The chosen class must be restricted to the positive class of TFDs of Cohen's class, that is, smoothed STFTs [15], [61c].

## 9.7 SIGNAL SYNTHESIS AND TIME-VARYING FILTERING

### 9.7.1 Pattern Recognition

In this section, the problem of estimating and extracting a signal from a noise background is considered, and a solution is presented, based on the use of the WVD. Noise may be considered as any undesirable component of the signal, either deterministic or random. For simplicity, the discussion is initially restricted to the class of monocomponent asymptotic nonstationary signals previously discussed, although it can be conceptually defined for a broader class of signals.

The estimation procedure uses the instantaneous frequency as a critical characteristic of the signal. In the case of monocomponent signals, since the signal contribution is concentrated around  $f_i(t)$ , the application of a two-dimensional windowing that preserves all the points  $(t, f)$  that are in its neighborhood and filters out the others, preserves the useful information contained in the signal, and indeed increases by an order of magnitude the signal-to-noise ratio. For example, given a cross-linear FM signal in additive noise, we may wish to extract the only desirable feature represented by the increasing linear FM (see the next section). Once the WVD has been filtered by applying the appropriate windowing, it is then necessary to be able to reconstruct the filtered signal,  $s_f(t)$ , that corresponds to the filtered WVD by using a WVD synthesis algorithm.

### 9.7.2 Signal Synthesis Using the WVD

The problem of synthesizing a signal from some given time-frequency characteristics can be addressed by using the WVD. Several methods are available [62], [63], [64]. Following the approach in [64], the problem can be formulated as follows: "Find the analytic discrete sequence,  $z(n)$ , whose discrete-time WVD,  $W_z(n, k)$ , best approximates some given desirable TFD,  $W_{z_m}(n, k)$ ."

The basis for the solution is the inversion property of the WVD shown in (9.55). From (9.55), taking the inverse Fourier transform of  $W(t, f)$  and letting  $t_1 = t + \tau/2$  and  $t_2 = t - \tau/2$ , we get

$$\int_{-\infty}^{+\infty} W\left(\frac{t_1 + t_2}{2}, f\right) e^{j2\pi f(t_1 - t_2)} df = z(t_1)z^*(t_2). \quad (9.115)$$

When  $t_1 = t_2 = t$ , (9.115) becomes

$$\int_{-\infty}^{+\infty} W(t, f) df = |z(t)|^2, \quad (9.116)$$

which is the marginal property of (9.30); similarly, when  $t_1 = t$  and  $t_2 = 0$ , (9.115) becomes

$$\int_{-\infty}^{+\infty} W\left(\frac{t}{2}, f\right) e^{j2\pi ft} df = z(t)z^*(0). \quad (9.117)$$

Combining (9.116) and (9.117) demonstrates that the signal may be reconstructed to within a complex exponential constant if  $|z(0)| \neq 0$ :

$$\frac{z^*(0)}{|z(0)|} = e^{j\alpha}. \quad (9.118)$$

#### Representability of a Two-Dimensional Function as a Wigner-Ville Distribution

To reconstruct exactly a signal from a given two-dimensional function (representing a time-frequency distribution) using a WVD synthesis procedure, this two-dimensional function must be expressible as the WVD of a signal. To ensure the WVD validity, two properties that must be satisfied by a function of time and frequency,  $\rho_z(t, f)$ , are described by (9.29) and (9.30); see Section 9.2.2. However, these conditions are not sufficient to ensure the WVD validity, because several TFDs that are members of Cohen's class [17] of TFDs satisfy these conditions [9]. The following approach is used to discriminate between them. If  $\rho_z(t, f)$  is a WVD, then

$$K_z(t, \tau) = \int_{-\infty}^{+\infty} \rho_z(t, f) e^{j2\pi f\tau} df = z(t + \tau/2)z^*(t - \tau/2). \quad (9.119)$$

### Sec. 9.7 Signal Synthesis and Time-Varying Filtering

For convenience, the function,  $A(u, v)$ , is defined such that

$$A(u, v) = K[(u + v)/2, u - v]. \quad (9.120)$$

If  $\rho_z(t, f)$  is a WVD, by combining (9.119) and (9.120), we get:

$$A(u, v) = z(u)z^*(v). \quad (9.121)$$

Then, if  $\rho_z(t, f)$  is a valid WVD, integrating  $A(u, v)$  with respect to  $u$  and with respect to  $v$  yields the following respective results:

$$\hat{A}_1(v) = \int_{-\infty}^{+\infty} A(u, v) du = k z^*(v)$$

and

$$\hat{A}_2(u) = \int_{-\infty}^{+\infty} A(u, v) dv = k^* z(u),$$

where  $k$  is a complex constant.

If  $\rho_z(t, f)$  is a valid WVD, then it must satisfy the condition

$$\hat{A}_1(u) = \hat{A}_2^*(u). \quad (9.122)$$

Thus a necessary and sufficient condition for a two-dimensional function  $\rho(t, f)$  to be a WVD is that the marginals are satisfied and that (9.122) is verified [64]. Additional insight is provided in [31].

For a discrete-time signal of length  $N = 2L + 1$ , the discrete WVD is defined as

$$W_{z_m}(n, k) = 2 \sum_{m=-L}^L z_m(n+m)z_m^*(n-m)e^{-j4\pi km/N} \quad (9.123)$$

and the equivalent expression for (9.115) is given by

$$\frac{1}{2} \sum_{k=-L}^L W\left(\frac{n_1 + n_2}{2}, k\right) e^{j2\pi(n_1 - n_2)k/N} = z(n_1)z^*(n_2). \quad (9.124)$$

When  $n_1 = n_2 = n$ , (9.124) gives

$$\frac{1}{2} \sum_{k=-L}^L W(n, k) = |z(n)|^2 \quad (9.125)$$

and, when  $n_1 = 2n$  and  $n_2 = 0$ , we obtain

$$\frac{1}{2} \sum_{k=-L}^L W(n, k) e^{j4\pi nk/N} = z(2n)z^*(0), \quad (9.126)$$

which yields the even samples to within a complex constant. Similarly, when  $n_1 = 2n - 1$ ,  $n_2 = 1$ , we obtain

$$\frac{1}{2} \sum_{k=-L}^L W(n, k) e^{j4\pi(n-1)k/N} = z(2n-1)z^*(1). \quad (9.127)$$

This gives the odd samples to within a complex constant. Therefore, in the discrete case, by combining (9.126) and (9.127), the signal  $z(n)$  may be reconstructed to within complex exponential constants as shown by

$$\frac{z^*(0)}{|z(0)|} = e^{j\alpha_e} \quad \text{and} \quad \frac{z^*(1)}{|z(1)|} = e^{j\alpha_o}. \quad (9.128a), (9.128b)$$

Equations (9.126) and (9.127) show that the problem of inversion of the discrete WVD may be split into two smaller problems—finding the odd samples and finding the even samples [64], and (9.128) shows that exact reconstruction can be achieved if we know two consecutive (or one even and one odd) nonzero samples of the signal. However, since the signal is analytic, the amplitudes of its spectral components at negative frequencies are zero, and it can therefore be undersampled. This means that only the even samples are necessary for exact reconstruction of the signal. The odd samples can be obtained by passing the sequence formed with the even samples in a reconstruction filter of impulse response,  $b(t) = \sin\pi f_s t / \pi f_s t$ , and transfer function,  $H(f) = T\Pi_{f_s}(f)$ , where  $f_s$  is the sampling frequency.

### 9.7.3 The Synthesis Algorithm

There are two cases to be considered: either the available time-frequency function is a valid TFD, or it is not.

#### Solution to the Case Where the Time-Frequency Function is a Valid DWVD

Equation (9.119) indicates that the first step for synthesizing  $z_m(n)$  is to take the IDFT (in the “ $k$ ” variable) to yield a kernel  $K_{z_m}(n, m)$ :

$$K_{z_m}(n, m) = \frac{1}{2} \sum_{k=-L}^L W_m(n, k) e^{j4\pi km/N} = z_m(n+m)z_m^*(n-m). \quad (9.129)$$

As indicated previously, the problem of finding  $z_m(n)$  in (9.123) reduces to that of solving for the even samples only of  $z_m(n)$ , that is,  $z_e(n') = z_m(2n')$ .

This is done by forming an  $N/2$  by  $N/2$  matrix,  $\mathbf{A}_e$ , the elements of which are defined by:

$$a_e(i, j) = K_{z_m}(i+j, i-j) = z_e(i)z_e^*(j). \quad (9.130)$$

$\mathbf{A}_e$  is of rank one since it is the outer product of the even samples of the required signal. An *eigensystem decomposition* of this matrix yields:

$$\mathbf{A}_e = \sum_{i=1}^{N/2} \lambda_{e_i} \mathbf{e}_{e_i} \mathbf{e}_{e_i}^\dagger = \lambda_{e_1} \mathbf{e}_{e_1} \mathbf{e}_{e_1}^\dagger, \quad (9.131)$$

where  $\lambda_{e_i}$  represents the  $i$ th eigenvalue of  $\mathbf{A}_e$  ( $\lambda_{e_1}$  nonzero),  $\mathbf{e}_{e_i}$  denotes the  $i$ th normalized eigenvector, and  $\mathbf{e}_{e_i}^\dagger$  denotes the conjugate (Hermitian) transpose of  $\mathbf{e}_{e_i}$ . Equation (9.131) simplifies because  $\mathbf{A}_e$  has  $N/2 - 1$  zero eigenvalues. The even samples of the reconstructed signal are then given (in vector form) by:

$$\mathbf{z}_e = \sqrt{\lambda_{e_1}} \mathbf{e}_{e_1} e^{j\alpha_e}, \quad (9.132)$$

where

$$\mathbf{z}_e = [z(0) \ z(2) \ \cdots \ z(N/2)]^T. \quad (9.133)$$

As (9.132) shows, the original even samples may be reconstructed to within a complex exponential constant.

*Note.* This method is sometimes used without the analytic signal [64]. In this case, several complications arise, because odd samples can no longer be reconstructed from the even samples, since the real signal cannot be undersampled without risking aliasing, and therefore the same procedure (9.130)–(9.133) must be repeated for the odd samples (all variables defined with subscript  $e$  will have corresponding variables with subscript  $o$ ) [64].

The phase constants,  $\alpha_e$  and  $\alpha_o$ , will in general, be unequal. Thus, to reconstruct the full signal correctly (meaning to combine both even and odd samples), assumptions about the phase of the reconstructed signal must be made. In fact, the algorithm presented in [64], assumes knowledge of the desired signal,  $z_d(n)$ , to obtain  $\alpha_e$  and  $\alpha_o$ . Consequently, if the signal was originally sampled at exactly the minimum sampling frequency (the Nyquist rate), then the even and odd sample phases must be reconstructed separately, increasing the computational burden by a factor of 2.

#### Solution to the Case Where TFD is Not a Valid DWVD

In the general case where the TFD to be inverted is not a valid  $W_{z_m}(n, k)$ , a *least squares error synthesis procedure* is used. The solution for  $z_m(n)$  is found by minimizing the error term [64]:

$$\varepsilon = \sum_{n,m} \left| a_e(n, m) - z_{me}(n)z_{me}^*(m) \right|^2, \quad (9.134)$$

where  $z_{me}(n) = z_m(2n)$ . In Case 2, the matrix  $\mathbf{A}_e$  will no longer be of rank one. Thus the eigensystem decomposition of (9.131) no longer holds. However, the error term,  $\varepsilon$ , in (9.134) will be minimized if  $z_{me}(n)$  (the vector of  $z_{me}$  values) is given by:

$$\mathbf{z}_{me} = \sqrt{\lambda_{e_{\max}}} \mathbf{e}_{e_{\max}}, \quad (9.135)$$

where  $\lambda_{e_{\max}}$  is the maximum eigenvalue of  $\mathbf{A}_e$ , and  $\mathbf{e}_{e_{\max}}$  is the corresponding eigenvector; the pertinent error energy is obtained from

$$\epsilon = \sum_{i=2}^{N/2} \lambda_i. \quad (9.136)$$

In the absence of additive noise, this error is a function of the window width used in the formation of the WVD.

#### 9.7.4 Influence of Window Length on Synthesis Accuracy

The effect of windowing on the synthesis operation was investigated by comparing  $\hat{z}(n)$  (the signal synthesized from  $W_z$ ) with the original  $z(n)$ .

Let the SNR,  $\sigma$ , be defined by

$$\sigma = 10 \log_{10} \left( \frac{\sum_{n=0}^{N-1} |z(n)|^2}{\sum_{n=0}^{N-1} |\hat{z}(n) - z(n)|^2} \right). \quad (9.137)$$

A zero-mean, Gaussian, white noise process was processed in the above manner and the synthesis errors noted for various DWVD window lengths. Fifty simulations at each window length were performed, and Fig. 9.28 shows that the error is largely independent of window length.

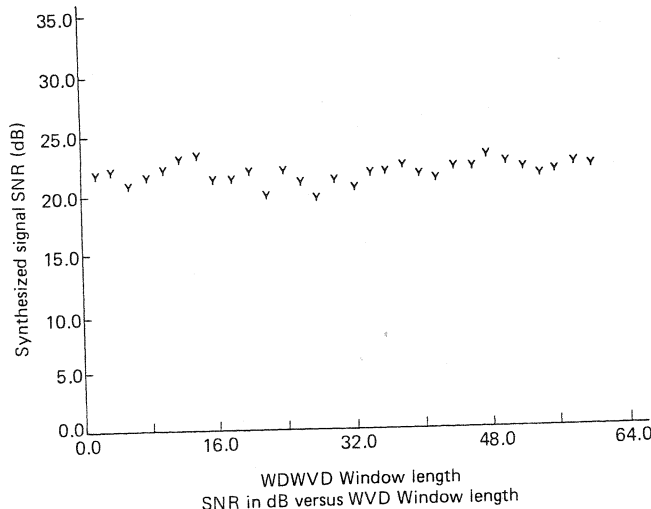


**FIGURE 9.28** WVD signal reconstruction error as a function of window length for wide-band signals.

The performance of the algorithm depends also on the performance of the Hilbert transform operation. A further simulation was carried out to test this dependence. The white noise process was bandpass filtered before the discrete windowed WVD and inversion processes were performed. The bandpass filter had a lower stopband frequency of  $0.05f_s$  ( $f_s$  = sampling frequency) and upper stopband frequency of  $0.45f_s$ , filtering out components which may adversely affect the calculation of the Hilbert transform. The results (Fig. 9.29) show an improvement of approximately 10dB between the original white noise case and the bandpass filtered case.

The following two examples illustrate the method.

#### Example 1: Application to Signal Enhancement

Figure 9.30 shows the DWVD of a noiseless increasing linear FM signal (chirp signal). Figure 9.31(a) is the DWVD of a similar signal with additive white Gaussian noise ( $f_{\min} = 10$  Hz,  $f_{\max} = 90$  Hz,  $f_s = 200$  Hz, SNR = 0.5 dB). The DWVD is then windowed by the function displayed in Fig. 9.31(b). The TFD thus formed is shown in Fig. 9.31(c). The signal reconstructed from this TFD is shown in Fig. 9.31(d) along with the original uncorrupted increasing linear FM signal (Fig. 9.31[e]).

#### Example 2: Application to Signal Separation

Figure 9.32a shows the DWVD of crossed increasing/decreasing linear FM signals (with the same parameters as above in the noise reduction example). Figure 9.32(a) is then windowed using Fig. 9.31(b) resulting in the TFD displayed in Fig. 9.32(b). Figure 9.32(c) then shows the reconstructed signal.

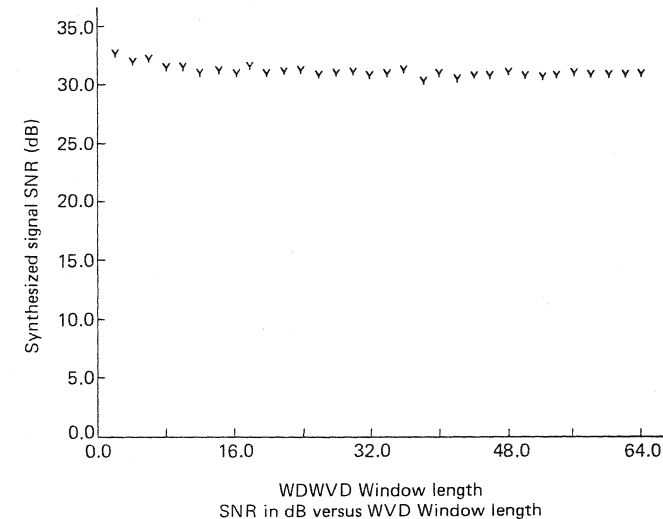


**FIGURE 9.29** WVD signal reconstruction error as a function of window length for narrow-band signals.

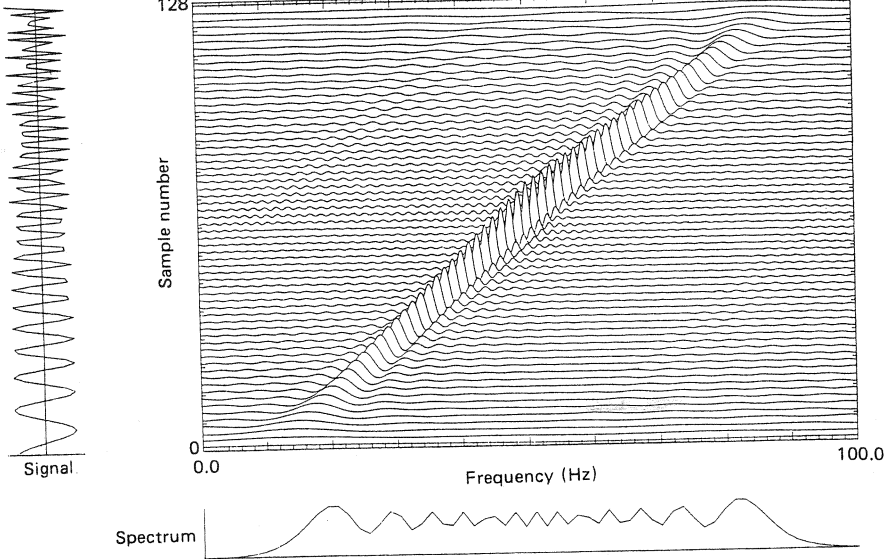


**Figure 9.30** WVD of noiseless chirp signal.

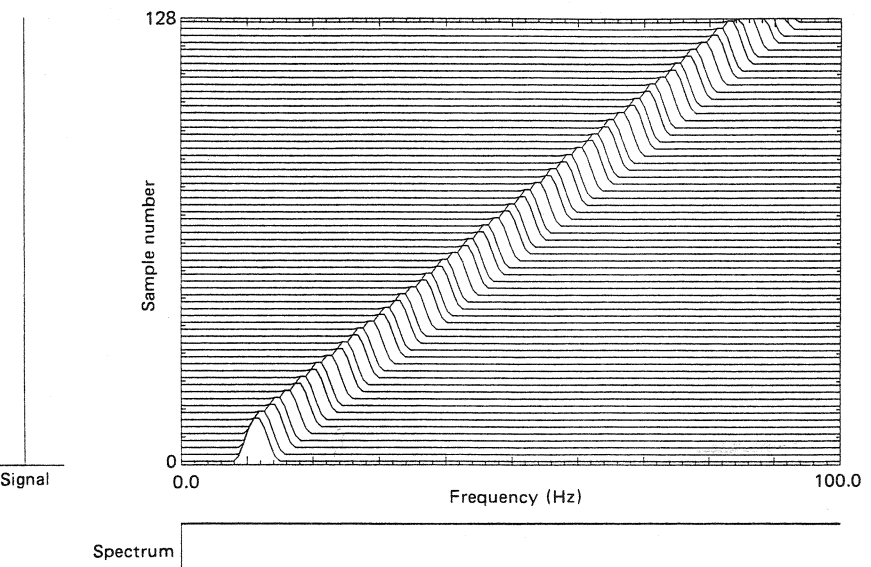


**Figure 9.31 (b)**

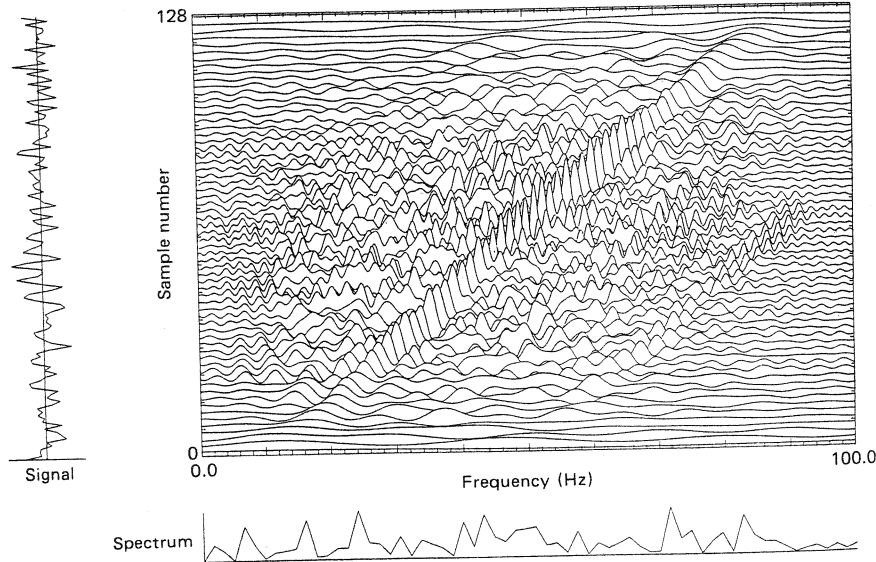


**Figure 9.31 (a)**

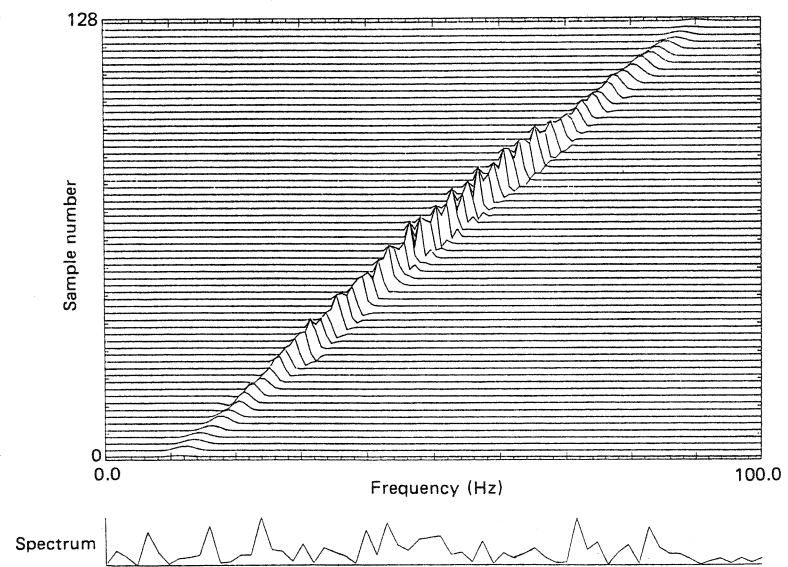


**Figure 9.31 (c)**

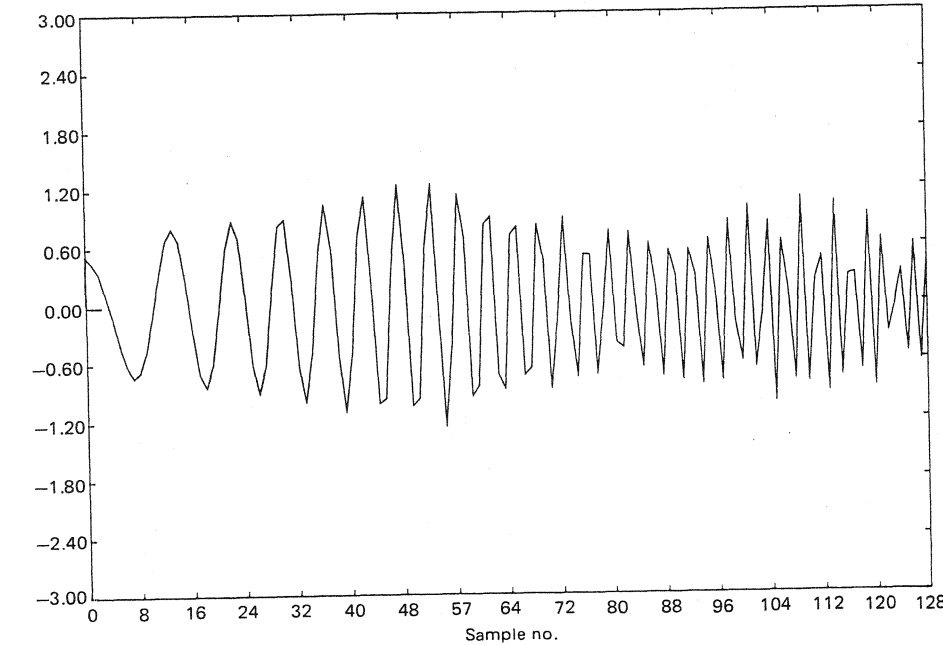


**Figure 9.31 (d)**

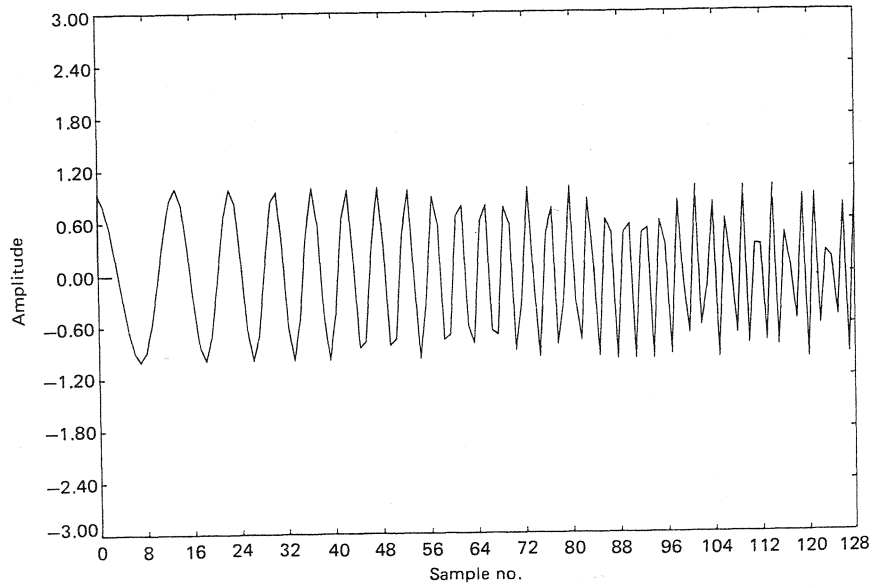


**Figure 9.31 (e)** Signal enhancement by time-frequency filtering. (a) WVD of chirp signal in 0.5dB Gaussian noise, (b) window function, (c) windowed WVD, (d) reconstructed signal, (e) original signal.

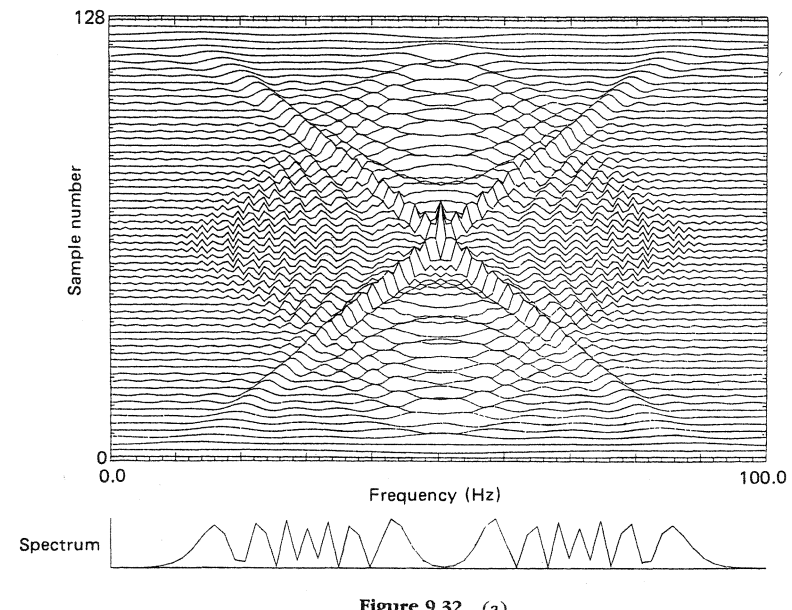
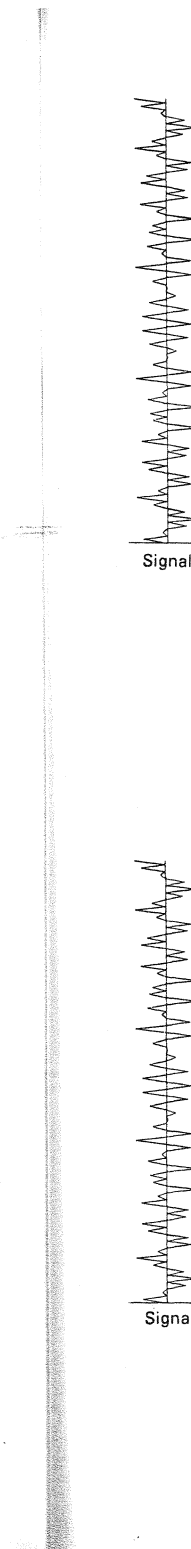


**Figure 9.32 (a)**

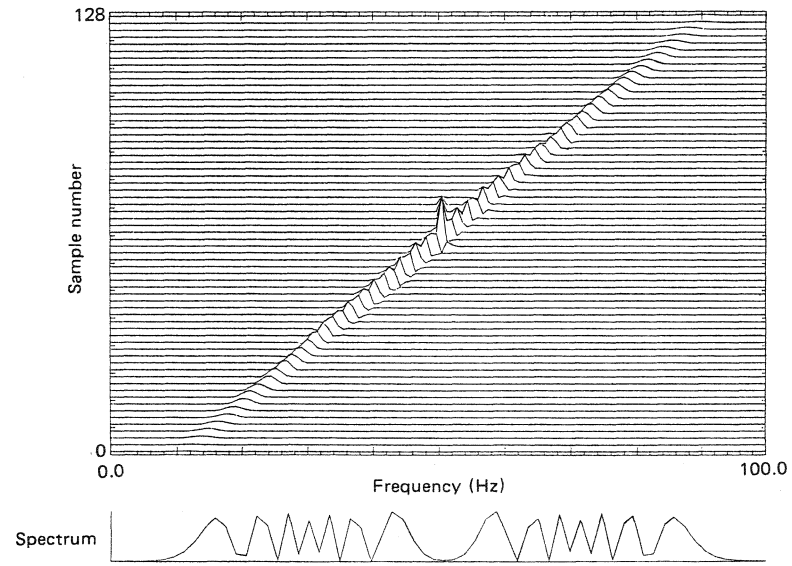


**Figure 9.32 (b)**

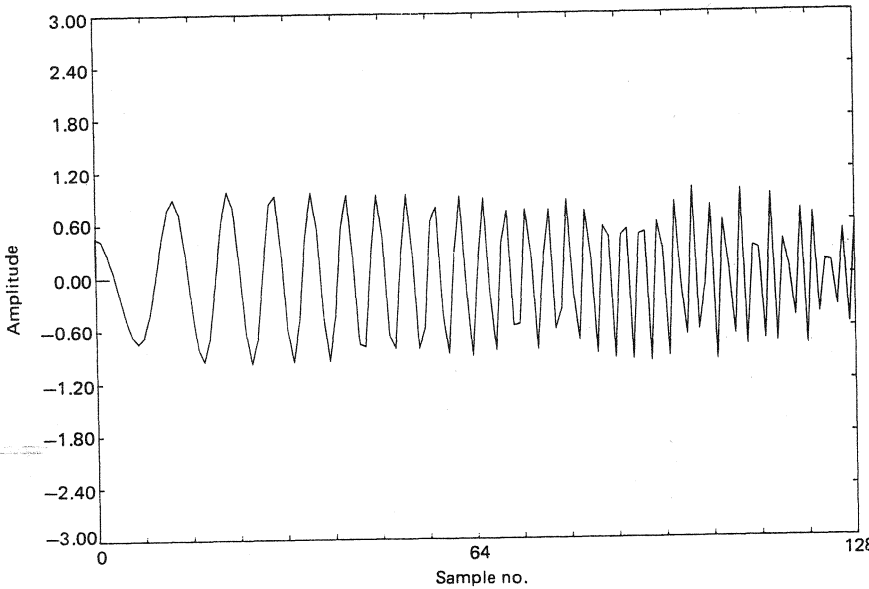


**Figure 9.32** (c) Signal component separation by time-frequency filtering. (a) WVD of the sum of two chirp signals, (b) windowed WVD, (c) reconstructed signal.

## 9.8 SIGNAL DETECTION BY TIME-FREQUENCY ANALYSIS

Several authors have proposed detection and estimation methods based on time-frequency distributions. *Spectrogram correlators*, for example, have been used for transient analysis for some time, and are reviewed in [65]. While they provide very good intuitive representations of the signal's spectral content, resolution is poor, the detector is suboptimal due to the loss of phase information, and reconstruction of the signal often occurs at some cost.

The *Gabor representation* has also been used to detect transients of unknown waveshape and arrival time [66]. This representation was chosen largely because of its inherent ability to localize signals in time and frequency. More recently, interest in the WVD spread to the area of signal detection [67], [68], [69], and [70]. For convenience, the WVD is redefined as

$$W_{zs}(t, f) = \int_{-\infty}^{+\infty} z_s(t + \tau/2) z_s^*(t - \tau/2) e^{-j2\pi f\tau} d\tau, \quad (9.138)$$

where  $z_s(t)$  is the analytic signal corresponding to  $s(t)$ . Similarly, the *cross Wigner-Ville-distribution* (XWVD) of two signals,  $s(t)$  and  $r(t)$ , is

$$W_{zs_r}(t, f) = \int_{-\infty}^{+\infty} z_s(t + \tau/2) z_r^*(t - \tau/2) e^{-j2\pi f\tau} d\tau, \quad (9.139)$$

where  $z_s(t)$  and  $z_r(t)$  are the analytic signals corresponding to  $s(t)$  and  $r(t)$ , respectively.

One of the reasons for using the WVD and XWVD for detection purposes is that there is an equivalence between time-domain correlations and XWVD correlations. The time-domain correlations that appear as the solutions to many classical detection problems, then, may be replaced by equivalent XWVD correlations. The advantage of this replacement is that time-frequency feature isolation and consequent noise suppression using time-varying filtering is then easier [71], especially where the signal waveshape is unknown.

Another justification for using the WVD as the basis for a detection scheme is its ability to detect signals subject to a Doppler shift. This problem is usually solved by methods that rely on the use of the ambiguity function. Since the AF of a signal is complex, its magnitude squared is used and the phase information is discarded. On the other hand, the WVD is real and can be shown to be the two-dimensional FT of the AF. Since the FT is a unitary linear transform the WVD and AF provide essentially the same information.

### 9.8.1 Matched-Filter, WVD, and XWVD-Based Detection

In this section a performance comparison is made between classical detection (the matched filter) and WVD- and XWVD-based detection [68].

#### Detection with a Matched Filter

The detection problem is to determine whether or not a signal is present at some time reference. A *detection statistic* ( $\eta$ ) is formed, such that if  $\eta$  exceeds a certain *threshold*, the signal is considered to be present (hypothesis  $H_1$ ). If not, it is decided that no signal is present (hypothesis  $H_0$ ), that is, the recorded waveform corresponds to noise only; the noise is assumed to be of zero mean, Gaussian, and white. The SNR, which provides a measure for noise performance comparison between WVD, XWVD, and the matched-filter detection methods, is defined as [68]

$$\text{SNR} = \frac{\sqrt{2}|E\{\eta|H_1\} - E\{\eta|H_0\}|}{(\text{var}\{\eta|H_1\} + \text{var}\{\eta|H_0\})^{1/2}}, \quad (9.140)$$

where  $E\{\eta|H_1\}$  is the expected value of  $\eta$  given  $H_1$ ,  $\text{var}\{\eta|H_1\}$  is the variance of  $\eta$  given  $H_1$ ,  $E\{\eta|H_0\}$  is the expected value of  $\eta$  given  $H_0$ , and  $\text{var}\{\eta|H_0\}$  is the variance of  $\eta$  given  $H_0$ . (See Fig. 9.33.) For a *matched filter*, we have

$$\eta = \int_{-\infty}^{+\infty} z_r(t) z_s^*(t) dt = \langle z_r | z_s \rangle, \quad (9.141)$$

where  $\langle z_r | z_s \rangle$  denotes the inner product of  $z_r(t)$  and  $z_s(t)$  as defined by (9.141). The average value of  $\eta$  is expected to be 0 if there is only noise, while if a signal is present, the average value for  $\eta$  would be equal to the signal energy. That is,

$$\begin{aligned} E\{\eta|H_0\} &= 0, \\ E\{\eta|H_1\} &= A = \text{signal energy}. \end{aligned} \quad (9.142a)$$

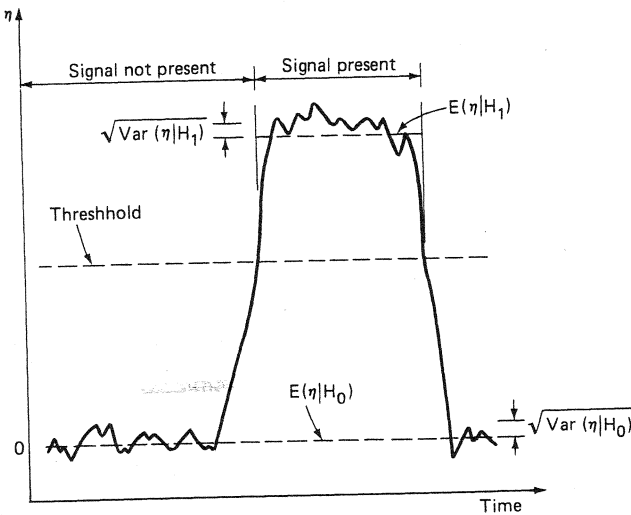


Figure 9.33 Principle of signal detection by thresholding.

The standard deviation of the measured value of  $\eta$  in both cases would be expected to be equal to  $\sqrt{N_0 A}$ , that is,

$$\text{var}\{\eta|H_0\} = \text{var}\{\eta|H_1\} = N_0 A. \quad (9.142b)$$

Substitution in (9.140) yields

$$\text{SNR} = \sqrt{A/N_0}. \quad (9.143)$$

### Detection with the WVD

The WVD-based detection statistic is a two-dimensional correlation between the WVDs of the transmitted and received signals,  $z_r(t)$  and  $z_s(t)$ :

$$\eta_{\text{wvd}} = \int_{-\infty}^{+\infty} \int_{-\infty}^{+\infty} W_{z_r}(t, f) W_{z_s}(t, f) dt df. \quad (9.144)$$

To find the relevant statistics for  $\eta_{\text{wvd}}$ , a relationship known as *Moyal's formula* may be used. This relation is shown below [72]:

$$\int_{-\infty}^{+\infty} \int_{-\infty}^{+\infty} W_{z_1 z_2}(t, f) W_{z_3 z_4}^*(t, f) dt df = \int_{-\infty}^{+\infty} z_1(t) z_3^*(t) dt \int_{-\infty}^{+\infty} z_2(t) z_4^*(t) dt \quad (9.145a)$$

$$= \langle z_1 | z_3 \rangle \langle z_2 | z_4 \rangle, \quad (9.145b)$$

where  $z_1(t)$ ,  $z_2(t)$ ,  $z_3(t)$ , and  $z_4(t)$  are arbitrary signals.

Applying Moyal's formula to (9.144) yields

$$\eta_{\text{wvd}} = \left| \int_{-\infty}^{+\infty} z_r(t) z_s^*(t) dt \right|^2 \quad (9.146a)$$

$$= \left| \int_{-\infty}^{+\infty} Z_r(f) Z_s^*(f) df \right|^2, \quad (9.146b)$$

where  $Z_r(f)$  and  $Z_s(f)$  are the FTs of  $z_r(t)$  and  $z_s(t)$ .

For this statistic, the average value obtained if no signal is present is  $N_0 A$ . The average value obtained if a signal is present is  $N_0 A + A^2$ ; that is,

$$E\{\eta_{\text{wvd}}|H_0\} = N_0 A$$

and

$$E\{\eta_{\text{wvd}}|H_1\} = N_0 A + A^2. \quad (9.147a)$$

The variances, for the cases of signal not present and signal present are given by, respectively,

$$\text{var}\{\eta_{\text{wvd}}|H_0\} = N_0^2 A^2, \quad (9.147b)$$

$$\text{var}\{\eta_{\text{wvd}}|H_1\} = N_0^2 A^2 + 2N_0 A^3, \quad (9.147c)$$

and

$$\text{SNR} = \sqrt{A/N_0} \cdot \frac{1}{\sqrt{1 + N_0/A}}. \quad (9.148)$$

This expression equals the SNR for a matched filter scaled by a factor of  $1/\sqrt{1 + N_0/A}$ . For large values of  $A/N_0$  the scaling factor approaches 1, and the SNR is not significantly degraded. For small values, however, the SNR is reduced substantially. This is explained by the nonlinearity of the WVD that accentuates the effects of noise by producing artifacts. However, for low SNR, estimators based on the WVD can be more useful than matched-filter-based estimators, since they allow a "built-in" time-varying filtering operation that is not possible with the matched filter [73].

**Detection with the XWVD** The XWVD formed between the transmitted and received signals becomes a linear operator of the signal (that is, it is no longer bilinear). The XWVD-based detection statistic is:

$$\eta_{\text{xwvd}} = \int_{-\infty}^{+\infty} \int_{-\infty}^{+\infty} W_{z_r z_s}(t, f) W_{z_s}(t, f) dt df. \quad (9.149)$$

Using Moyal's formula, (9.149) becomes

$$\eta_{\text{xwvd}} = \langle z_r | z_s \rangle \langle z_s | z_s \rangle \quad (9.150a)$$

$$= A \langle z_r | z_s \rangle. \quad (9.150b)$$

Equation (9.150) illustrates two interesting results. First, the XWVD detection statistic is the matched-filter detection statistic multiplied by a constant,  $A$ . Hence, the SNR for XWVD detection will be identical to that of the matched filter. The expected values and standard deviations of  $\eta$  for  $H_0$  and  $H_1$  will be the same as those for the matched filter, except for the multiplicative constant,  $A$ .

$$E\{\eta_{\text{xwvd}}|H_0\} = 0, \quad E\{\eta_{\text{xwvd}}|H_1\} = A^2, \quad (9.151a)$$

$$\text{var}\{\eta_{\text{xwvd}}|H_0\} = \text{var}\{\eta_{\text{xwvd}}|H_1\} = N_0 A^3, \quad (9.151b)$$

and

$$\text{SNR} = \sqrt{A/N_0}. \quad (9.152)$$

Second, because  $\eta_{\text{xwvd}}$  is also equal to  $\langle r|s \rangle$  multiplied by a constant, the detection statistic will be real—this makes the task of interpretation easier.

Thus, the detection statistic formed by the correlation of the reference signal WVD and the XWVD of the reference and observed signals, is the same as that of the standard cross-correlator except for a constant. The former statistic may then be used equivalently in any detection scheme. Due to the extra degree of freedom given by the two-dimensional nature of the WVD, estimators based on the XWVD can perform better if this extra flexibility is used; that is, the reference WVD pattern is chosen as a windowed version of the original WVD of the signal, thereby preserving only the region of the time-frequency domain where the signal is concentrated.

### 9.8.2 Interpretation of the XWVD Detection Scheme

In general the XWVD is complex, and becomes the WVD (which is real) for  $z_r = z_s$ . Thus any distortion of the signal (other than a real-valued scaling), causes real and imaginary oscillating “noise” components to appear in the XWVD. When a two-dimensional correlation with the reference WVD is performed over the time-frequency plane, the imaginary part is completely rejected, and additionally, almost all the real oscillations are smoothed out, accounting for the improved noise performance.

For practical purposes we may also form a modified XWVD detection statistic

$$\eta_m = \int_{-\infty}^{+\infty} \int_{-\infty}^{+\infty} W_{z_r z_x}(t, f) W_{z_s z_x}^*(t, f) dt df \quad (9.153)$$

$$= \langle z_r | z_s \rangle \langle z_x | z_x \rangle = A_x \langle z_r | z_s \rangle, \quad (9.154)$$

where  $A_x$  is the energy of the arbitrary signal,  $z_x(t)$ .

This statistic is again equivalent to the cross-correlator statistic so that it will be possible to form a class of optimal linear two-dimensional correlation statistics by varying  $z_x(t)$ . The class of detectors specified by (9.153) is especially useful for situations where  $s(t)$  is not known, but must first be estimated. (This is the case when detecting signals of unknown waveshape.) For such cases, the detectors given

by (9.153) allow estimation of  $s(t)$  to be replaced equivalently by estimation of  $W_{z_s z_x}(t, f)$ . Thus, the estimation problem has been transferred into a time-frequency space, where feature selection and time-varying filtering are much easier. Normally, in the WVD (XWVD) plane the presence of cross-terms makes it very difficult to distinguish multicomponent signals from the noise, and therefore to do the appropriate filtering. If, however,  $z_x(t)$  is chosen appropriately, the autoterms and the cross-terms can be isolated, with a resultant ability to perform two-dimensional feature extraction with built-in noise suppression. This idea is expanded in the next section.

### 9.8.3 Examples Using the XWVD Scheme

Consider the monocomponent FM signal embedded in noise, shown in Fig. 9.34. A preliminary analysis is performed to estimate the instantaneous frequency law, about which the signal is concentrated. A signal,  $x(t)$ , which exhibits this instantaneous frequency law, is then formed, according to the relationship

$$x(t) = \text{Re}\{z_x(t)\} \quad \text{and} \quad z_x(t) = \Pi_T(t - T/2) \exp^{j2\pi f_0 t f_i(\alpha) d\alpha + \phi_0}, \quad (9.155)$$

where  $\phi_0$  is the initial phase of the signal, and which may be obtained by comparing the original signal with the reconstructed one.

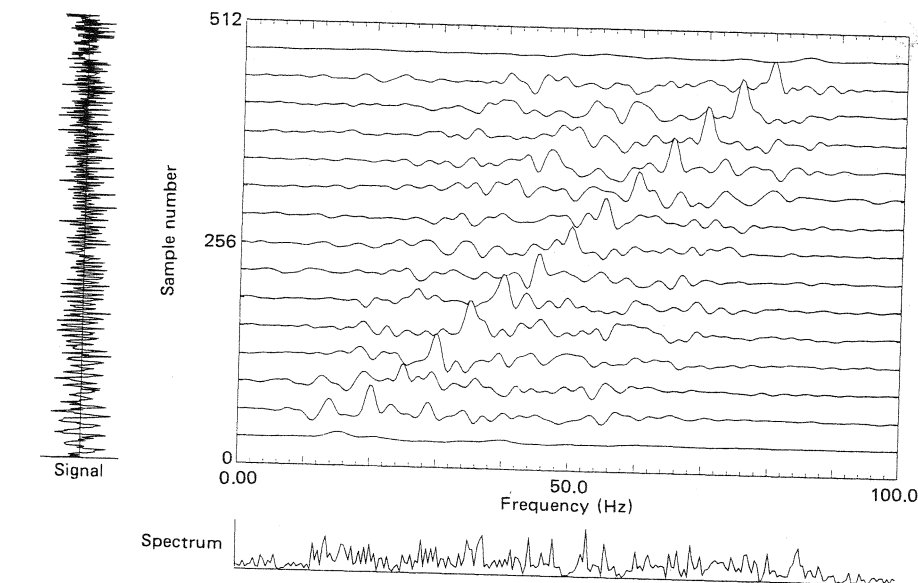


Figure 9.34 WVD of chirp signal in 0-dB noise.

From this signal, we can construct the cross Wigner-Ville distribution,  $W_{z_s z_x}(t, f)$  as seen in Fig. 9.35, followed by noise reduction through thresholding or windowing to yield the estimate,  $\hat{W}_{z_s z_x}(t, f)$  in Fig. 9.36. This can now be used in (9.153) to form the appropriate detection statistic,  $\eta_m$ . The usefulness of this approach is its ability to localize the signal in the time-frequency plane, so that the noise (which is dispersed broadly over the time-frequency plane) can be largely eliminated. This localization is not sensitive to the accuracy of the initial estimation of the frequency law, and hence, small errors in that stage should not cause large errors in the detection stage. (Both frequency and amplitude information are preserved in the XWVD.)

The method may be generalized to multicomponent signals, by forming a signal,  $x(t)$ , such that

$$x(t) = \sum_{i=1}^n x_i(t), \quad (9.156)$$

where the  $x_i(t)$  represent the instantaneous frequency laws of the various components. The procedure for estimating  $\hat{W}_{z_s z_x}(t, f)$  then involves estimation of the individual  $\hat{W}_{z_s z_{x_i}}(t, f)$  and summing:

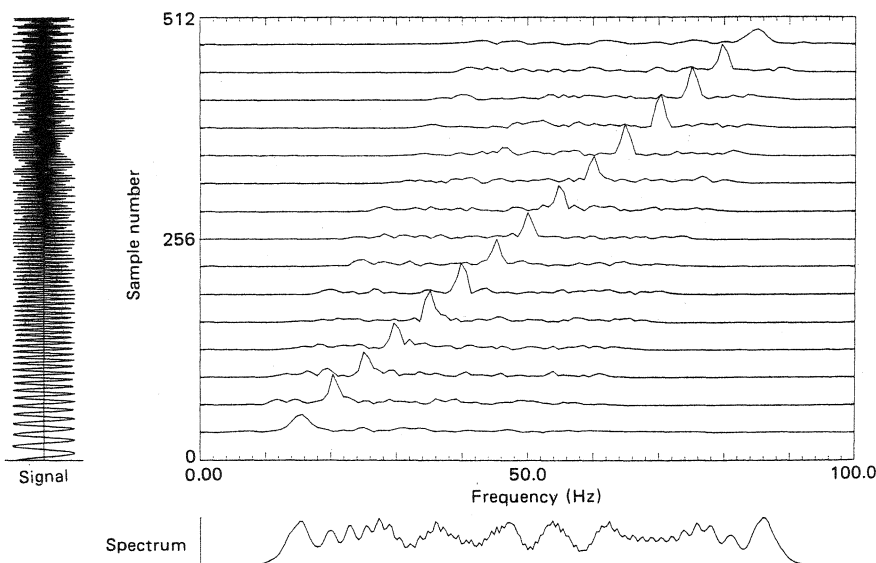


**Figure 9.35** XWVD of chirp signal  $s(t)$  in 0-dB noise and signal reconstructed from an estimate of the instantaneous frequency of  $s(t)$ .

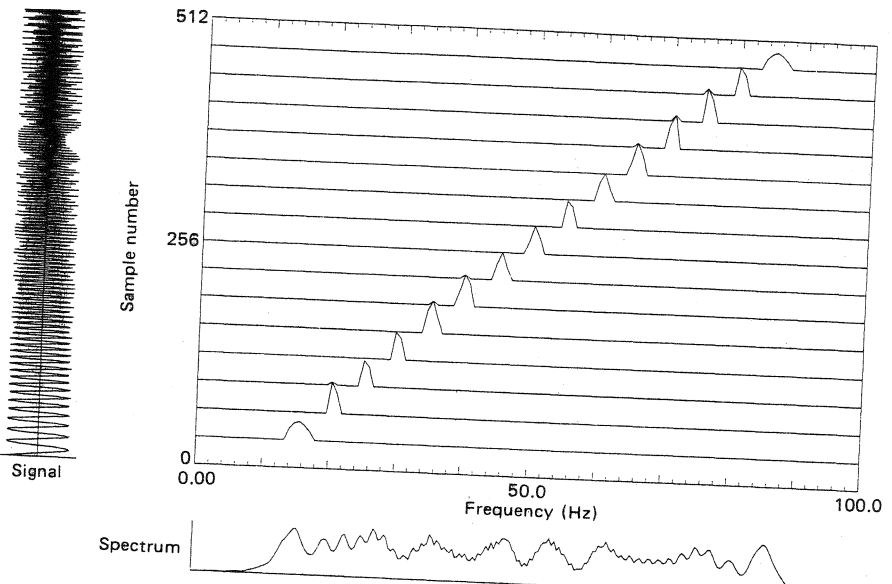


**Figure 9.36** Windowed XWVD of chirp signal in 0-dB noise.

$$\hat{W}_{z_s z_x}(t, f) = \sum_{i=1}^n \hat{W}_{z_s z_{x_i}}(t, f). \quad (9.157)$$

With this approach, the cross-terms can be isolated from the autoterms, with resultant noise suppression and time-frequency feature selection. Figure 9.37 shows the WVD of three linear FM signals of unknown slope in 3-dB noise. Fig. 9.38 shows a  $\hat{W}_{z_s z_x}(t, f)$  estimate, where the frequency laws have been estimated by an algorithm based on dechirping techniques [74]. The cross-terms have been eliminated to achieve good noise suppression.

## 9.9 APPLICATIONS

### 9.9.1 Detection of Transients

This section presents an example of detection of a transient using real data [71], [75]. It shows the effectiveness of time-frequency correlations incorporating time-varying filtering. The problem involves detection of a signal with unknown waveshape in Gaussian noise. The optimal detection procedure for such a problem involves first estimating the signal and then using this estimate as the true signal in a conventional detector such as a matched filter [76]. The equivalent procedure used here is first to

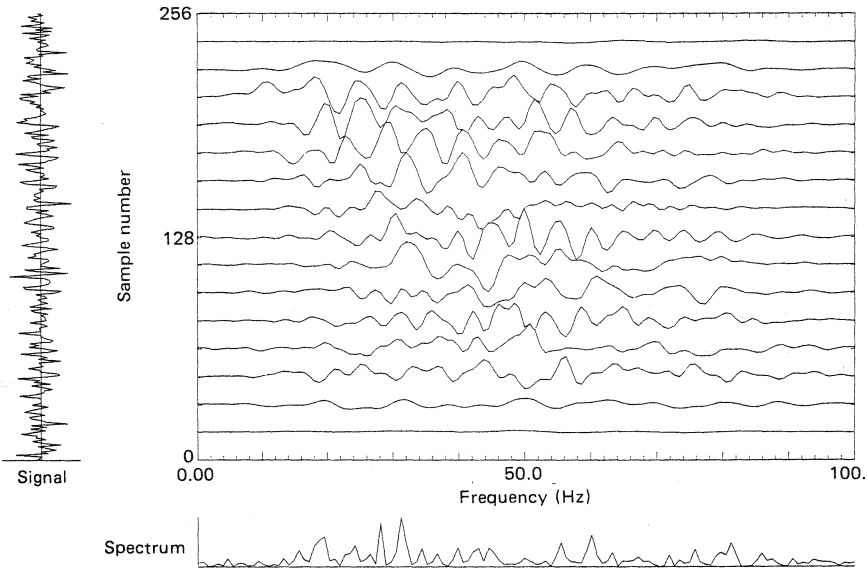


Figure 9.37 WVD of three chirp signals in 3-dB noise.

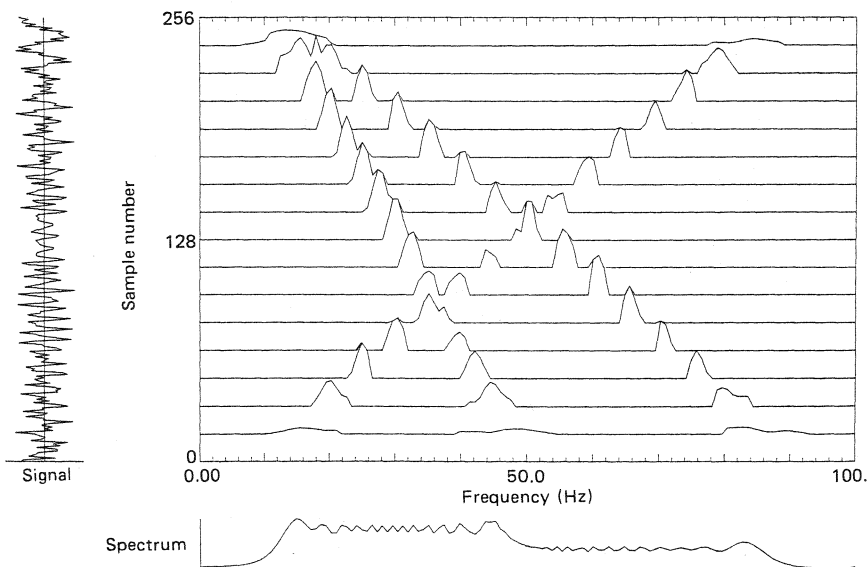


Figure 9.38 XWVD of three chirp signals with cross-terms eliminated.

estimate the time-frequency representation for the signal and then to use this as the true representation in a time-frequency detection scheme.

Figure 9.39 represents the WVD of a real transient in 3-dB noise. The techniques described in Section 9.8 are used first to estimate the signal (by noting the region in the time-frequency domain where the signal energy is concentrated) and then to detect the signal. The procedure is as follows:

1. The instantaneous frequency,  $f_i(t)$ , of the signal is first estimated using the algorithm described in Section 9.4.
2.  $f_i(t)$  is used to resynthesize a signal  $x(t)$ .
3. The XWVD,  $W_{z_r z_x}(t, f)$  is then formed, with its magnitude being shown in Fig. 9.40.
4. From this magnitude representation, a preliminary bandpass filtering operation is performed, and then threshholding is applied to form a time-frequency window function,  $W_b(t, f)$ . (See Fig. 9.41.) This is expected to enhance the important features of the signal and to eliminate noise.
5. The final estimate for  $W_{z_s z_x}(t, f)$  is obtained by multiplying  $W_{z_r z_x}(t, f)$  by  $W_b(t, f)$  and is shown in Fig. 9.42. Note that only the real part is shown in Fig. 9.42, since it is this part that is important for the correlations; the imaginary part will contribute nothing to the correlations.

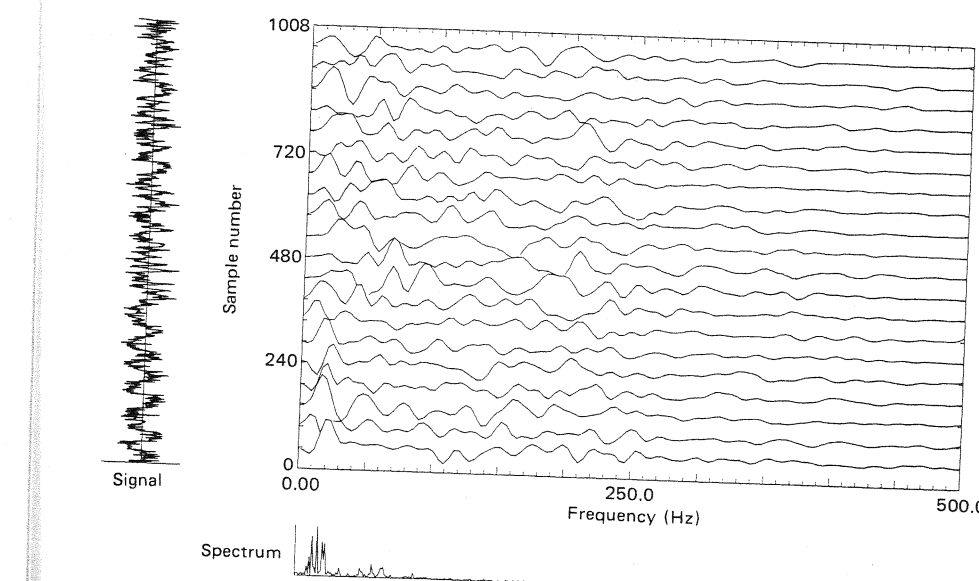


Figure 9.39 WVD of transient signal in 3-dB noise.

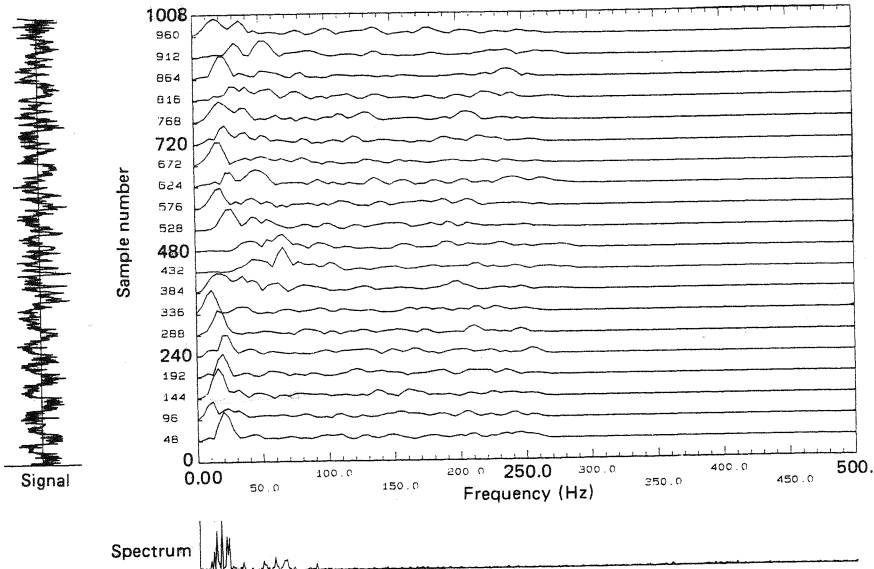


Figure 9.40 Magnitude of the XWVD of transient signal in 3-dB noise.

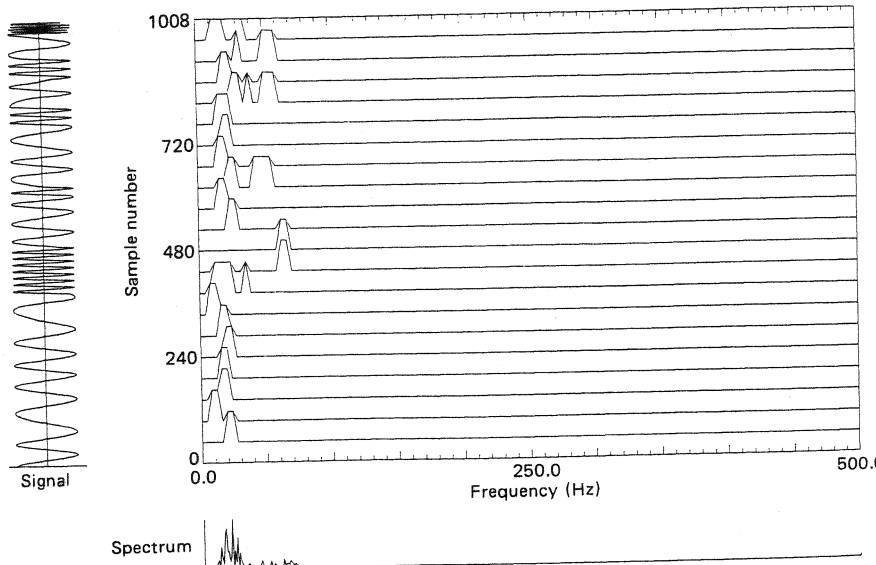


Figure 9.41 Window function.

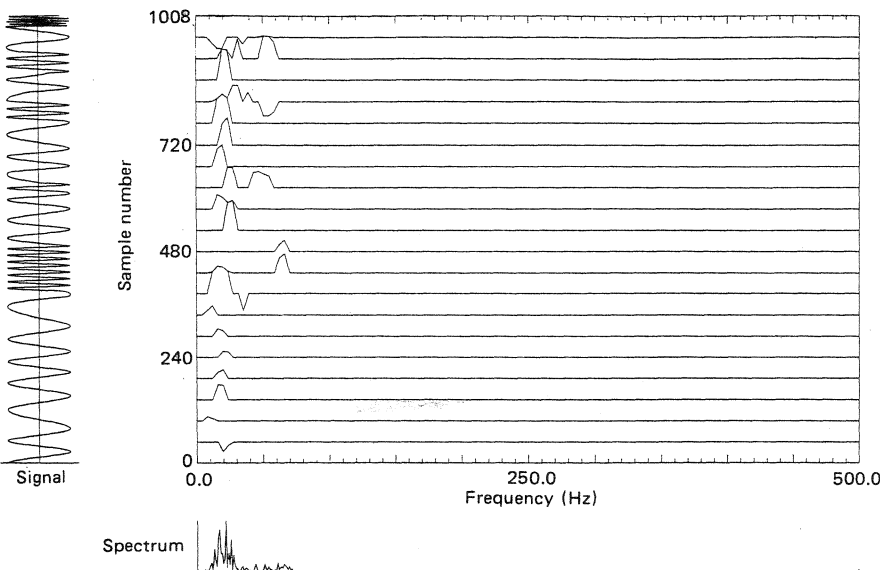


Figure 9.42 Windowed XWVD of transient (real part).

The value of the detection statistic  $\eta_m$  for  $H_1$  divided by the statistic for  $H_0$ , determined according to (9.153), was found to be 12.9. (Appropriate scaling was used so that the energy of  $x(t)$  under  $H_0$  and  $H_1$  were the same.) The corresponding ratio for matched filtering (where conventional filtering only is used to form the signal estimate) was found to be 9.7.

Note that the quantity referred to in the previous paragraph,  $\eta|H_1/\eta_m|H_0$ , represents the ratio of the energy of the signal estimate under  $H_1$  to the energy of the signal estimate under  $H_0$ . If no time-varying filtering (i.e., two-dimensional windowing) were applied in the above scheme, it would reduce to the conventional energy detector [76]. The improvement over the energy detector arises because of the two-dimensional windowing operation. In the case of noise only (hypothesis  $H_0$ ), a windowing around the "instantaneous frequency law" should eliminate a large proportion of the noise, since the noise energy would in general be distributed over the entire plane. In the case of a signal being present (hypothesis  $H_1$ ), however, provided the signal exhibits a concentration around the instantaneous frequency law, most of the signal energy will be retained in the windowing operation. The ratio  $\eta_m|H_1/\eta_m|H_0$ , would then be much greater than the corresponding ratio for the energy detector, the degree of improvement depending on the concentration of the signal around the instantaneous frequency law.

If the SNR is low, to allow for the uncertainty in the instantaneous frequency estimate, the window applied in step 4 consists of a narrow-band time-frequency window function convolved with the PDF of the estimator. Alternatively, adjunct methods, such as in band eigenvalue filtering may be used. This is an open question, and it has not yet been investigated.

### 9.9.2 Machine Noise Identification

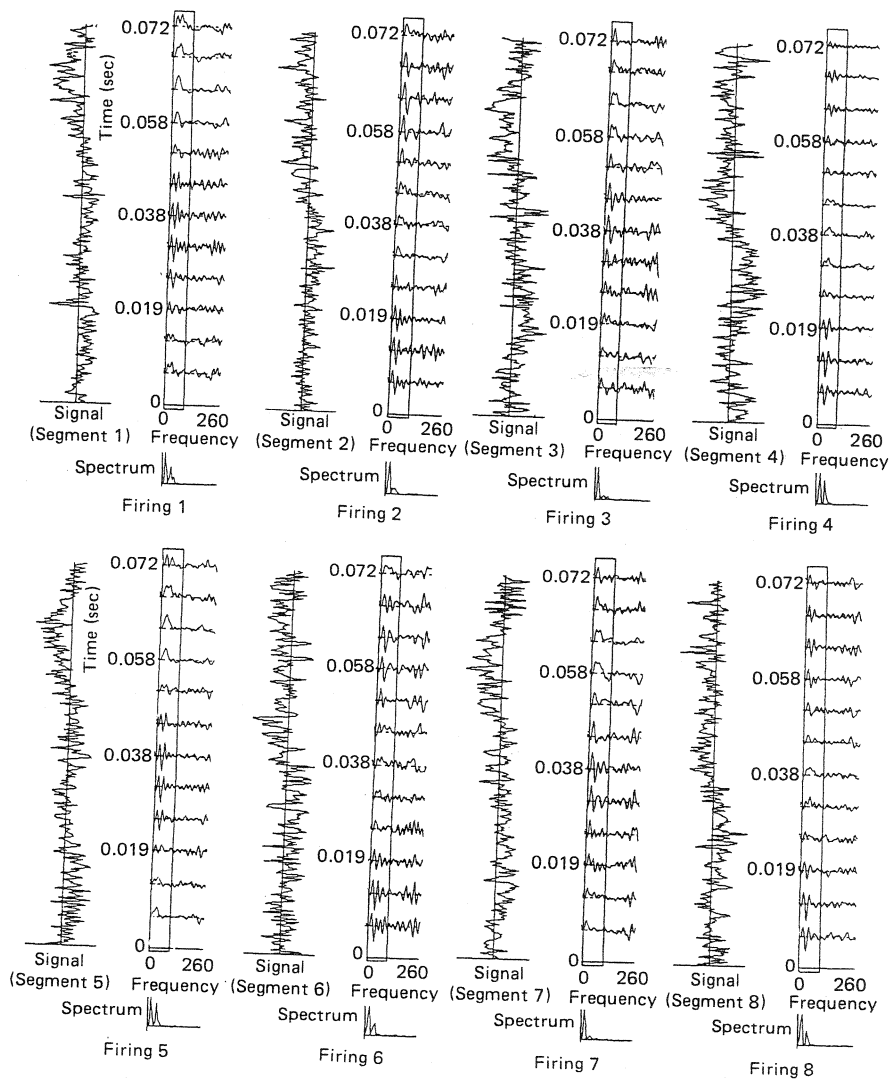
In this application the WVD is used to develop signatures for the individual cylinders of a diesel engine, and to discriminate one cylinder from the other [73]. The XWVD is also used for the same purpose, providing even better discrimination.

The signal from a diesel engine, produced predominantly by cylinder firing activity, was chosen for analysis. To develop signatures for these nonstationary transient type signals, time-frequency analysis using the WVD was used. The signal was first segmented, with each segment length corresponding to one "cylinder length." This was done using correlation techniques. Wigner-Ville analysis was then performed on eight segments of signal (numbered 1 through 8), with a view to reliably discriminating the signatures of each cylinder. Segments 1 and 5 corresponded to consecutive firings of cylinder 1, segments 2 and 6 corresponded to consecutive firings of cylinder 2, and so on. An appropriate window length was selected, and WVD plots were produced for all eight signal segments. Each of these segments contained 400 sample points (generated with a sample frequency of 5 KHz), and the WVDs were produced by applying a 400-point rectangular window (with 50 percent overlap) at varying positions along the segment. It was observed that good correspondence existed in the low frequency region of the WVD for segments corresponding to the same cylinder. This result is illustrated in Fig. 9.43, which shows side by side the low-frequency region of the WVD for segments 1 to 8. (Rectangles have been used to highlight the relevant parts of the WVDs.) It can be clearly seen that the time-frequency representations of firings 1 and 5, 2 and 6, 3 and 7, and 4 and 8 correspond very closely.

To quantify these similarities, WVD correlation techniques were employed. The two dimensional normalized cross-correlation between the two WVDs is given by

$$R(t_0, f_0) = \frac{\int_{-\infty}^{+\infty} \int_{-\infty}^{+\infty} W_{z_1}(t, f) W_{z_2}(t - t_0, f - f_0) dt df}{\left[ \int_{-\infty}^{+\infty} \int_{-\infty}^{+\infty} W_{z_1}^2(t, f) dt df \int_{-\infty}^{+\infty} \int_{-\infty}^{+\infty} W_{z_2}^2(t, f) dt df \right]^{1/2}} \quad (9.158)$$

This translates into the discrete-time domain in a straightforward way. For this practical example, the two-dimensional cross-correlation is performed not over an infinite frequency range, but over the low-frequency region shown bounded by rectangles in the time-frequency plots. (See Fig. 9.43.) This corresponds to an effective



Low frequency regions of WVD'S for 8 consecutive firings of underwater diesel

Figure 9.43 WVDs of cylinder firings from four-cylinder diesel engine.

prefiltering with a low-pass filter. Note that it could in fact be obtained in the time domain in this simple case. This approach suffers from problems due to the WVD's nonlinearity, but as discussed previously, these can be overcome by using the XWVD instead.

These low-frequency parts of the WVDs from all eight signal segments were taken, and the cross-correlation table (Table 9.3) was constructed. For this table, the rows correspond to segment  $i$ , ( $i = 5$  to 8), the columns correspond to segment  $j$ , ( $j = 1$  to 4), and the elements of the table are the peak cross-correlation values between the WVDs for segments  $i$  and  $j$ .

The table reveals comparatively high correlation values along the diagonal and lower values elsewhere. Since the diagonal elements represent cross-correlations from signals that correspond to the same cylinder, it is possible to make an objective claim that the cylinders have been signatured. Furthermore, the correlation table itself may prove useful in the process of machine identification, since it provides quantitative information as to the similarity relationships between each of the cylinders.

The eight signal segments were also analyzed using the short time Fourier transform and the XWVD. It was found that discriminating between the cylinders using the STFT was not possible in the same way that it was with the WVD, while with the XWVD, even better discrimination between cylinders was achieved [71], [73].

### 9.3 Analysis and Modeling of ECG Signals

#### Origin of the Electrocardiogram

The rhythmic contractions of the heart are initiated by a traversing electrical impulse that originates in the conduction system of the heart. The formation and propagation of the electrical impulse through the heart muscle results in a time-varying potential on the surface of the body, which is commonly known as the electrocardiographic signal.

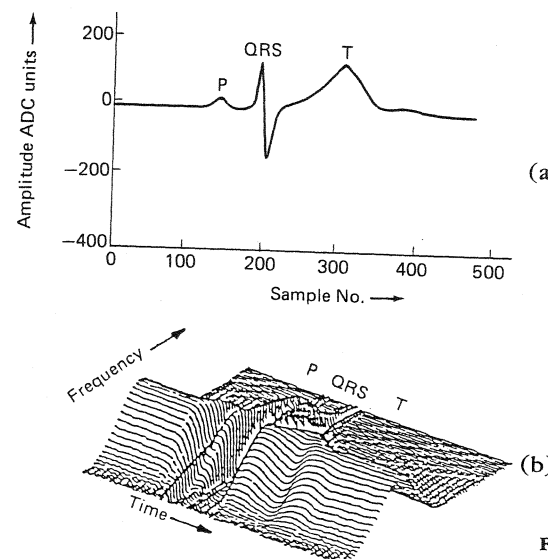
The cardioelectric impulse propagates from one node to the other (an activity known as the P wave). After a pause, the impulse enters the bundle branches, resulting in a subsequent contraction of the ventricular walls, known as the QRS complex on an ECG trace. Then the ventricular muscles regain their original size and shape (activity known as the T wave). Sometimes the impulse conduction in the bundle branches are obstructed due to blocks, and these cases are identified as bundle

TABLE 9.3

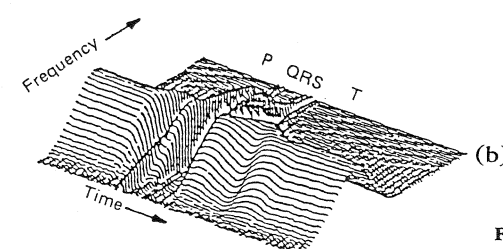
Seg. 1	Seg. 2	Seg. 3	Seg. 4
Seg. 5	0.813	0.490	0.496
Seg. 6	0.487	0.747	0.468
Seg. 7	0.628	0.515	0.737
Seg. 8	0.393	0.604	0.428
			0.784

branch blocks. The typical shapes and durations of P, QRS, and T waves for a normal heart beat are shown in Fig. 9.44.

Traditional diagnosis algorithms use the features of P, QRS, and T waves obtained in the time domain [77]. The frequency domain is also increasingly used as an adjunct or even an alternative. A difficulty is that the interbeat interval of the heart rhythm varies markedly due to irregularities in the initiation of the cardiac impulse in the atrium. The result is that the correlation function for ECG data, even for normal healthy subjects, tends to be time variant. These nonstationarities become severe in abnormal cardiac rhythms due to additional transient behavior of the signal. Time-frequency analysis has been proposed to circumvent this problem.



(a)



(b)

Figure 9.44 The ECG signal. (a) A normal ECG beat, (b) its WVD.

#### Time-Frequency Domain Features of ECG

Figure 9.45(b) shows a normalized contour plot of the STFT of the signal of Figure 9.44(a). Fig. 9.45(a) shows the WVD of the same signal with the same window. The time-frequency behavior of the signal is clearly represented in this figure. The STFT is smeared, resulting in inadequate resolution for the energy distribution along both the time and frequency axes and is inferior to the WVD. Additionally, the WVD shows negative areas that provide additional information about the time-frequency behavior of the ECG signals. The presence of these cross-terms creates interesting patterns for recognition [77].

These cross-terms are due to the interaction between the components that are localized at different positions on the time-frequency plane. In general, these cross-terms produce oscillatory components. However, in the case of ECG signals, due to

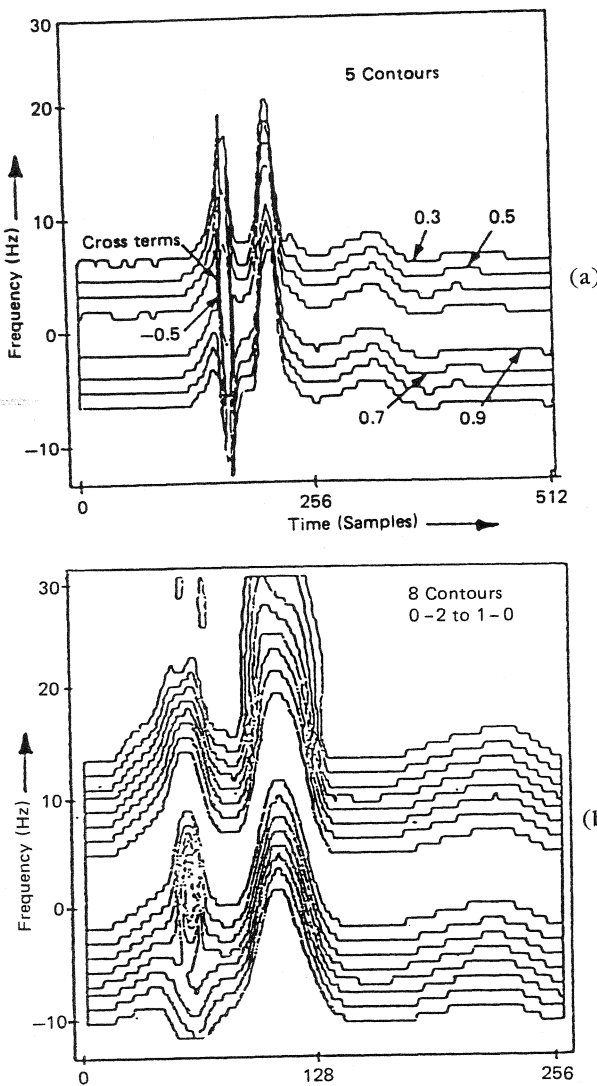


Figure 9.45 A normal ECG beat. (a) Its WVD, (b) its STFT.

the closeness of the positions of the signals in the time-frequency plane, these cross-terms are limited to a single negative area. In a WVD of a normal ECG signal, these cross-terms appear in the later part of the QRS complex (during the late ventricular depolarization), and also during the P wave (after atrial depolarization). The T wave produces no cross-terms and, hence, essentially shows a monocomponent nature [77].

The time-frequency patterns during the normal QRS complex can be described by two independent events that are concentrated at different time and frequency locations thus producing cross-terms in the WVD. The cross-terms of the WVD during a QRS complex are attributed to the travel time difference of the depolarization waves in the bundle branches [77]. Another area where cross terms are seen in the WVD is immediately after P activity.

Careful observation of Fig. 9.45 shows that the energies of the P, QRS, and T waves are concentrated at frequencies around 3, 9, and 1 Hz, respectively. This information is used in the ECG modeling procedure discussed in the following section [77].

### Modeling ECG Signals in Time-Frequency Domain

The first step of time-frequency modeling is to select suitable basis functions which result in the desired shapes for the instantaneous frequency law. An instantaneous frequency variation of the form:

$$f_i(t) \frac{1}{\sqrt{1 + (t/\alpha)^2}} \quad (9.159)$$

was selected.

The following basis function,  $u(t)$ , was selected to represent the ECG signals:

$$u(t) = A \cos\{2\pi f_p \sinh^{-1}[2\pi f_w (t - \tau) + 2\pi f_0 (t - \tau)]\} e^{-(t-\tau)/\tau_w} \quad (9.160)$$

where  $\sinh(x) = (e^x - e^{-x})/2$ .

$A$ ,  $\tau$ , and  $\tau_w$  are three time-domain parameters that specify the temporal amplitude, position and width, respectively. The three frequency-domain parameters,  $f_p$ ,  $f_0$ , and  $f_w$  specify the maximum frequency, base frequency, and the frequency width of the instantaneous frequency respectively. As time-frequency patterns during P and QRS activities show multicomponent behavior, two basis functions were selected to represent each low- and high-frequency activity. In the case of modeling the T wave, a single basis function was used. By selecting the six parameters appropriately, various basis functions for P, QRS, and T waves were selected. (Due to the low BT product of the basis functions, independent selection of the time and frequency parameters is not possible. The selection was done using trial and error to achieve the required time-frequency behavior.)

The basis functions used to simulate P and QRS waveforms were selected to generate the cross-terms as appearing in the actual ECG waveforms.

### Simulation of Normal and Abnormal Beats

Basis functions,  $u(t)$ , were selected to simulate the normal signals. The simulated waveforms and their time-frequency distributions are shown in Fig. 9.46(a). The parameters used for the generations of basis functions can be found in [77].

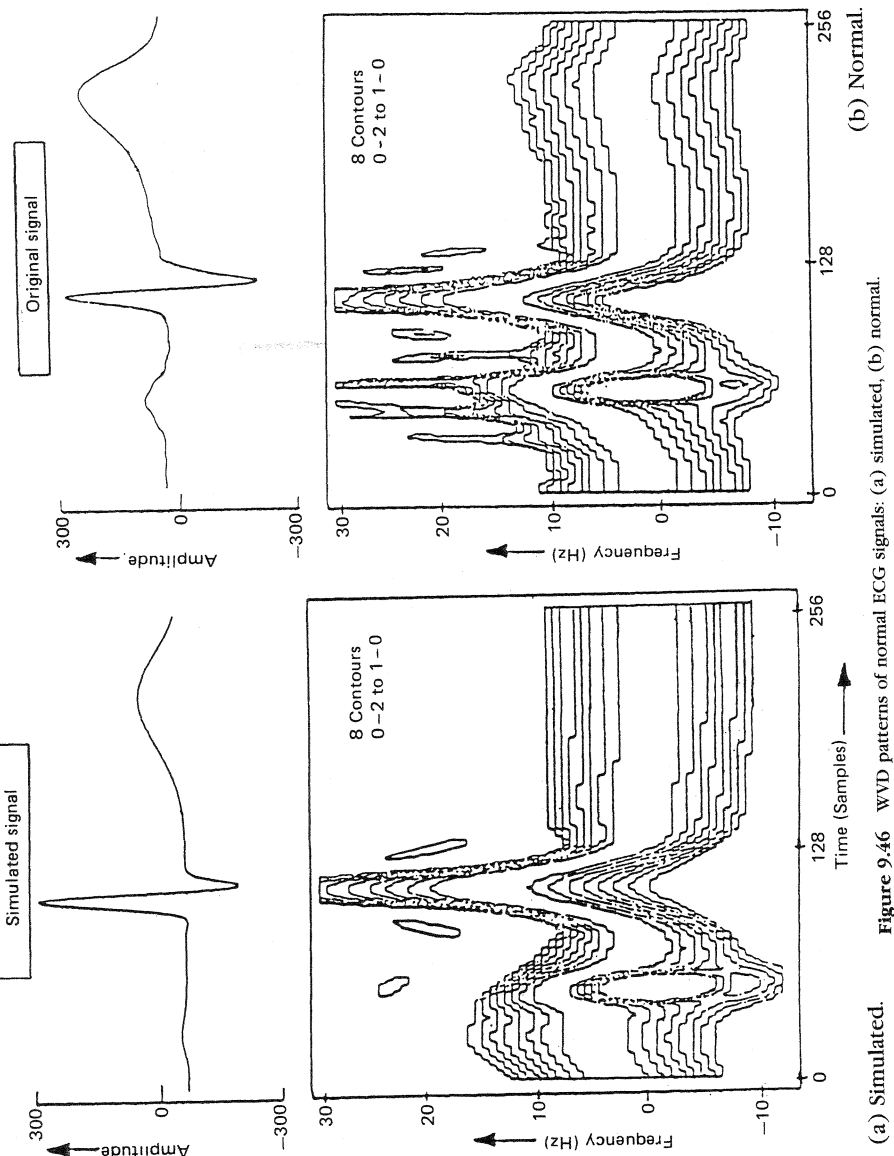


Figure 9.46 WVD patterns of normal ECG signals: (a) simulated, (b) normal.

Figure 9.47 shows the simulation of a bundle branch block waveform. Typical time-frequency patterns of ECG signals having these abnormalities obtained from real ECG signals are also shown. It can be seen that the simulated ECG waveforms of normal bundle branch block signals provide close time-frequency similarity to actual signals. The P wave and QRS complex were modeled with two basis functions to produce the cross-terms, while the T wave was modeled using a single basis function. Appearance of the cross-terms in the WVD plays an important role in successful time-frequency domain modeling of P waves and QRS complexes [78].

#### 9.4 Seismic Exploration, Sonar/Radar Echolocation, Passive Detection, and Oceanography

##### Seismic Exploration

Modern methods of seismic exploration are based on linear FM signals that are used as source instead of classical explosives. These FM signals are emitted by multiple large trucks with vibrating plates in contact with the surface of the ground. Under the assumption of the convolution model (weak reflection), then the Wigner-Ville distribution of the received signal is the convolution between the WVD of the emitted signal and the WVD of the sequence of reflectors. If the WVD of the sequence of reflectors was known, then using the invertibility property of the WVD, the sequence of reflectors can be recovered up to a multiplicative constant. Thus the practical problem of Wigner-Ville analysis of the seismic problem is a classical inverse scattering problem in which it is desired to deconvolve the instrument response function, that is, the WVD of the transmitted signal from the WVD corresponding to the sequence of reflectors.

The WVD provides one method for achieving better identification of fine strata; this can provide enhanced interpretation of seismic sections by revealing more detail about the thin layers and by allowing estimation of important parameters such as absorption and dispersion [37], [38], [79], [34], [13], [80].

##### Sonar/Radar Echolocation

The sonar/radar echolocation problem is a generalization of the seismic problem in that the individual reflectors (targets) may also be in motion so that they provide both a delay and a frequency shift of the signal. This problem is normally described in terms of the ambiguity function of the narrow-band transmitted waveform that may be viewed as the output of a matched filter, matched to the signal waveform when that waveform is delayed and frequency shifted. The WVD is equal to the two-dimensional FT of the ambiguity function, and therefore the whole echolocation system can be described in terms of the WVD [81].

### Passive Detection

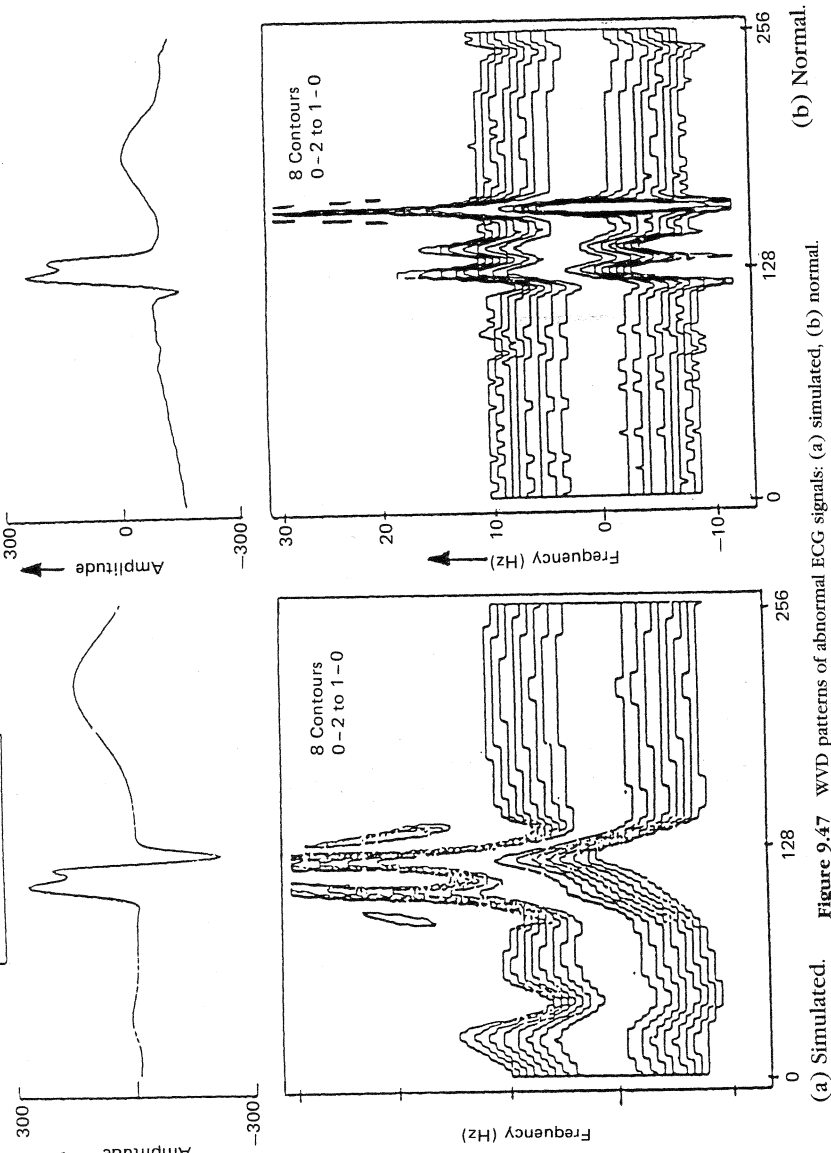
In the passive localization problem, multiple spherical waves are received by a uniformly spaced line array of sensors such as geophones and hydrophones on electromagnetic antennas. In the far field, the spherical waves may be approximated by plane waves, and then the distribution of phase along the sensors will be linear and different ratios of phase shifts correspond to different angles of arrival; thus the problem of estimating the direction of arrival is equivalent to the spectral analysis of the time signal corresponding to the spatial samples of the signal. This type of signal processing is equivalent to decomposing the incoming signal field into a frequency, wavenumber spectrum [82] [84]. When the sources are in the Fresnel zone of the array, then the curvature of the spherical wavefront must be properly accounted for. Inspection shows that it is now a linear FM, which again corresponds to the signal for which the proposed WVD method will be most effective [57], [82], [84].

### Oceanography

Natural signals found in oceanography are often extremely nonstationary. They cannot be analyzed using Fourier analysis techniques because they lead to loss of temporal and spatial resolution. Examples of such signals are obtained when, in an attempt to determine turbulence in a body, temperature-gradient microstructure measurements are made. In this application the WVD is used to compute the local instantaneous and maximum frequencies of the signals as a function of depth, and these frequencies are then related to the dissipation of turbulent kinetic energy. A high-resolution estimate of the dissipation is then obtained that provides insight into the patchiness, the wavenumber content, and the Reynolds-Froude number (measure of variability of the integral scales of motion in a strongly stratified water column). Use of the WVD circumvents the difficulties associated with other methods as there is no requirement, *a priori*, that the turbulent signatures be stationary [36], [35].

Other applications of the WVD that have been reported and that may be consulted are the following:

1. Oceanography: [36], [22].
2. Underwater acoustics: [83].
3. Detection, estimation: [84], [85], [68], [83].
4. Pattern recognition: [15], [77], [86], [73], [71], [67].
5. Speech: [87], [88].
6. Acoustics: [89], [90], [91], [92].
7. Optics: [93], [48].
8. Image analysis: [94].
9. Sonar: [82]. General [96] [97].



## 9.10 CONCLUSION AND PERSPECTIVES

This chapter explained the need for defining time-frequency distributions when dealing with nonstationary signals. An attempt was made to provide a comparison between all available TFDs and a clear basis for choice. The criterion of choice is based on one's intuition of how a TFD should perform under some particular condition, for a practical and suitable analysis. The Wigner-Ville distribution has been preferred because it is the closest fit to the ideal time-frequency analysis tool that most signal analysts envisage; it verifies most of the desirable properties and is easily calculated. The notions of instantaneous frequency and time delay of a signal were also reviewed, and it was shown how these parameters are related to time-frequency signal analysis based on the Wigner-Ville distribution.

Other properties of the WVD were reviewed and their usefulness for a practical analysis emphasized. The condition of positivity that seems intuitively basic to the concept of a TFD is shown not to be essential in many applications, but it is stressed that what is important is to find a relation between some physical parameters, and some features of the time-frequency distribution, (e.g., energy dissipation and instantaneous frequency [36], [22].

The limitation of the WVD with regard to cross-terms was addressed. An experienced user of the WVD should be able to interpret correctly these time-frequency representations by discriminating these interferences when they are not too close together. Alternatively, a smoothing procedure will reduce their effect, at the expense of decreased resolution. Potential users of the WD should incorporate the analytic signal (i.e., in fact use the WVD) if they want to avoid artifacts and aliasing created by the Wigner distribution (which uses the real signal).

Implementation procedures of WVD analysis were shown to be relatively straightforward, in the case of both deterministic and random signals. The potential importance of the method for time-varying filtering of nonstationary signals was demonstrated, and examples were provided.

As is the case in standard spectral analysis, there is no "best" method in time-frequency signal analysis. The correct approach is to select a TFD that will be optimal for the particular class of signals under consideration. In practice the most useful TFDs, in the author's opinion, are the STFT and the WVD — the STFT because of its negligible cross-terms and the WVD because it gives the least blurred time-frequency representation in the case of monocomponent signals.

Other techniques are being currently developed which cater specifically for multicomponent signals. In some specific applications, for example speech, it could be advantageous to use methods such as those developed by Williams and co-workers [20], and Atlas and co-workers [35b].

There are still a number of open questions with regards to time-frequency analysis: positivity, cross-terms, instantaneous frequency, and so on. For further reading it is recommended that a recent tutorial by Mecklenbrauker [95] and a recent review paper by Cohen [32] be consulted.

New developments in this field are reported at the annual session on Time-Frequency Signal Analysis organized by SPIE as part of the international conference on advanced signal processing algorithms and architectures, and at the "time-varying spectral analysis" session of the IEEE International Conference on Acoustics, Speech, and Signal Processing, as well as other conferences.

## ACKNOWLEDGMENTS

The author wishes to thank all the staff of the CRISSP research laboratory for their help and contribution, in particular Peter O'Shea, research fellow, for generating the plots incorporated in this chapter, as well as for reviewing and editing the manuscript. The assistance of Patricia White in preparing diagrams is also acknowledged. The author is also grateful to Leon Cohen for stimulating discussions on the notions of instantaneous frequency and multicomponent signals, and for reviewing this manuscript. Additionally, the ongoing discussions and assistance in reviewing this material, which were provided by Ross Barrett and Langford White from the Defense Science and Technology Organization, and the late reviews provided by Jeffrey Speiser, Naval Ocean Systems Center and Ted Posch, Hughes Aircraft, are appreciated. The original developments presented in this chapter are part of a research project funded by the Australian Research Council, the Australian Telecommunication and Electronics Research Board, the Australian Defense Science and Technology Organization, and the U.S. Naval Ocean Systems Center.

## REFERENCES

1. D. Gabor, "Theory of Communication," *J. IEE (London)* 93:114 (1946), 429–457.
2. A. Spataru, "Theorie de la transmission de l'information — 1: Signaux et bruits," 685 pp., translation from *Editura Technica*, Bucarest, Romania, 1970.
3. A. V. Oppenheim and J. S. Lim, "The Importance of Phase in Signals," *Proc. IEEE* 65:5, (1981), 529–541.
4. J. Ville, "Theorie et application de la notion de signal analytique, *Cables et Transmissions*, Vol. 2A(1), pp. 61–74, Paris (1948). Translation by I. Selin, "Theory and Applications of the Notion of Complex Signal," Report T-92, RAND Corporation, Santa Monica, California.
5. B. Bouachache, "Representation temps-fréquence," Doctoral thesis, Inst. Nat. Polytechnique, Univ. Grenoble, France, May 1982.
6. H. Landau, D. Slepian, and H. Pollack "Prolate Spheroidal Wave Functions, Fourier Analysis and Uncertainty," *Bell Syst. Tech. J.* 40:1 (January 1961), 43–63, 65–84.
7. D. Slepian, "On Bandwidth," *Proc. IEEE* 64:3 (March 1976).
8. B. Bouachache and P. Flandrin, "Wigner-Ville Analysis of Time-Varying Signals," *IEEE Inter. Conf. Acoustics, Speech, and Signal Processing*, Paris, May 1982, pp. 1329–1333.

9. L. Cohen and C. Lee, "Instantaneous Quantities, Standard Deviation and Cross-Terms," *Proc. SPIE Conf., Advanced Algorithms and Architectures for Signal Processing III*, Vol. 975, San Diego, California, August, 1988, pp. 186–208.
10. A. W. Rihaczek, "Signal Energy Distribution in Time and Frequency," *IEEE Trans. Inform. Theory* **14**:3 (May 1968), 369–374.
11. E. Bedrosian, "A Product Theorem for Hilbert Transforms," *Proc. IRE* **51** (May 1963), 868–869.
12. L. Qiu, "Wigner-Ville Distribution of Multicomponent Signals – Theoretical Consideration and Implementation," Masters thesis, University of Queensland, Australia, 1989.
13. B. Boashash and H. J. Whitehouse, "Seismic Applications of the Wigner-Ville Distribution," *Proc. 1986 IEEE Int. Symp. on Circuits and Systems*, Vol. 1, San Jose, California, May 1986, pp. 34–37.
14. B. Kodera, R. Gendrin, and C. Villedary, "Analysis of Time-Varying Signals with Small BT Values," *IEEE Trans. Acoustics, Speech, and Signal Processing* **26**:1 (February 1978), 64–76.
15. L. B. White, "Some Aspects of Time-Frequency Analysis of Non-Stationary Random Signals," Ph.D. thesis, University of Queensland, Australia, 1989.
16. E. P. Wigner, "On the Quantum Correction for Thermodynamic Equilibrium," *Phys. Rev.* **40** (1932), 748–759.
17. L. Cohen, "Generalized Phase-Space Distribution Functions," thesis, Yale University, New Haven, Connecticut, 1966.
18. J. L. Flanagan, *Speech Analysis and Perception* (Berlin, New York: Springer-Verlag, 1965).
19. C. H. Page, "Instantaneous Power Spectra," *J. Appl. Phys.* **23**:1 (1952), 103–106.
20. H. L. Choi and W. J. Williams, "Improved Time-Frequency Representation of Multicomponent Signals Using Exponential Kernels," *IEEE Trans. Acoustics, Speech, and Signal Processing* **37** (June 1989), 862–871.
21. L. R. O. Storey, "An Investigation of Whistling Atmospherics," *Phil. Trans. Roy. Soc. A* **246** (1953), 113–141.
22. J. Imberger and B. Boashash, "Application of the Wigner-Ville distribution to Temperature Gradient Microstructure: A New Technique to Study Small Scale Variations," *J. Phys. Ocean.* **16** (December 1986), 1997–2012.
23. L. Cohen, "Generalized Phase Space Distributions," *J. Math. Phys.* **7** (1966), 781–786.
24. T. A. C. M. Classen and W. F. G. Mecklenbrauker, "The Wigner Distribution – Part III," *Philips Res. J.* **35** (1980), 372–389.
24. (b) L. Cohen and T. E. Posch, "Generalized Ambiguity Functions," *Proc. IEEE Conf. on Acoustics, Speech, and Signal Processing*, Tampa, March 1985, pp. 27.6.1–27.6.4.
25. S. M. Sussman, "Least Squares Synthesis of Radar Ambiguity Functions," *Trans. IRE* (1962), 246–254.
26. M. H. Ackroyd, "Short Time Spectra and Time Frequency Energy Distribution," *J. Acoust. Soc. Am.* **50**:5 (1970), 1229–1231.
27. B. Bouachache, "Representation temps-frequence," Master's thesis (DEA), Cephag Inst. Nat. Polytechnique, Grenoble, France, 1979.

28. B. Bouachache, B. Escudie, P. Flandrin, and J. Grea, "Sur une condition nécessaire et suffisante de positivité de la représentation conjointe en temps et fréquence," *Compte Rend. Acad. Sci.* **288** (1979), pp. 307–309.
29. L. Cohen and T. Posh, "Positivity of Time-Frequency Distribution," *IEEE Trans. Acoustics, Speech, and Signal Processing* **33**:1 (February 1985), 31–37.
30. L. Cohen and C. A. Pickover, "A comparison of Joint Time-Frequency Distributions for Speech Signals," *Proc. 1988 IEEE Int. Symp. on Circuits and Systems*, San Jose, California, May 1988, pp. 42–45.
30. (b) A. J. E. M. Janssen and T. A. C. M. Claasen, "On Positivity of Time-Frequency Distributions," *IEEE Trans. on Acoustics, Speech, and Signal Processing*, **33**:4 (August 1985), 1029–1032.
31. T. A. C. M. Classen and W. F. G. Mecklenbrauker, "On the Time-Frequency Discrimination of Energy Distributions – Can They Look Sharper than Heisenberg," *Proc. IEEE Int. Conf. on Acoustics, Speech, and Signal Processing*, San Diego, California, 1984, pp. 41B7.1–7.4.
32. L. Cohen, "Time-Frequency Distributions," *Proc. IEEE*, vol. 77, No. 7, July 1989, pp. 941–981.
33. A. J. Janssen, "Application of the Wigner Distribution to Harmonic Analysis of Generalised Stochastic Processes," Ph.D. thesis, University of Eindhoven, Amsterdam, 1979.
34. B. Bouachache, B. Escudie, and J. M. Komatitsch, "Sur la possibilité d'utiliser la représentation conjointe en temps et fréquence dans l'analyse des signaux modulés en fréquence émis en vibroismiques," *Proc. Gretsi Conf.*, Nice, 1979, pp. 121/1–121/6.
35. B. Boashash, B. Lovell, and P. J. Kootsookos, "Time-Frequency Signal Analysis and Instantaneous Frequency Estimation: Their Inter-relationship and Applications," *Proc. IEEE Conf. on Circuits and Systems*, Portland, Oregon, April 1989, pp. 1237–1242.
35. (b) Y. Zhao, L. E. Atlas, R. J. Marks II, "The Use of Cone-Shaped Kernels for Generalized Time-Frequency Representations of Non-Stationary Signals," submitted to *IEEE Trans. Acoustics, Speech, and Signal Processing*, July 1989.
36. B. Boashash, L. White, and J. Imberger, "Wigner-Ville Analysis of Random Signals," *Proc. IEEE Int. Conf. on Acoustics, Speech, and Signal Processing*, Tokyo, 1986, pp. 2231–2233.
37. B. Bouachache, "Wigner Analysis of Time Varying Signals and Application to Seismic Prospecting," (Erlangen, Germany: Eusipco, 1983); North Holland edition, Amsterdam, 1983, pp. 703–705.
38. B. Boashash and B. Escudie, "Wigner-Ville Analysis of Asymptotic Signals," *Signal Process.* **8** (June 1985), pp. 315–327.
39. T. A. C. M. Classen and W. F. G. Mecklenbrauker, "The Wigner Distribution – Part I," *Philips Res. J.* **35** (1980), pp. 217–250.
40. B. Boashash, "Note on the use of the Wigner Distribution for Time-Frequency Signal Analysis," *IEEE Trans. Acoustics, Speech, and Signal Processing* **36** (September 1988), pp. 1518–1521.
41. T. A. C. M. Claasen and W. F. G. Mecklenbrauker, "The Wigner Distribution – Part II," *Philips Res. J.* **35** (1980), pp. 276–300.

42. B. Boashash and P. Black, "An Efficient Real Time Implementation of the Wigner-Ville Distribution," *IEEE Trans. Acoustics, Speech, and Signal Processing* 35:11 (November 1987), pp. 1611–1618.
43. A. V. Oppenheim and R. W. Schaffer, *Digital Signal Processing* (Englewood Cliffs, NJ.: Prentice-Hall, 1975).
44. L. R. Rabiner and B. Gold, *Theory and Application of Digital Signal Processing* (Englewood Cliffs, NJ.: Prentice-Hall, 1975).
45. B. Boashash and H. J. Whitehouse, "High Resolution Wigner-Ville Analysis," paper presented at 11th Gretsi Conf., Nice, France, June 1987, pp. 205–208.
46. P. Ramamoorthy, V. Iyer, and Y. Polysongsang, "Autoregressive Modeling of the Wigner Spectrum," *IEEE Conf. on Acoustics, Speech, and Signal Processing* (April 1987), pp. 1509–1512.
47. H. J. Whitehouse, B. Boashash and J. M. Speiser, "High Resolution Techniques for Temporal and Spatial Signals," presented at the Workshop on High Resolution Methods for Underwater Acoustics, organized by GRETSI, Juan les Pins, France, June 16, 1989. To appear as a chapter in a volume edited by M. Bouvet and G. Bienvenu, in the Springer-Verlag *Lecture Notes in Computer Science* (1990).
48. O. Kenny and B. Boashash, "An Optical Signal Processor for Time-Frequency Signal Analysis Using the Wigner-Ville Distribution," *J. EEE, (Australia)* 8:3 (September 1988), pp. 152–158.
49. K. V. Mardia, *Statistics of Directional Data*, (London: Academic Press, 1972).
50. F. J. Harris and H. Abu Salem, "Performance Comparison of Wigner-Ville Based Techniques to Standard FM Discrimination for Estimating Instantaneous Frequency of a Rapidly Slewling FM Sinusoid in the Presence of Noise," *Proc. SPIE Conf., Advanced Algorithms and Architectures for Signal Processing III*, Vol. 975, San Diego, August 1988, pp. 232–244.
51. B. Boashash, G. Jones, and P. O'Shea, "Instantaneous Frequency Estimation: Implementations and Applications," *Proc. of SPIE Conf., Advanced Algorithms and Architectures for Signal Processing*, vol. 1152, San Diego, August 1989.
51. (b) L. B. White and B. Boashash, "Estimating the Instantaneous Frequency of a Gaussian Random Process," *IEEE Trans. Acoustics, Speech, and Signal Processing* 36:3 (March 1988), 417–420.
51. (c) L. B. White, L. Qiu, and B. Boashash, "Instantaneous Frequency Estimation: Statistical Properties; Application to Time-Varying Filtering," *Proc. IEEE Intern. Conf. on Acoustics, Speech, and Signal Processing*, Albuquerque, 1990.
51. (d) L. B. White, "Robust Methods for Instantaneous Frequency Estimation," *Proc. SPIE Intern. Conf. on Advanced Signal Processing Algorithms and Architectures*, San Diego, July 1990.
51. (e) P. Rao and F. J. Taylor, "Estimation of Instantaneous Frequency Using the Wigner Distribution," *Electronics Letters*, vol. 26, No. 4 (Feb. 1990), pp. 246–248.
51. (f) K. M. Wong and Q. Jin, "Estimation of the Time-Varying Frequency of a Signal: the Cramer-Rao Bound and the Application of Wigner Distribution," *IEEE Trans. Acoustics, Speech, and Signal Processing* 38:3 (March 1990), pp. 519–536.
52. R. A. Altes, "Sonar for a Generalised Target Description and Its Similarity to Animal Echolocation," *Journal of Acoustic Society of America* 59:1 (January 1976).

53. A. Papoulis, *Systems and Transforms with Applications to Optics* (New York: McGraw-Hill, 1972).
54. R. L. Hudson, "When Is the Wigner Quasi-Probability Density Non-negative?" *Rep. Math. Phys.* 6 (1974), pp. 249–252.
55. A. H. Nutall, "The Wigner Distribution Function with Minimum Spread," *NUSC Technical Report* 8317, June 1988.
56. W. Martin, "Time-Frequency Analysis of Random Signals," *IEEE Int. Conf. on Acoustics, Speech, and Signal Processing*, Paris, 1982, pp. 1325–1328.
56. (b) Priestly, M. B. "Evolutionary Spectra and Non-Stationary Processes," *J. Roy. Stat. Soc. (Ser. B)* 27:2 (1965), 204–237.
56. (c) Hammond J. K. and R. F. Harrison, "Wigner-Ville and Evolutionary Spectra for Covariance Equivalent Non-Stationary Random Process," *Proc. IEEE Intern. Conf. on Acoustics, Speech, and Signal Processing*, 1985.
57. A. Nutall, "Wigner Distribution Function: Relation to Short-Term Spectral Estimation, Smoothing, and Performance in Noise," *NUSC Technical Report* 8225, February 16, 1988.
58. M. Amin, "Smoothing and Recursion in Time-Varying Spectrum Estimation," *Proc. SPIE Conf., Advanced Algorithms and Architectures for Signal Processing IV*, vol. 1152, San Diego, August 1989.
59. M. Amin, "Time and Lag Window Selection in the Wigner-Ville Distribution," *Proc. IEEE Int. Conf. on Acoustics, Speech, and Signal Processing*, Dallas, Texas, 1987.
60. L. B. White and B. Boashash, "A Design Methodology for the Optimal Estimation of the Spectral Characteristics of Non-stationary Random Signals," *Acoustics, Speech, and Signal Processing Workshop on Spectrum Estimation and Modeling*, Minnesota, 1988, pp. 65–70.
61. U. Appel and A. V. Brandt, "Adaptive Sequential Segmentation of Piecewise Stationary Time Series," *Infor. Sci.* 29 (1983), pp. 27–56.
61. (b) L. B. White and B. Boashash, "Time-Frequency Coherence: A Theoretical Basis for Cross-spectral Analysis of Non-Stationary Signals," *Proc. IASTED Int. Symp. on Signal Processing and Its Applications*, edited by B. Boashash, Vol. 1, pp. 18–23, Brisbane, Australia, August 1987.
61. (c) L. B. White and B. Boashash, "Cross-Analysis of Non-Stationary Random Processes," *IEEE Transactions on Information Theory*, to appear, July 1990.
62. K. B. Yu and S. Cheng, "Signal Synthesis from the Pseudo-Wigner Distribution and Applications," *IEEE Trans. Acoustics, Speech, and Signal Processing* 35:9 (1987), pp. 1289–1302.
63. B. E. A. Saleh and N. S. Subotic, "Time-Variant Filtering of Signals in the Mixed Time-Frequency Domain," *IEEE Trans. Acoustics, Speech, and Signal Processing* 33:6 (1985), pp. 1479–1485.
64. G. F. Boudreaux-Bartels and T. W. Parks, "Time-Varying Filtering and Signal Estimation Using Wigner Distribution Synthesis Techniques," *IEEE Trans. Acoustics, Speech, and Signal Processing* 34:3 (1985), pp. 442–451.
65. R. A. Altes, "Detection, Estimation, and Classification with Spectrograms," *J. Acoust. Soc. Amer.* 67:4 (1980), pp. 1232–1246.

66. B. Friedlander and B. Porat, "Detection of Transients by the Gabor Representation," *Proc. IEEE Int. Conf. on Acoustics, Speech, and Signal Processing*, 1987, pp. 40.1.1–4. See also "Detection of Transient Signals by the Gabor Representation," *IEEE Trans. on Acoustics, Speech, and Signal Processing* 37:2 (1989), pp. 169–180.
67. B. Bouachache and F. Rodriguez, "Recognition of Time-Varying Signals in the Time-Frequency Domain by Means of the Wigner Distribution," *Proceedings of Int. Conf. Acoustics, Speech, and Signal Processing*, 1984, pp. 22.5.1–4.
68. V. J. Kumar and C. Carroll, "Performance of Wigner Distribution Function Based Detection Methods," *Opt. Eng.* 23:6 (November 1984), pp. 732–737.
69. S. Kay and G. F. Boudreault-Bartels, "On the Optimality of the Wigner Distribution for Detection," *IEEE Int. Conf. on Acoustics, Speech, and Signal Processing*, Vol. 3, Tampa, Florida, 1985, pp. 1263–1265.
70. B. Boashash, "Theory, Implementation and Application of Time-Frequency Signal Analysis Using the Wigner-Ville Distribution," *J. EEE (Australia)* 7:3 (1987), pp. 166–177.
71. B. Boashash and P. O'Shea, "Application of the Wigner-Ville Distribution to the Identification of Machine Noise," *Proc. SPIE Conference, Advanced Algorithms and Architectures for Signal Processing III*, Vol. 975, August 1988.
72. J. E. Moyal, "Quantum Mechanics as a Statistical Theory," *Proc. Cambridge Phil. Soc.*, Vol. 45 (1949), pp. 99–132.
73. B. Boashash and P. O'Shea, "Time-Frequency Analysis Applied to Signaturing of Underwater Acoustics Signals," *Proc. Int. Conf. Acoustics, Speech, and Signal Processing*, New York, April 1988, pp. 2817–2820.
74. W. Li, "Wigner Distribution Method Equivalent to Dechirp Method for Detecting a Chirp Signal," *IEEE Trans. Acoustics, Speech, and Signal Processing*, 35:8 (August 1987).
75. B. Boashash, P. O'Shea, and G. Jones, "Time-Frequency Analysis Applied to Underwater Acoustics — Final Report on DSTO Project No. CDS 10/87-DST 86/726," *Dept. Electr. Eng. Report EE88/7*, Vol. 2, University of Queensland, Australia, 1988.
76. F. B. Tuteur, "On the Detection of Broadband Targets on Noise of Uncertain Level," *IEEE Trans. Commun. Tech.* 15:1 (1962).
77. R. M. S. S. Abeysekera, "Time-Frequency Domain Features of ECG Signals: An Interpretation and Their Application in Computer Aided Diagnosis," Ph.D. thesis, University of Queensland, St. Lucia, Brisbane, Australia, January 1989.
78. R. M. S. S. Abeysekera and B. Boashash, "Time-Frequency Domain Features of ECG Signals: Their Application in P Wave Detection Using the Cross Wigner-Ville Distribution," *IEEE Int. Conf. on Acoustics, Speech, and Signal Processing*, Glasgow, 1989.
79. P. Boles and B. Boashash, "The Cross WVD — A Two-Dimensional Analysis Method for the Processing of Vibroseis Seismic Signals," *Proc. Int. Conf. on Acoustics, Speech, and Signal Processing*, New York, April 1988, pp. 904–907.
80. S. K. Mullick and V. A. Topkar, "A Wigner Distribution Based Receiver," *Signal Processing*, Vol. 14, pp. 185–196 (Amsterdam: North Holland, 1988).
81. H. H. Szu, "Two-Dimensional Optical Processing of One-Dimensional Acoustic Data," *Opt. Eng.* 21:5 (September–October 1982), pp. 804–813.
82. A. L. Swindellhurst and T. Kailath, "Near-Field Source Parameter Estimation Using a Spatial Wigner Approach," *Proc. SPIE Conference, Advanced Algorithms and Architectures for Signal Processing III*, Vol. 975, San Diego, California, August 1988.

83. P. Flandrin, "A Time-Frequency Formulation of Optimum Detection," *IEE Tran. on Acoustics, Speech, and Signal Processing*, Vol. ASSP-36, 1988, pp. 1377–1384.
84. B. P. Breed and T. E. Posch, "A Range and Azimuth Estimator Based on Forming the Spatial Wigner Distribution," *Proc. Int. Conf. on Acoustics, Speech, and Signal Processing*, San Diego (1984), pp. 41B.9.1–2.
85. F. Cohen, G. F. Boudreau-Bartels, and S. Kadambé, "Tracking of Unknown Non-Stationary Chirp Signals Using Unsupervised Clustering in the Wigner Distribution Space," *Proc. Int. Conf. on Acoustics, Speech, and Signal Processing*, New York, April 1988, pp. 2180–2183.
86. N. M. Marinovic and G. Eichmann, "Feature Extraction and Pattern Classification in Space Frequency Domain," *Proc. SPIE Conf. on Intelligent Robots and Computer Vision*, 1985, pp. 15–20.
87. D. Chester, F. Taylor, and M. Doyle, "The Wigner Distribution in Speech Processing," *J. Franklin Inst.*, 318 (1984), 415–430.
88. H. Garudari et al., "Identification of Invariant Acoustic Cues in Stop Consonants Using the Wigner Distribution," *IASTED Conference Proceedings*, edited by M. H. Hamza, Calgary, 1985.
89. D. D. Day, "The Modified Wigner Distribution with Application to Acoustic Well Logging," *Proc. Int. Conf. on Acoustics, Speech, and Signal Processing*, New York, April 1988, pp. 2713–2717.
90. C. P. Janse and A. Kaiser, "Time-Frequency Distributions of Loud-Speakers: The Application of the Wigner Distribution," *J. Audio Eng. Soc.* 37 (1983), 198–223.
91. N. M. Marinovic and W. Smith, "Suppression of Noise to Extract the Intrinsic Frequency Variation from an Ultrasonic Echo," *Proc. IEEE Ultrasonics Symp.*, 1985.
92. N. M. Marinovic and W. Smith, "Application of Joint Time-Frequency Distributions to Ultrasonic Transducers," *IEEE Int. Symp. on Circuits and Systems*, San Jose, California, 1986.
93. M. J. Bastiaans, "Application of the Wigner Distribution to Partially Coherent Light," *J. Opt. Soc. Am.*, 3 (1986), 1227–1238.
94. G. Cristobal, J. Bescos, and J. Santamaría, "Application of the Wigner Distribution for Image Representation and Analysis," *Proc. IEEE 8th Int. Conf. on Pattern Recognition*, 1986, pp. 998–1000.
95. W. F. G. Mecklenbrauker, "A Tutorial on Non-Parametric Bilinear Time-Frequency Signal Representations," *Les Houches, Session XLV, 1985, Signal Processing*, editors J. L. Lacoume, T. S. Durrani, and R. Stora, Les Houches, France 1987.
96. N. M. Marinovic, and G. Eichmann, "An Expansion of Wigner Distribution and Its Applications," *Proc. IEEE Int. Conf. on Acoustics, Speech, and Signal Processing*, 1985, pp. 1021–1024.
97. W. D. Mark, "Spectral Analysis of the Convolution and Filtering of Non-Stationary Stochastic Processes," *J. Sound Vib.* 11 (1970), p. 19.

*Library of Congress Cataloging-in-Publication Data*

Advances in spectrum analysis and array processing / Simon Haykin,  
editor.

p. cm.

Includes bibliographical references.

ISBN 0-13-007444-6 (v. 1)

1. Signal processing. 2. Signal theory (Telecommunication)

I. Haykin, Simon S.

TK5102.5.A334 1991

621.382'23—dc20

89-26459  
CIP

Editorial/production supervision: *Jean Lapidus*

Interior design: *Brendan M. Stewart*

Cover design: *Karen A. Stephens*

Manufacturing buyers: *Kelly Bebr* and *Susan Brunke*



©1991 by Prentice-Hall, Inc.  
A Division of Simon & Schuster  
Englewood Cliffs, New Jersey 07632

This book can be made available to businesses  
and organizations at a special discount when  
ordered in large quantities. For more information  
contact:

Prentice-Hall, Inc.  
Special Sales and Markets  
College Division  
Englewood Cliffs, N.J. 07632

All rights reserved. No part of this book may be  
reproduced, in any form or by any means,  
without permission in writing from the publisher.

Printed in the United States of America

10 9 8 7 6 5 4 3 2 1

ISBN 0-13-007444-6

Prentice-Hall International (UK) Limited, *London*

Prentice-Hall of Australia Pty. Limited, *Sydney*

Prentice-Hall Canada Inc., *Toronto*

Prentice-Hall Hispanoamericana, S.A., *Mexico*

Prentice-Hall of India Private Limited, *New Delhi*

Prentice-Hall of Japan, Inc., *Tokyo*

Simon & Schuster Asia Pte. Ltd., *Singapore*

Editora Prentice-Hall do Brasil, Ltda., *Rio de Janeiro*

# Advances in Spectrum Analysis and Array Processing

## Volume I

Simon Haykin, editor

McMaster University  
Hamilton, Ontario  
Canada



PRENTICE HALL, Englewood Cliffs, New Jersey 07632